



EUROPEAN
COMMISSION

Community research

STAR

(Contract Number:Fission-2010-3.5.1-269672)

DELIVERABLE D4.2

Tools for assessing availability and exposure in a multiple contaminant context: the scientific basis and associated tools to assess radionuclide availability and exposure under multiple contaminant conditions

Author(s): Steve Lofts, Nele Horemans, Hans-Christian Teien, Laureline Février, Rodolphe Gilbin, Claus Svendsen, Hildegard Vandenhove

Editors: Laureline Février

Reporting period: [01/02/2014– 31/07/2015](#)

Date of issue of this report: [28/07/2015](#)

Start date of project : [01/02/2011](#)

Duration : [54 Months](#)



[[STAR](#)]



DISTRIBUTION LIST

Name	Number of copies	Comments
André Jouve, STAR EC Project Officer	1	Electronically
Laureline Février, STAR Co-ordinator (WP-1), IRSN	1	Electronically (pdf file)
STAR Management Team members: WP-1: T. Hinton, IRSN WP-2: T. Ikaheimonen, STUK WP-3: A. Liland, NRPA WP-4: H. Vandenhove, SCK•CEN WP-5: F. Alonzo, IRSN WP-6: L. Skipperud, NMBU WP-7: B. Howard, NERC	1 per member	Electronically (pdf file)
STAR Steering Committee M. Steiner, BfS A. Real, CIEMAT J-C. Gariel, IRSN T. Ikaheimonen, STUK H. Vandenhove, SCK•CEN C. Bradshaw, SU A. Liland, NRPA B. Howard, NERC B. Salbu, NMBU N. Fisher, SUNY J. Nishikawa, Tokai Univ.	1 per member	Electronically (pdf file)
STAR Wiki site		Electronically (pdf file)
STAR's External Advisory Board	1 per member	Electronically (pdf file)
ALLIANCE members	1 per member	Electronically (pdf file)

Project co-funded by the European Commission under the Seventh Euratom Framework Programme for Nuclear Research & Training Activities (2007-2011)		
Dissemination Level		
PU	Public	PU (after 01/07/2017)
RE	Restricted to a group specified by the partners of the [STAR] project	RE (before 01/07/2017)
CO	Confidential, only for partners of the [STAR] project	

Table of Contents

Table of Contents	3
Foreword	5
1 Background	7
1.1 Speciation models.....	8
1.2 Tools for bioavailability	10
1.2.1 Biotic Ligand Model for single and multiple metals.....	10
1.2.2 Predicting toxic effects of single metals and mixtures from bioaccumulation ..	13
2 Objectives and tested hypotheses	14
2.1 Objectives	14
2.2 Hypotheses.....	14
3 Speciation modelling for BLM development.....	14
4 Development of a bioavailability model under mixed contaminant conditions.....	15
4.1 General experimental strategy for uranium BLM development.....	15
4.2 General modelling strategy for BLM development.....	15
4.3 Experimental approaches for specific organisms	17
4.3.1 <i>Salmo salar</i>	17
4.3.2 <i>Lemna minor</i>	19
4.3.3 <i>Daphnia magna</i>	21
4.4 Results	25
4.4.1 <i>Observed U accumulation: Lemna minor and Salmo salar</i>	25
4.4.2 <i>U accumulation modelling: Lemna minor and Salmo salar</i>	28
4.4.3 <i>Modelling: one-site model</i>	29
4.4.4 <i>Modelling: two-site model</i>	37
4.4.5 <i>U toxicity modelling: Lemna minor and Salmo salar</i>	41
4.4.6 <i>U toxicity modelling: Daphnia magna</i>	49
5 Modelling mixture accumulation and toxicity	58
5.1 Lemna minor.....	58
5.1.1 <i>Cadmium accumulation and toxicity</i>	58

5.1.2	<i>Mixture accumulation</i>	60
5.1.3	<i>Mixture toxicity</i>	62
5.2	<i>Salmo salar</i>	65
5.2.1	<i>Cadmium accumulation and toxicity</i>	65
5.2.2	<i>Mixture accumulation</i>	67
5.2.3	<i>Mixture toxicity</i>	71
5.3	<i>Daphnia magna</i>	73
6	Discussion, Highlights and Conclusions	78
6.1	Biotic ligand modelling of uranium–cadmium mixture accumulation and toxicity..	82
6.2	Extension of the BLM to other radionuclides	84
6.3	Highlights and Conclusions	84
7	References	85
8	Annex 1: List of papers and presentations issued from this work	91
9	Annex 2: One-site toxicity model results, <i>L. minor</i>	92
10	Annex 3: One-site toxicity model results, <i>S. salar</i>	96
11	Annex 4: Mixture BLM effect predictions, <i>S. salar</i>	100
12	Annex 5: Two-site model results, <i>D. magna</i>	103

Foreword

The overarching goal of the STAR Work Package 4 "Radiation Protection in a Mixed Contaminant Context" was to determine if radiation protection criteria for wildlife are robust, even within a mixed contaminant context.

To achieve this goal, four specific objectives were pursued:

1. Critically review existing approaches, methods and tools developed in ecotoxicology for assessing exposures, effects and risks in a mixed contaminant context and evaluate their applicability for radioecological research and radioecological risk assessments (task 1, D-N°4.1, Vandenhove et al., 2012a).
2. Test and improve selected ecotoxicological approaches and tools for reliable radionuclide (bio)availability and exposure assessment under mixed contaminant conditions, and improve the understanding of underlying mechanisms and processes (task 2).
3. Apply selected approaches developed in ecotoxicology to assess the impact of mixed contaminant conditions on radiation induced effects, and improve the understanding of underlying mechanisms and processes (task 3).
4. Integration of all research and technology development results for a critical evaluation on how mixed contaminant conditions may affect radiation protection standards (task 4).

This document is the final Deliverable for the second task. The goals of this task, as noted above, were (i) to test and improve selected ecotoxicological approaches and tools for reliable radionuclide (bio)availability and exposure assessment under mixed contaminant conditions, and (ii) improve the understanding of underlying mechanisms and processes. Based on the outcomes of Deliverable N°4.1, (Vandenhove et al., 2012b), a STAR workshop (November 2011) and a STAR expert consultation workshop (January 2012), a research/experimental plan (Milestone 43, Vandenhove et al., 2012a) was developed setting out the proposed work to evaluate whether radiation protection criteria need to consider contaminant mixture effects. Within the plan, three pieces of work were proposed under the common heading of 'Availability':

Availability 1. Paper project – Influence of co-contaminants on the speciation of natural radionuclides at uranium mining sites.

Availability 2. Preliminary characterization and environmental availability assessment at the Observatory Site(s).

Availability 3. Development of a bioavailability model under mixed contaminant conditions.

Availability 1 comprises the production of a paper based on the results presented in D-N°4.1 (Vandenhove et al., 2012b). On the advice of the STAR External Advisory Board (EAB) and since the establishment of an Observatory Site was not done due to the lack of a suitable site, one of these items (Availability 2) was dropped from consideration. Thus this deliverable focuses on the outcomes of Availability 3.

The work mobilised the existing collective experience of the partner institutions in the development (NERC) and application (NERC, SCK•CEN, IRSN) of speciation modelling tools and for experimentation using the test organisms *Lemna minor* (SCK•CEN with assistance from STUK and BfS), *Salmo salar* (NMBU) and *Daphnia magna* (IRSN). Adoption of common approaches to experimental design and data treatment, coupled with exchange of knowledge and expertise among the partners, was intended to drive integration among the STAR partners and to collectively derive datasets and tools that can be viewed in an integrated manner across the tested organisms. Specific activities driving partner integration were:

- The paper project was conducted jointly across SCK•CEN, NERC and IRSN, with each partner applying their selected geochemical modelling tool(s) to a common set of scenarios derived from uranium mining sites, to provide a broad and integrated assessment of the role of co-contaminants on the speciation of radionuclides;
- NERC provided an online training session to familiarise the experimental partners with the underlying theory and practical development of Biotic Ligand Models (BLMs);
- SCK•CEN, in collaboration with STUK and BfS, performed single and mixture exposure experiments with *L. minor*;
- NMBU, in collaboration with NRPA, performed single and mixture exposure experiments with *S. salar*;
- IRSN performed single and mixture exposure experiments with *D. magna*
- NERC developed an updated speciation model (WHAM7) for all partners to use in speciation of exposure media and hence to generate the data required for bioavailability evaluation and BLM development;
- NERC supported all groups in the interpretation of the results and was essential in the development of the BLMs for the different species.

A list of outputs (Papers, conference presentations) of the work is provided in Annex 1.

Note that many of the results presented in this report are preliminary and still unpublished. In some cases, further data analyses, experiments and interpretation may actually change slightly the conclusions given in this document. The definitive conclusion of each series of experiments will be given in the peer-reviewed papers to be submitted.

***The diffusion of this document is Restricted,
only for partners of the [STAR] project, during 2 years.
It will be publically available after 01/07/2017.***

1 Background

Within the overarching goal of STAR Workpackage 4 – to determine whether radiation protection criteria for wildlife are sufficiently robust in a mixed contaminant context – the work described had the aims of (i) testing and improving selected ecotoxicological approaches and tools for reliable radionuclide (bio)availability and exposure assessment under mixed contaminant conditions, (ii) and improve the understanding of underlying mechanisms and processes.

Organism exposure to contaminants, including radionuclides, in the environment almost invariably entails exposure to multiple contaminants. In order to robustly assess the potential risks to organisms of multiple contaminant exposure, there needs to be a good understanding of how co-occurrence of contaminants influences (i) their availability to the organisms and (ii) the resulting exposure and toxic effects. The general issue of multiple contaminant effects has been addressed in many studies (e.g. Van Gestel et al., 2011; Altenburger et al., 2013) yet the inclusion of radionuclides as co-contaminants is uncommon.

The chain of processes involved in controlling contaminant exposure, uptake and effect was described in three categories by Hamelink et al. (1994):

Environmental availability relates to the processes influencing the distribution of chemical form(s) (speciation) of the contaminant in the exposure medium. The variability in said distribution in time and space may have a significant influence on the exposure of organisms to contaminants, for example if particular forms are more amenable to interacting with the organism than others.

Environmental bioavailability relates to the processes influencing the uptake of contaminants from the medium. For example, binding of a contaminant to a receptor site on a cell wall or membrane, as the first stage of uptake, may be subject to competitive inhibition by other contaminant moieties in the medium.

Toxicological bioavailability is concerned with the processes relating the amount of contaminant taken up, to the concentration in tissues that is toxicologically active and thus contributing to effects on the organism. For example, internal sequestration processes may render a portion of the accumulated contaminant into a nontoxic form (e.g. Morgan and Morgan, 1998).

The work described here is focused on the processes controlling exposure to radionuclides (and by extension, the resulting effects) in a mixed contaminant context. Therefore we consider the processes of environmental availability and bioavailability. For familiarity, we will henceforth use the common terms ‘speciation’ and ‘bioavailability’ respectively.

Co-occurrence of contaminants may influence speciation and bioavailability and hence toxicity, for example:

- A metallic contaminant may cause changes in the form (speciation) of other metallic contaminants, by outcompeting them for binding to ligands and causing an increase in the free ionic form of the other contaminants (e.g. Tipping et al., 2002);

- Contaminants may compete with each other for binding to receptor sites on cell walls or membranes (e.g. Winter et al., 2012).

Robust assessment of the impacts of co-contaminant interactions on exposure therefore requires understanding of the interactions among contaminants influencing their speciation and bioavailability. In practice, toxic mixture modelling frequently relates patterns of mixture effects directly to the total exposure concentrations, without explicit consideration of speciation or bioavailability. This makes the understanding of what controls the observed mixture effects challenging, since it could be due to interactions at any of the levels described above. By studying mixture interactions at each stage along of the chain of processes from exposure to effect, the potential exists to quantify interactions at each stage in the chain. This can in principle be used to develop a fundamental understanding of the factors that ultimately control the effects of co-contaminant mixtures, and so move towards *a priori* effect predictions.

As noted in the Foreword, the main objective was to ‘test and improve selected ecotoxicological approaches and tools for reliable radionuclide (bio)availability and exposure assessment under mixed contaminant conditions’. Since exposure and effect are closely linked the work focuses on the chain of processes from speciation in the exposure media, through exposure (accumulation), to effect.

The choice of uranyl and cadmium as the radionuclide and co-contaminant respectively is provided in detail by Vandenhove et al. (2012a). Briefly, uranyl was chosen as the radionuclide as it is a metallic, cationic species whose uptake and toxicity was already known to be influenced by the same water quality parameters as other metals, and was thus considerable the most suitable radionuclide candidate for BLM development. Cadmium was chosen as co-contaminant due to its known occurrence at uranium mining and milling sites and the existing body of knowledge on the factors influencing its bioavailability. This choice had the added advantage of the availability of existing tools for speciation and bioavailability that were either already applicable for selected radionuclides (speciation tools), or were in principle amendable to parameterisation for radionuclides (bioavailability tools). Of the main chemical classes of contaminants, metals have the most extensively developed tools. Since a considerable proportion of radionuclides are metallic in nature, it made sense to focus on these and to apply or develop existing tools for metals for mixtures of radionuclides and non-radioactive metals. The remainder of this section provides a brief review of two such tools/groups of tools: speciation modelling tools, and the Biotic Ligand Model (BLM) as a model of contaminant bioavailability for the prediction of exposure and effect.

1.1 Speciation models

A key aim of our research was to study how co-contaminants influence radionuclide availability to biota by impacting their chemical speciation. Speciation models provide the capability to do this.

A considerable body of work exists demonstrating that the exposure of organisms to potentially toxic chemicals in the environment is not a simple function of the total

concentration of the contaminant in the exposure medium. For metallic contaminants, including many important radionuclide contaminants such as strontium and uranium, research has demonstrated that exposure may be a complex function of the chemistry of the medium. The overall exposure can be considered as a combination of the speciation and bioavailability of the contaminant. In waters, metallic contaminants can occur in a large number of forms, as the free ion (e.g. UO_2^{2+} in the case of U(VI)) or bound to naturally-occurring or anthropogenically-derived ligands. Examples of natural ligands in surface waters are the inorganic anions chloride (Cl^-), sulphate (SO_4^{2-}) and carbonate (CO_3^{2-} , HCO_3^{2-}). Natural organic matter, which is usually dominated by humic substances, is well known to be a significant ligand for many metals (Tipping, 2005). Anthropogenic ligands are typically small organic molecules such as EDTA, NTA.

Research into the bioavailability of metals has clearly demonstrated the need to link organism exposure to their speciation in the exposure medium, and thus considerable research is devoted to measuring metal speciation, particularly to quantify the free ion (Unsworth et al., 2006), which is a key determinant of bioavailability. However speciation methods are complex and potentially subject to poor validation and bias. Application of such methods to radionuclides (e.g. Unsworth et al., 2005), particularly under field conditions, is relatively uncommon. Given these difficulties in speciation measurement, the role of speciation modelling, as a complement and an alternative to measurement, has assumed central importance in studies of speciation and bioavailability.

A speciation model will predict the distribution of a metal among its possible forms at thermodynamic equilibrium, given a sufficiently comprehensive dataset on the chemistry of the medium and a set of binding constants for the possible equilibria occurring in the system. There is a wide selection of models available for use, of varying complexity, such as the Geochemist's Workbench, Visual MINTEQ (<http://vminteq.lwr.kth.se/>), CHESSE (<http://chess.geosciences.enscm.fr/>; Van der Lee, 1998), PHREEQC (http://wwwbrr.cr.usgs.gov/projects/GWC_coupled/phreeqc/) and WHAM7 (<http://www.ceh.ac.uk/products/software/wham/>). Differences among models in their capabilities typically relate to their ability to simulate specific types of reactions beyond conventional solution equilibria, e.g. oxidation-reduction, the precipitation/dissolution of minerals and adsorption of solutes to the surfaces of minerals. Of notable relevance is the capability to simulate the complex, heterogeneous chemistry of humic substances, since these are frequently key ligands for the speciation of metallic contaminants. A number of models have this capability, including Visual MINTEQ and ECOSAT (Keizer and van Riemsdijk, 2009), both of which use the NICA–Donnan model (Kinniburgh et al., 1996), and WHAM7, which uses Humic-Ion Binding Model VII (Tipping et al., 2011).

A database of equilibrium constants is essential for use of a speciation model. A model may incorporate multiple databases, each one providing a specific (though certainly, not necessarily mutually exclusive) set of equilibrium constants. Use of different databases may thus produce quite different predictions of speciation, even if used with the same model. As knowledge of environmentally-relevant equilibria increases, a database may become somewhat obsolete over time, if not reviewed and updated. This is particularly so for the important actinide nuclides (e.g. uranium, thorium) since they exhibit relatively complex

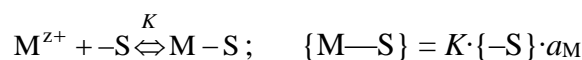
interactions with simple ligands and other species in solution. This can include formation of mixed complexes (complexes with two or more chemically different ligands) or mixed-metal complexes (complexes with another metal and a ligand). Knowledge of the formation and importance of such complexes continues to develop, making the need to keep databases up to date clear. In the case of metallic radionuclides, bodies such as the Nuclear Energy Authority of the OECD periodically collate, review and publish up-to-date collections of equilibrium constants for radionuclides (e.g. Guillaumont et al., 2003).

1.2 Tools for bioavailability

1.2.1 Biotic Ligand Model for single and multiple metals

As noted in Section 1.1, a considerable body of work exists demonstrating that exposure of aquatic organisms to cationic metals is not solely a function of the dissolved metal concentration, but is also a function of the chemistry of the exposure medium. For example, Sinley et al. (1974) showed that zinc was both acutely and chronically less toxic to rainbow trout (*Onchorhynchus mykiss*) in hard water compared to soft water, Howarth and Sprague (1977) showed effects of pH and water hardness on the acute lethality of copper to rainbow trout, and Wildish et al. (1971) demonstrated that humic substances decreased the acute toxicity of zinc and copper to Atlantic salmon (*Salmo salar*) fry and parr. Further work suggested a strong role of complexation of the toxic metal in the exposure medium on toxicity. For example, Zitko et al. (1973) showed that at constant pH and hardness, the potential measured using a copper(II) ion selective electrode was a useful predictor of copper lethality to juvenile Atlantic salmon when the concentration of humic acid, a strong binder of copper, was varied. Since the potential measured by an ion selective electrode is related to the activity of the uncomplexed metal species (the free ion, Cu^{2+}) in the medium, Zitko et al. (1973) suggested a relationship between the activity of the free ion and the toxic effect. This type of finding was further reinforced by a number of studies of metal toxicity in the presence of metal complexing reagents. For example, Allen et al. (1980) exposed the blue-green alga *Microcystis aeruginosa* to zinc in the presence of a number of complexing agents. By using the same exposure medium and a constant concentration of zinc, and by computing the equilibrium zinc free ion concentration from the medium composition, they showed that the toxic effect was related to the zinc free ion concentration. At the same time, investigations on the influence of hardness on toxicity suggested that competition for uptake between the hardness cations (Mg^{2+} , Ca^{2+}) and the metal free ion could explain the trends in toxicity (Zitko and Carson, 1976). Subsequent research has demonstrated similar trends for a wider range of metals, including uranyl (e.g. Charles et al., 2002) and cadmium (e.g. Calamari et al., 1980), the metals used in the work presented here. Such work has led to the development of BLMs for cadmium (e.g. Clifford et al., 2010) and to some bioavailability-based modelling of U toxicity (Alves et al., 2008).

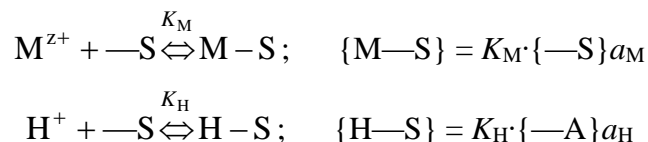
The accumulating body of knowledge on the role of solution complexation of metals in controlling toxicity led Morel (1983) to formulate the free ion activity model (FIAM) of metal–organism interactions. Fundamentally, the FIAM postulates that metal may be taken up by organisms by equilibrium binding of the free ion and/or specific metal complexes to receptors (—S) in or on the cell:



Where M^{Z+} is the free metal ion, a_M is the free ion activity, $-S$ is a receptor not binding metal, $M-S$ is a receptor binding metal and K is an equilibrium binding constant.

The key assumption of the FIAM is that organism response is directly related to the concentration of metal bound to the cell receptors, $\{M-S\}$. The model also assumes that (i) solution complexation of the metal, transport of the binding species to the cell membrane and establishment of the binding equilibrium are all rapid, and (ii) that the cell surface receptor is either itself the site of toxic action, or is a transport site that allows bound metal to pass the cell membrane to the site of toxic action. If the latter is the case then the rate of transport is assumed to be slow relative to the rate of binding at the cell surface. Loss of metal from the binding site across the cell membrane is then compensated by rapid binding of metal from the solution. If the amount of metal taken up by the organism is small relative to the amount of metal in the exposure medium, then the free ion a_M will be approximately constant through the exposure, and if the proportion of cell surface ligands not binding metal ($\{-R_{cell}\}/(\{-R_{cell}\} + \{M-R_{cell}\})$) is large across the range of metal concentrations of interest, then $\{M-R_{cell}\}$ will be approximately proportional to a_M and thus also approximately constant through the exposure.

The FIAM is largely focused on explaining observed relationships between organism response and a_M when the latter is varied by the use of complexing agents but the major chemistry of the exposure medium (e.g. pH, hardness) remains constant. The central assumption of metal binding at cell surface ligands implies the possibility of the competitive binding of other ions (e.g. H^+ , Mg^{2+} , Ca^{2+}), which would reduce metal binding and hence toxic effect. Such competitive binding was invoked by Pagenkopf (1983) to explain the toxicity of copper, zinc, cadmium and lead to fish under varying alkalinity, hardness and pH. Using competition from H^+ as an example, we can write



and derive an expression for the cell ligand sites occupied by M:

$$\{M-S\} = \{S_{total}\} \cdot \frac{K_M a_M}{1 + K_M a_M + K_H a_H}$$

where $\{R_{cell, total}\}$ is the total number of cell surface receptors. Inspection of the expression shows that as a_H increases, $\{M-S\}$ and thus organism response are predicted to decrease. Inclusion of additional competing ions results in additional terms in the denominator, of the form $K_X a_X$ where X is the activity of the competing ion.

This latter expression is the basis of the Biotic Ligand Model (BLM) (Paquin et al., 2002), which allows the toxicity of a cationic metal ($L(E)C_x$ as dissolved metal) to be described and predicted as a function of exposure water chemistry. The BLM has been parameterised for a range of organisms, metals and exposure times (e.g. De Schampelaere and Janssen, 2002;

Peters et al., 2011; Thakali et al., 2006) – largely focusing on acute exposures, but with some application to chronic exposures also (e.g. De Schamphelaere and Janssen, 2004; 2006). In application to standard laboratory toxicity tests, BLMs are largely successful in predicting the variability in point toxicity estimates, e.g. L(E)C50 values, to within a factor of 2–3 of the measured values (e.g. Di Toro et al., 2001). The standard BLM has been extended, for example to allow the binding of metal species besides the free ion (De Schamphelaere et al., 2002; De Schamphelaere and Janssen, 2004) and for multiple receptor types (e.g. Borgmann et al., 2005), yet there is currently no BLM for a radionuclide element.

In multiple metal exposures, the BLM readily allows for the possibility of accounting for the competition among the toxic metals for uptake. To take a simple example of competition among two potentially toxic metals (M_1 and M_2) and the proton at a single biotic ligand, we can write expressions for the amounts of each metal binding:

$$\{M_1 - S\} = \{S_{\text{total}}\} \cdot \frac{K_{M_1} a_{M_1}}{1 + K_{M_1} a_{M_1} + K_H a_H + K_{M_2} a_{M_2}}, \text{ and}$$

$$\{M_2 - S\} = \{S_{\text{total}}\} \cdot \frac{K_{M_2} a_{M_2}}{1 + K_{M_1} a_{M_1} + K_H a_H + K_{M_2} a_{M_2}}.$$

So, if the binding parameters K_{M_1} , K_{M_2} and K_H are known (i.e. by parameterisation on single metal exposures) the BLM-bound concentrations of both metals in a mixture exposure may be computed.

Prediction of mixture effects may be done with reference to either the concentration addition (CA) or independent action (IA) models. Prediction may be done by first fitting dose-response curves for single metal exposures. For a response which has a value zero at zero dose and increases to a maximum under increasing dose (e.g. mortality), the dose-response expressions are

$$Y = Y_{\text{max}} - \frac{Y_{\text{max}}}{1 + \left(\frac{\{M_1 - S\}}{\{M_1 - S\}_{\text{EC50}}} \right)^{\beta_{M_1}}} \text{ and } Y = Y_{\text{max}} - \frac{Y_{\text{max}}}{1 + \left(\frac{\{M_2 - S\}}{\{M_2 - S\}_{\text{EC50}}} \right)^{\beta_{M_2}}}.$$

These expressions can be fitted to obtain values for $\{M_i - S\}_{\text{EC50}}$, the BL occupancy at the 50% effect level, and β_{M_i} , the slope of the dose-response relationship, for each metal acting alone. For the CA approach, the expression for the reference model is then

$$\frac{\{M_1 - S\}}{\{M_1 - S\}_{\text{EC50}} \left(\frac{Y_{\text{mix}}}{Y_{\text{max}} - Y_{\text{mix}}} \right)^{1/\beta_{M_1}}} + \frac{\{M_2 - S\}}{\{M_2 - S\}_{\text{EC50}} \left(\frac{Y_{\text{mix}}}{Y_{\text{max}} - Y_{\text{mix}}} \right)^{1/\beta_{M_2}}} = 1$$

and the predicted mixture effect Y_{mix} is found by iteration. For the IA approach the corresponding expression is

$$Y_{\text{mix}} = Y_{\text{max}} \left(1 - \frac{Y_{\text{max}}}{\left[1 + \left(\frac{\{M_1 - S\}}{\{M_1 - S\}_{\text{EC50}}} \right)^{\beta_{M1}} \right] \cdot \left[1 + \left(\frac{\{M_2 - S\}}{\{M_2 - S\}_{\text{EC50}}} \right)^{\beta_{M2}} \right]} \right)$$

and the predicted mixture effect is directly calculated.

The simple example given above is only of a number of ways in which a multi-metal BLM may be constructed. For example, Santore and Ryan (2015) constructed a multi-site mixture BLM where the number of biotic ligands equals the number of metal in the exposure medium and each metal has a toxicologically-relevant biotic ligand for which its binding induces effects. The other metals may also bind to this ligand, but only as competitors, their binding induces no toxic effect. An alternative approach is the WHAM- F_{TOX} model (Tipping and Lofts, 2015), in which the competitive binding of protons and metals to humic acid is assumed to be a surrogate for their accumulation in metabolically active form in organisms.

Many radionuclides are metallic in nature and so their uptake and toxicity are amenable in principle to modelling with a BLM. The effects of water chemistry on uranium (as uranyl) uptake and toxicity have been the subject of a number of studies (e.g. Charles et al., 2002; Fortin et al., 2007) yet only the study of Alves et al. (2008) has developed a model incorporating competition effects on exposure. The effects of water chemistry on uranyl uptake and toxicity appear to be somewhat more complex than those for other metals (Fortin et al., 2007), which may explain why no concerted effort to develop BLMs for multiple species has yet been done.

1.2.2 Predicting toxic effects of single metals and mixtures from bioaccumulation

A number of researchers have related toxic effects on organisms to concentrations of bioaccumulated metal, both in the field (e.g. De Jonge et al., 2013) and the laboratory (e.g. Alves et al., 2008). Particularly where direct uptake of metals from solution is likely to be the dominant pathway (e.g. in short-term laboratory tests), bioaccumulation should be subject to the same influences of water chemistry as are considered by the BLM. The bioaccumulated metal may therefore correlate well with the actual exposure, integrating the influence of water chemistry on toxicity and providing a more reliable indicator of toxicity than any single measurement of toxicant concentration in the medium. This was seen, for example, by Alves et al. (2008) for U toxicity to *Hyalella azteca* under laboratory conditions.

Some research has also been done into evaluating mixture toxicity based on multitoxicant accumulation data. Norwood et al. (2013) predicted the chronic toxicity of a mixture of eight metals to *H. azteca* on the basis of their background-corrected body burdens and an independent action (effects addition) approach. Such work highlights the potential utility of using accumulated concentrations as an alternative means of assessing mixture toxicity effects.

2 Objectives and tested hypotheses

2.1 Objectives

The detailed experimental plan for the work described here is given by Vandenhove et al. (2012a). The tasks to be done were:

1. Generate experimental data suitable for developing Biotic Ligand Models (BLMs) for uranium(VI) (uranyl) for three aquatic species: *Salmo salar* (fish), *Lemna minor* (plant) and *Daphnia magna* (invertebrate);
2. From the experimental data, develop and parameterise BLMs for the toxicity and/or accumulation of uranyl, acting alone, as a function of exposure chemistry;
3. Generate experimental data on the response (toxicity and/or accumulation) of the organisms to mixtures of uranyl and cadmium;
4. Parameterise a combined uranyl-cadmium BLM to describe toxicity and/or accumulation patterns in the mixture exposures.

A review of existing speciation tools was published as D-N^o4.1 (Vandenhove et al., 2012b). Here, Section 3 summarises only those outcomes of this exercise that were important for the subsequent work. The overall experimental strategy for this work is described in Sections 4.1 and 4.2. Species-specific experimental and analytical approaches are described in Section 4.3.

2.2 Hypotheses

A set of hypotheses was formulated against which to assess the ultimate outcomes of the BLM development work:

- H1: The bioavailability of U(VI) to organisms will exhibit statistically significant variations in response to the exposure medium used;
- H2: The variation in U(VI) bioavailability can be described by organism-specific Biotic Ligand Models (BLMs) that take into account the speciation of U(VI) and competition of binding U(VI) species with major cations;
- H3: Cationic trace metal co-contaminants will influence the bioavailability of U(VI). The magnitude of this influence will be consistent with a BLM-based description of uptake competition.

3 Speciation modelling for BLM development

This Section describes the relevant outcomes of the speciation modelling exercise (Vandenhove et al., 2012a) that influenced the subsequent BLM development. In the speciation exercise we used a set of speciation models and associated databases to assess the potential influence of co-contaminants on U(VI) and thorium speciation at uranium mining sites. A key finding of this exercise, for U(VI), was that the predicted speciation was highly dependent upon the set of complexes that were allowed to form and the values of their

binding constants. Given this fact, during subsequent development of the experimental plan it was decided that a single model/database combination should be chosen for use in the BLM development work. Of the models used, WHAM7 was chosen. This was done because (a) since the model is owned by a participant in the WP (NERC), modifications to the model code could be done if required, and (b) WHAM7 was one of two models of the four tested which could simulate the binding of metals (including uranyl) to natural organic matter. For any future application of developed BLMs to risk assessment in the field the ability to simulate binding to natural organic matter is likely to be important, as it is for metals for which BLMs have previously been developed, such as copper, zinc and cadmium.

Prior to use it was decided to update the database of solution binding constants in WHAM7, as the speciation modelling had shown that a number of uranyl complexes not included in the model database were important for speciation in natural waters. The complexes added to the database were the ternary alkaline earth–carbonate complexes $\text{MgUO}_2(\text{CO}_3)_3^{2-}$, $\text{CaUO}_2(\text{CO}_3)_3^{2-}$, $\text{Ca}_2\text{UO}_2(\text{CO}_3)_3^0$, $\text{SrUO}_2(\text{CO}_3)_3^{2-}$, $\text{BaUO}_2(\text{CO}_3)_3^{2-}$, and $\text{Ba}_2\text{UO}_2(\text{CO}_3)_3^0$ (Dong and Brooks, 2006; Geipel et al., 2008), and the ternary hydroxy–carbonate complexes $(\text{UO}_2)_2(\text{OH})_3\text{CO}_3^-$, $(\text{UO}_2)_3(\text{OH})_3\text{CO}_3^+$ and $(\text{UO}_2)_{11}(\text{OH})_{12}(\text{CO}_3)_6^{2-}$. Furthermore, the model was updated to allow the precipitation of common uranyl minerals to be simulated if required. Code was added to allow the precipitation of minerals of formula $\text{UO}_2(\text{OH})_2(\text{s})$ (e.g. gummite), $\text{UO}_3(\text{s})$ (schoepite), or $\text{CaUO}_4(\text{s})$ (calcium uranate).

4 Development of a bioavailability model under mixed contaminant conditions

4.1 General experimental strategy for uranium BLM development

Development of a BLM, incorporating knowledge of the competitive effect of individual medium components on the accumulation and/or toxicity of the chemical under study, entails systematic generation of data showing the response of the organism to the chemical in the presence of varying concentrations of those medium components considered likely to exert competitive effects. An established method of accomplishing this is to generate dose–(accumulation and/or response) curves for the organism in series of media where the concentration of one potentially competing component is systematically varied through an environmentally relevant range, while keeping the concentrations of the other potentially competing components constant. De Schamphelaere and Janssen (2002) present such an approach for studying the acute toxicity of copper to *Daphnia magna*. Knowledge gained from past studies on metals strongly suggests that the medium components most likely to exert competitive effects are the proton (H^+) and the major ions sodium (Na^+), magnesium (Mg^{2+}), potassium (K^+) and calcium (Ca^{2+}). Therefore, this list of competing ions was considered for inclusion.

4.2 General modelling strategy for BLM development

Past modelling strategies for BLM development have focused either on modelling the variability across media of the observed endpoint concentrations (e.g. LC50s) (e.g. De

Schamphelaere and Janssen, 2002) or the whole dose–response relationship (e.g. Peters et al., 2011). Here we take the latter approach. This is largely because we wished to model the variability in response in the mixture exposures, which would not have been possible with an approach based on effect prediction only. Furthermore, since we wished where possible to initial model the variability in accumulation before developing the models for toxicity, modelling the whole accumulation–response relationship across doses and media was required.

The general steps in BLM development to model toxicity are then:

1. For each individual exposure, calculate the chemical speciation of the system to obtain the activities of free uranyl, UO_2^{2+} , and its complexes, and of the major competing ions (e.g. H^+ , Na^+ , Mg^{2+} , K^+ , Ca^{2+}).
2. Construct an initial BLM allowing for binding parameters for U(VI) and the major competing ions, and a density of binding sites.
3. Fix the fractional occupancy of the biotic ligand that will cause a 50% effect level. In the absence of information on the total number of binding sites, this parameter must be fixed since it is not independent of the U(VI) binding strength. A fractional occupancy of 0.1 is reasonable.
4. Link the fractional occupancy of the biotic ligand to effect using a standard dose–response curve, e.g.

$$R = \frac{R_0}{1 + \left(\frac{f_{\text{UO}_2\text{BL}}}{f_{\text{UO}_2\text{BL},L(E)C50}} \right)^\beta}$$

where R is the predicted response, R_0 is the control response for the medium in question, $f_{\text{UO}_2\text{BL}}$ is the modelled fractional occupancy of the biotic ligand, $f_{\text{UO}_2\text{BL}}$ is the fractional occupancy for a 50% response and β is the slope of the dose–response curve.

5. Fit the binding constants for U(VI) and the significant competing ions using a stepwise approach. Firstly a BLM where only free uranyl (UO_2^{2+}) can bind to the biotic ligand is fitted, to act as a null model for statistical comparison. Then derive binding constants for each competing ion in turn, initially by fitting allowing the binding of UO_2^{2+} and one competing ion. The statistical significance of adding a competing ion to the model is assessed by χ^2 testing (e.g. Jonker et al., 2005). After each round of testing competing ions, the ion providing the most statistically significant ($p < 0.05$) improvement to the model fit is retained in the model and further testing of each remaining competing ion is done. The procedure is continued until statistically significant binding constants for all the competing ions are fitted, or no further statistically significant improvement to the fit can be achieved.

In practice, to obtain an optimal fit it may be necessary to perform several iterations of the above steps, adjusting the structure of the model. For example, it has been shown previously that optimal fitting may require invoking the binding of multiple solution species to the biotic

ligand. This was shown by De Schampelaere and Janssen (2004) for the chronic toxicity of copper to *D. magna*, for which optimal fitting of the BLM required the binding of the CuOH^+ and CuCO_3^0 species as well as the free ion Cu^{2+} . Some workers have also invoked more complex binding structures to explain observations, such as multiple proton binding (Alves et al., 2008) or multiple binding sites (Peters et al., 2011) to explain observed trends in toxicity and/or accumulation.

4.3 Experimental approaches for specific organisms

4.3.1 *Salmo salar*

In total about 1200 Atlantic salmon juvenile parr were exposed (96h) to commercially available depleted uranium (DU) in controlled experiments conducted in accordance with the OECD guidelines 203 for acute toxicity tests (OECD, 1992) and the Norwegian Welfare Act and research animal legislation. The experiment was approved in advance by the Norwegian Animal Research Authority (NARA ID: 4615). Atlantic salmon was used based on its economic importance as a valuable food source and its sensitivity to water pollutants.

Speciation, uptake and induced toxicity of U as a function of varying water concentrations of H^+ , Ca^{2+} , Mg^{2+} , Na^+ and K^+ as well as U were studied at 9°C based on US EPA very soft water (US EPA, 2002). The concentration ranges of the different ions (i.e. H^+ , K^+ , Na^+ , Mg^{2+} and Ca^{2+}) were selected to be within an environmentally relevant range, as well as a range that is sufficient for optimal survival and growth of this freshwater life stage. The impact of H^+ , Ca^{2+} , Mg^{2+} , Na^+ and K^+ were studied systematically according to the media compositions (Table 1).

Table 1. Nominal concentrations (mM) of major cations and anions in the US EPA very soft water (“reference water”) and in the modified water qualities included in the test.

Group	pH	Ca ²⁺	Mg ²⁺	Na ⁺	K ⁺	CO ₃ ²⁻ ^a	SO ₄ ²⁻	Cl ⁻
Ref. water	6.7	0.044	0.062	0.14	0.078	0.14	0.11	0.0068
pH 5.2	~5.2-5.3	0.044	0.062	1.43	0.078	0.14	0.11	1.61–1.64
pH 5.7	~5.5-5.8	0.044	0.062	1.43	0.078	0.14	0.11	1.52–1.64
pH 6.0	~6.0	0.044	0.062	1.43	0.078	0.14	0.11	1.50–1.61
pH 7.2	~7.2	0.044	0.062	1.43	0.078	0.14	0.11	1.21
pH 7.9	~7.9	0.044	0.062	1.43	0.078	0.14	0.11	0.0412
Low Ca	6.7	0.022	0.062	0.14	0.078	0.14	0.087	0.0068
Medium Ca	6.7	0.087	0.062	0.14	0.078	0.14	0.11	0.094
High Ca	6.7	3.49	0.062	0.14	0.078	0.14	0.11	6.91
Low Mg	6.7	0.044	0.016	0.14	0.078	0.14	0.059	0.0068
High Mg	6.7	0.044	2.47	0.14	0.078	0.14	0.11	4.82
Medium Na	6.7	0.044	0.062	1.43	0.078	0.14	0.11	1.30
High Na	6.7	0.044	0.062	4.57	0.078	0.14	0.11	4.43
Low K	6.7	0.044	0.062	0.14	0.078	0.14	0.11	0.0034
High K	6.7	0.044	0.062	0.14	0.078	0.14	0.11	0.54

^a Nominal carbonate concentration, based on concentration in salts used to make water. Measured alkalinity was used in speciation calculations.

Uranium was added to experimental water units 48 hrs before the introduction of fish. Uranium was added from a stock solution (2.5 g U/L) prepared by dissolving uranyl nitrate hexahydrate (UO₂(NO₃)₂ x 6 H₂O) in Type 2 water (resistivity < 1 MΩ-cm). A series of U concentrations (0.5, 1, 2, 3 and 4 mg U/L; 2.1, 4.2, 8.4, 12.6, 16.8 μM) were selected to be used in the BLM experiments. In some dose-response tests, however, the concentration range was extended up to 100.8 μM (24 mg U/L). Each test unit consist of seven fishes exposed simultaneously to one batch of water, in a static setup.

The combined effect of U and Cd was studied in US EPA very soft water at pH 6.7. Cd was added to experimental units from stock solutions (3.5 mg Cd/L; 31.1 μM) prepared by dissolving CdCl₂ in Type 2 water. The experimental design for the combined exposures (Figure 1) comprised a series of dose–response curves for U with nominal dissolved U ranging from 0–20 μM, and fixed nominal dissolved Cd ranging from 0–0.01 μM.

A range of water quality parameters such as O₂, CO₂, NH₄, temperature were measured before and after exposure to ensure that the general water quality was within normal range for fish. In addition pH, conductivity, alkalinity, major cations and major anions were determined. pH

was measured daily and adjusted with 1 M HCl or NaOH to keep within ± 0.1 pH unit of the nominal value. To obtain information on the molecular mass of U and Cd in the water, fractionations with respect to size (0.45 μm membrane filtration and 10 kDa ultrafiltration) were performed according to Popic et al. (2011).

Mortality was recorded daily. In addition, blood samples were collected in surviving fish at the experimental period, using syringe and analysed for general stress parameters using i-STAT with EC8+ cartage prior to fish dissection. Collection of different tissues such as gills, liver and kidney were performed according to protocol (Rosseland et al. 2002). Fish tissues were freeze-dried and digested (10 % HNO_3) using an ultraclave (Mile-stone, Leutkirch, Germany). U and Cd concentration in water fractions and in digested tissues were determined using inductively coupled plasma mass spectrometry (8800 ICP-MS Triple Quad, Agilent Technologies). Concentration of Cd and U in tissues is presented as $\mu\text{g/g}$ dry weight.

Dose response curves for mortality were modelled using a log-logistic model in the drc add-on package in R, and lethal concentrations (i.e. LC50) and their standard errors were calculated for the different water qualities.

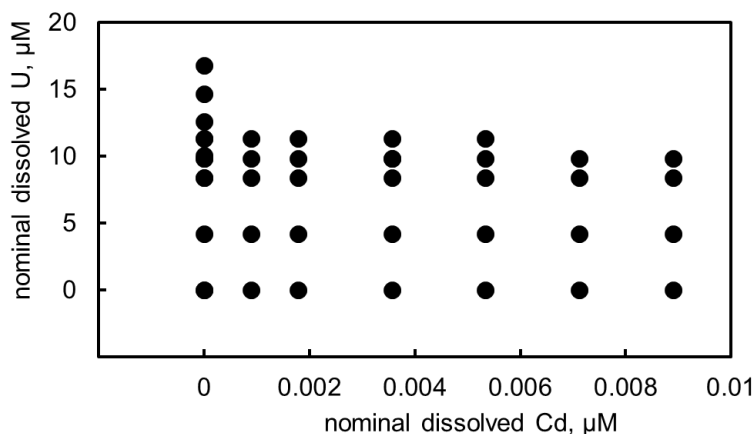


Figure 1. Design of *S. salar* U–Cd mixture experiment.

4.3.2 *Lemna minor*

To obtain experimental data to set up uranium BLM for *L. minor* a seven-day growth inhibition test was performed for a range of U concentrations to acquire full Dose Response Curves (DRC) in different exposure media, in which the concentration of competing cations (Ca^{2+} , Mg^{2+} , Na^+ , K^+ and H^+) are varied one by one. For the implementation of the U(VI)-Cd BLM, the seven-day growth inhibition test was performed in a basic medium in which only the concentrations of U and Cd were varied.

The stock culture of *Lemna minor* cv. Blarney was obtained from Dr. M. Jansen (University College Cork, Ireland) and cultured aseptically in 250 mL glass erlenmeyers containing half-strength Hütner medium (Brain and Solomon, 2007) under continuous light (Osram 400W HQI-BT daylight, 80-100 $\mu\text{mol/m}^2\cdot\text{s}$) at 24°C. Plants were sub-cultured every 10-12 days by transferring three plants to 100 mL of fresh growth medium. Exposure of *L. minor* to the

combination of U and Cd was essentially performed as described in Horemans et al. (2015) following the OECD guidelines for a *Lemna* growth inhibition test (OECD 2006) using as a test medium K-medium (Cedergreen et al. 2007) with phosphate concentrations lowered to 0.5 mg/L. To stabilise pH during toxicity tests, 5 mM filter-sterilised (0.22 µm) MES (2-(N-morpholino)ethanesulfonic acid) was added. For the experiments three plants (between 9 to 12 fronds) were aseptically transferred to polycarbonate-pots containing 100 mL of the modified K-medium. A 1 cm, surface-sterilised floating ruler was added for calibration of images. Pots were covered with a 9 cm plastic petridish and experiments were run for 7 days under the same light and temperature conditions as used for normal plant culture. To set up the single DRCs uranium was administered to the media with varying ion/proton concentrations as a filter-sterilised solutions of $\text{UO}_2(\text{NO}_3)_2 \cdot 6\text{H}_2\text{O}$ (SPI chemicals, USA dissolved in 100 mM HCl) in a final concentration ranging from 0-150 µM for U. Six replicas were used for control conditions and at least three for each of the U concentration applied. To evaluate *Lemna* growth, pictures were taken every 2 days and the frond number and frond area was determined by picture analysis (ImageJ software). After 7 days fresh and dry weight of the plants was measured. At the end of the growth inhibition test pH and conductivity of the medium was measured. Samples for U analysis were taken at the beginning and end of the growth inhibition test at the level of the roots of the *Lemna* plants (half way the pot). Samples were subsequently acidified and analysed for the presence of U or Cd using ICP-MS (Perkin-Elmer, elan 500). The plants were harvested per pot and after dry-weight was determined, further ashed and the U concentration was determined in the plants. As plant material was limited and exposure to higher metal concentrations resulted in fragile, damaged or dead plants this procedure could only be done for plants treated with up to 25 µM of U.

The single dose response curves were set up for five different pH levels ranging from 4.0-8.0 and different cation levels (five Ca-levels ranging from: 0.4-60 mM, three K-levels from 0.88-69 mM, three Na-levels and three Mg-levels both ranging from 0.02 to 4 mM). Normal cation levels were: pH 5.0, Ca 4 mM, K 8.9 mM, Na 0.02 mM and Mg 0.4 mM. For all cations except Na at least one concentration was chosen below the normal nutrient medium composition the others above. Samples for determination of cation concentrations in the medium and plants were taken identically as described above for U and were measured with ICP-MS. Measured concentrations of major cations are given in Table 2.

The mixture experiment followed a classical ray design based on U and Cd being present in 0U:1Cd, 1/3U:2/3Cd, 1/2U:1/2Cd, 2/3U:1/3Cd or 1U:0Cd ratio's (Figure 2), based on their respective IC50s. The concentration ranges were chosen based on initial single metal dose response experiments. U and Cd were administered to the plants as a filter sterilised solution of $\text{UO}_2(\text{NO}_3)_2 \cdot 6\text{H}_2\text{O}$ or CdCl_2 , respectively in a concentration range varying from 0 to 200 µM. Prior to addition of the plants the pH was readjusted by addition of filter sterilised NaOH. Cd concentrations were measured in medium and plants as described above for U determination.

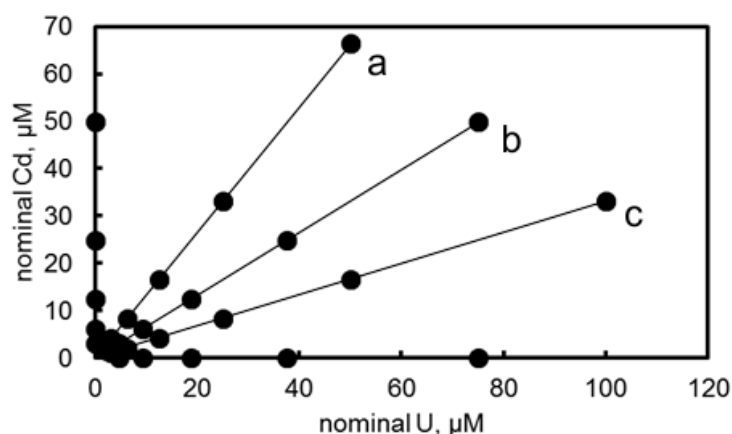


Figure 2. Mixture design for *L. minor* combined U-Cd exposures. The exposure series a,b, and c are connected by lines for information.

Table 2. Concentrations (mM) of major cations in the modified K–medium used for *L. minor* testing. Values given are ranges of measured concentrations with the exception of the potassium exposure exposures series LK, NK and HK for which nominal concentrations are given.

Exposure series	Na ⁺	Mg ²⁺	K ⁺	Ca ²⁺
p4	0.3-1.4	0.7-2.4	3.1-10.4	1.3-4.5
p6	0.2-0.9	0.7-2.4	2.9-10.4	1.2-4.4
p7	0.3-0.5	2.1-2.3	9.2-10.0	3.9-4.3
p8	0.1-2.4	2.1-2.2	9.2-9.7	3.9-4.1
LNa	0.05-0.16	2.1-2.2	9.5-10.1	3.9-4.1
NNa	0.4-0.5	2.1-2.2	9.7-10.1	3.9-4.1
HNa	3.7-4.2	2.1-2.2	9.5-10.1	3.9-4.1
LMg	0.4-0.6	0.2-0.3	13.1-13.6	3.9-4.0
NMg	0.4-0.7	2.0-2.2	8.8-9.3	3.8-4.1
HMg	0.5-0.9	21.4-21.9	9.2-9.5	4.1-4.5
LK	(0.02)	(0.40)	(0.88)	(4.0)
NK	(0.02)	(0.40)	(8.8)	(4.0)
HK	(0.02)	(0.40)	(68.8)	(4.0)
LCa	0.5-0.8	1.8-2.4	17.0-18.9	0.3-0.5
C20	0.4-0.8	2.2-2.3	9.2-9.9	18.6-25.0
C25	0.4-0.9	2.2-2.3	9.2-9.8	12.2-27.6
C40	0.6-0.9	2.1-2.2	9.1-9.5	39.8-44.6

4.3.3 *Daphnia magna*

The experimental plan for the implementation of the uranium BLM consists of the performance of acute toxicity tests and acquisition of full DRCs in different exposure media, in which the concentration of competing cations (Ca²⁺, Mg²⁺, Na⁺, K⁺ and H⁺) are varied one

by one. For the implementation on the U-Cd BLM, acute toxicity tests were performed in basic medium in which only the concentrations of U and Cd were varied.

Acute toxicity tests

Acute toxicity of U to *D. magna* was evaluated through a 48h-immobilisation assay performed on juvenile *D. magna* (< 24h old) from the fourth brood following the OECD test guideline. The test organisms originated from *D. magna* cultures maintained in continuous parthenogenic reproduction in M4 medium modified to maintain a pH of 7. The composition of the M4-pH7 medium as well as culture conditions are detailed in Zeman et al. (2008). For each tests, 10 groups of 5 animals were exposed in polycarbonate tubes containing 10 mL medium, without renewal. After 48 h exposure, the number of surviving animals in each tube was counted, considering that animals without response to gentle agitation after 15 s were dead. Four replicate exposures were carried out at each U concentration.

Dose response curves for mortality were modeled using a log-logistic model in the drc add-on package in R, and EC50s and its standard errors were calculated.

Test solutions for the U-BLM

The basic medium for all experiments was composed of $[Ca^{2+}] = 0.05$ mM, $[Mg^{2+}] = 0.05$ mM, $[K^+] = 0.078$ mM, $[Na^+] = 0.14$ mM and pH 7. From this medium, five series of acute toxicity tests were performed: Ca-series, Mg-series, Na-series, K-series and pH-series, where concentrations of Ca, Mg, Na, K and pH were varied to cover a range of concentration in which competition with U may appear. All series comprised from three to seven toxicity tests (Table 3). For each series, 10 to 12 different concentrations of U were tested to obtain a full DRC.

All test solutions were prepared by adding different volumes of stock solution of $CaCl_2$, $MgSO_4$, NaCl, KCl and $NaHCO_3$. All U solutions were prepared from a 1 g/l stock solution of uranyl nitrate hexahydrate in 0.2% HNO_3 , except for the experiments at pH 7.5 and 8 where stock solutions with higher concentration of U were used. In all solutions, pH was adjusted by adding $NaHCO_3$ and equilibrating them with the atmosphere (stirred vigorously for at least 12 h) prior to the addition of U.

Test solutions for the U-Cd BLM

The basic medium for the mixture experiments was composed of $[Ca^{2+}] = 0.05$ mM, $[Mg^{2+}] = 0.05$ mM, $[K^+] = 0.078$ mM, $[Na^+] = 1.4$ mM and pH 7. All test solutions were prepared as described above. Cd was prepared from a stock solution of $CdCl_2$.

Acute toxicity tests were performed the same day on U alone, Cd alone and U-Cd in mixture. Two different experimental design were used (Figure 5). In series a, the Cd concentration was kept constant all along the exposure to U at 1.08 μ M, corresponding to the EC₂₀ of Cd alone. In series b, the ratio of U to Cd was kept constant all along the exposure.

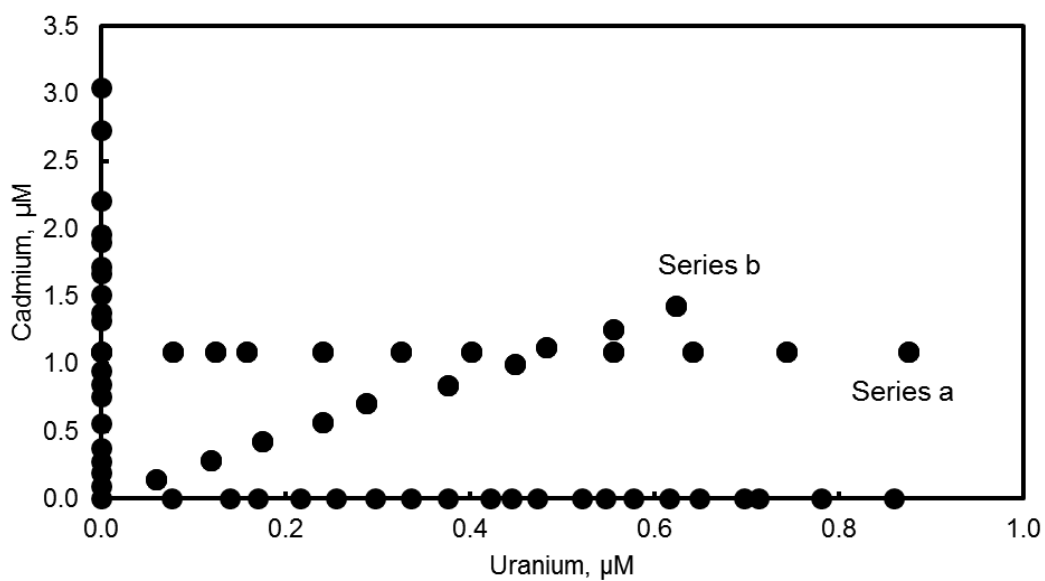


Figure 3. Mixture design for *D. magna* mixture U-Cd exposures, comprising two series of exposures: a and b.

Table 3 Chemical characteristics (pH and nominal concentrations (mM)) of the test solutions in the acute toxicity tests with *D. magna*.

Exposure series	pH	Na ⁺	Mg ²⁺	K ⁺	Ca ²⁺
Ca 0.05	6.85	0.14	0.10	0.078	0.05
Ca 0.1	6.9	0.14	0.10	0.078	0.1
Ca 0.2	6.85	0.14	0.10	0.078	0.2
Ca 0.4	6.85	0.14	0.10	0.078	0.4
Ca 0.8	6.85	0.14	0.10	0.078	0.8
Ca 1.6	6.65	0.14	0.10	0.078	1.6
Ca 3.2	6.65	0.14	0.10	0.078	3.2
Mg 0.05	6.85	0.14	0.05	0.078	0.05
Mg 0.1	6.85	0.14	0.1	0.078	0.05
Mg 0.2	6.85	0.14	0.2	0.078	0.05
Mg 0.4	6.85	0.14	0.4	0.078	0.05
Mg 0.8	6.85	0.14	0.8	0.078	0.05
Mg 1.6	6.85	0.14	1.6	0.078	0.05
Mg 3.2	6.85	0.14	3.2	0.078	0.05
Na 0.14	6.85	0.14	0.05	0.078	0.05
Na 0.3	6.9	0.30	0.05	0.078	0.05
Na 0.6	6.8	0.60	0.05	0.078	0.05
Na 1.4	6.85	1.4	0.05	0.078	0.05
Na 2.8	6.9	2.8	0.05	0.078	0.05
Na 5.6	6.85	5.6	0.05	0.078	0.05
K 0.078	7	0.14	0.05	0.078	0.05
K 1	7	0.14	0.05	1	0.05
K 2	7	0.14	0.05	2	0.05
pH 6	6	1.4	0.05	0.078	0.05
pH 6.5	6.5	1.4	0.05	0.078	0.05
pH 6.85	6.85	1.4	0.05	0.078	0.05
pH 7.5	7.5	1.4	0.05	0.078	0.05
pH 8	8	1.4	0.05	0.078	0.05
Cd_2807 ^a	7.05	1.4	0.05	0.078	0.05
Cd_09 ^a	7.05	1.4	0.05	0.078	0.05
U50_Cd50 ^b	6.9	1.4	0.05	0.078	0.05
U_Cd_040814 ^b	6.95	1.4	0.05	0.078	0.05

^a Cadmium only exposures

^b mixture exposures

Chemical measurements

U, Ca, Mg, Na, K and Cd concentrations were measured in both filtered (< 0.45 µm) or unfiltered samples at the start and at the end of the test with ICP-AES or ICP-MS depending

of the concentration ranges. Samples were acidified with ultra-pure HNO₃ prior to measurements.

pH was measured at the beginning of the test, before and after addition of U to the tests solution. The pH after the tests was checked on some samples only.

4.4 Results

4.4.1 Observed U accumulation: *Lemna minor* and *Salmo salar*

Accumulation of U in *L. minor* is summarised in Figure 4 according to exposure series. The clearest influence of exposure medium chemical composition on accumulation is seen in the pH series, where the accumulation in the p8 series (pH~8) is consistently 1–2 orders of magnitude lower than the accumulation in the other pH series. There is no clear trend in accumulation across the remaining pH series. This may be due to shifts in pH during testing, which resulted in overlapping pH ranges; the final pH ranges for series p4, p5, p6 and p7 were 4.2-5.0, 3.8-5.3, 4.6-6.1 and 6.6-7.3 respectively.

The influence of the medium chemical composition in the remaining series was less clear. Nonetheless, in the Ca series there is a clear trend for lower accumulation as the medium Ca concentration is increased. In both the Mg and Na series no clear trend can be seen.

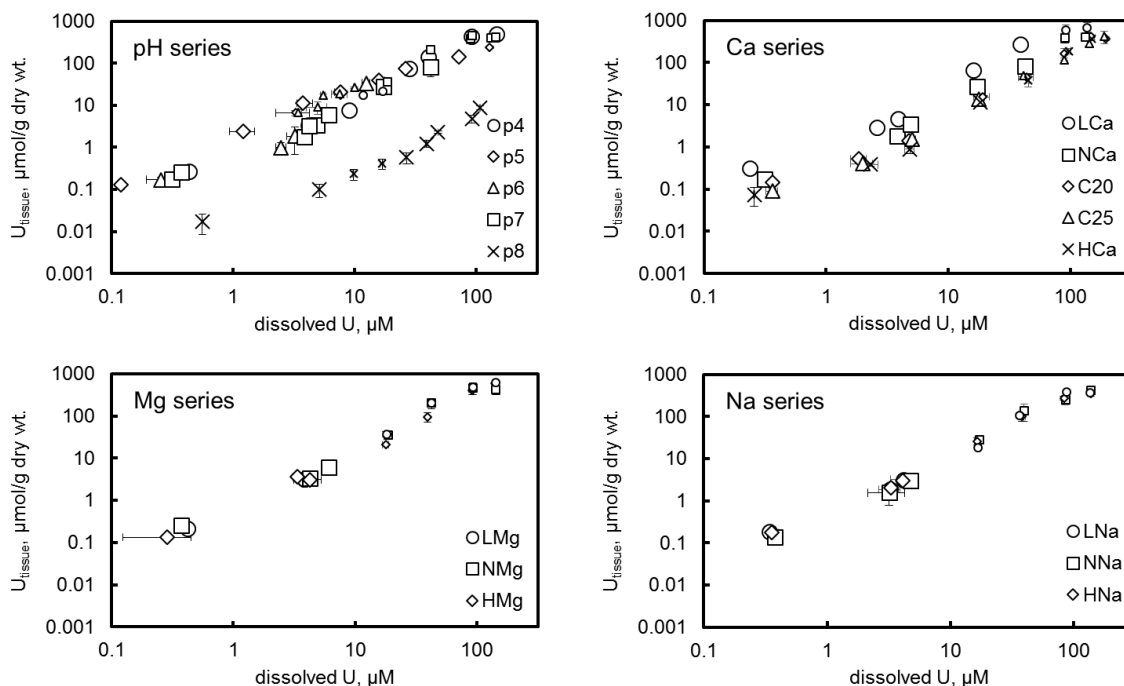


Figure 4. Relationship between U in solution and accumulated U for *L. minor* in seven-day chronic exposures, for the pH, Ca, Mg and Na series. Large points represent measurements on washed plants, small points represent exposures on unwashed plants. Values are means of up to three replicates, errors represent ± 1 SD.

Accumulation of U in *S. salar* gill tissue in U(VI)-only exposures is summarised in Figure 5. Accumulation of U in the gills under conditions of varying major ion (Na, Mg, Ca, K) but over a small pH range showed no clear influence of variations in exposure conditions on uptake (Figure 5) relative to the dissolved U concentration in the medium. In contrast, changing the exposure pH caused considerable variability in uptake. As the medium pH was increased from ~5.2 to ~7.9, the bioaccumulation factors (accumulated U/dissolved U, l/g dry wt.) decreased considerably; for example, on decreasing pH from 7.9 to 6.7, mean accumulation in response to dissolved U in the range 4.2–4.3 μM increased from 0.014 to 0.074 $\mu\text{mol/g}$ dry wt., i.e. by over five-fold. At pH 5.2 and in response to a slightly lower concentration of dissolved U (3.85 μM), accumulated U was even higher, with a mean of 1.38 $\mu\text{mol/g}$ dry wt..

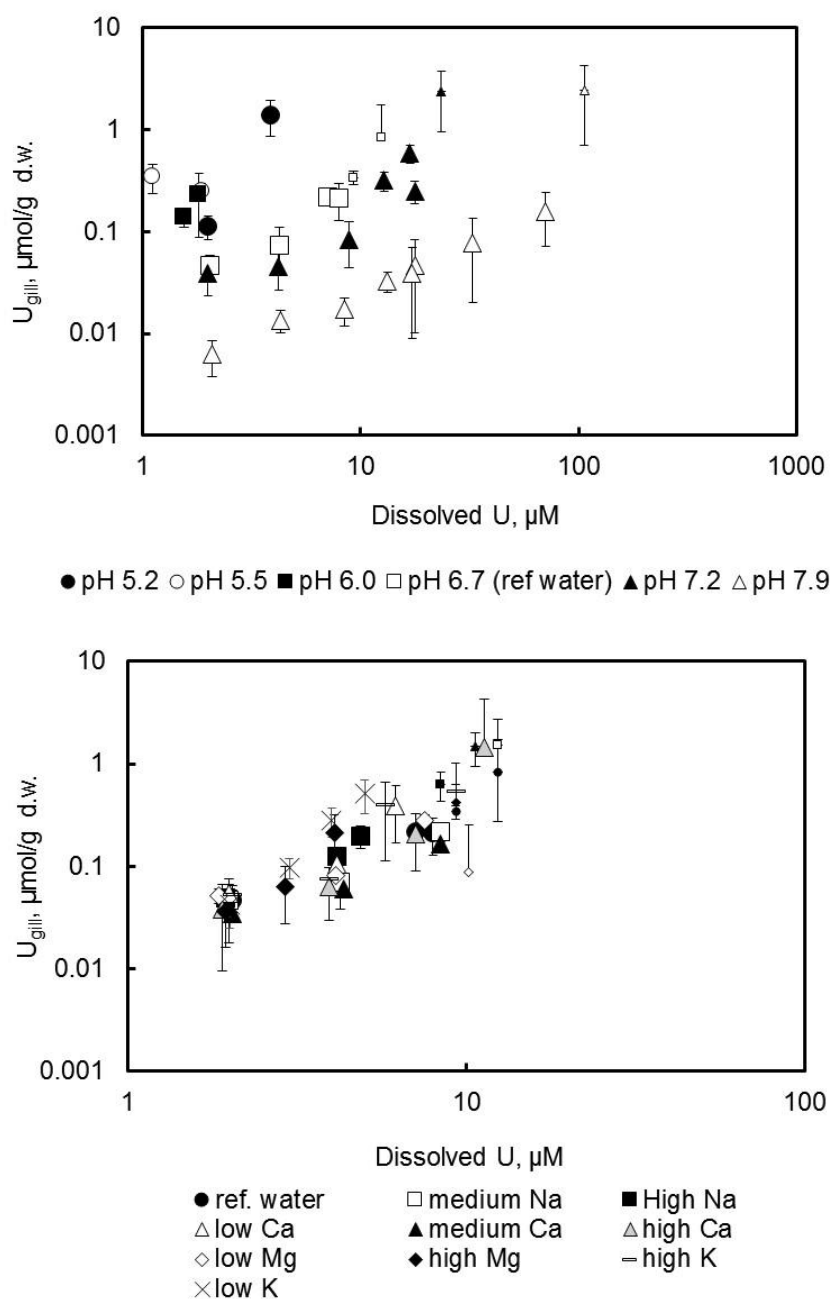


Figure 5. Relationship between U in solution and gill-accumulated U for *S. salar* in 96h acute exposures. Large points represent exposures with no mortality, small points represent exposures with partial mortality. Values are means of up to seven replicates, error bars represent ± 1 standard deviation.

For salmon, a trend to increasing bioaccumulation factor with increasing U exposure can be seen in the accumulation patterns of the pH 6.7 (ref. water), pH7.2 and pH7.9 exposures (Figure 5). This was most pronounced in the pH7.9 exposure, where in the dissolved U range from 2.08 μM to 70.8 μM the bioaccumulation factor was almost constant within the range

0.002–0.003 l/g dry wt., then abruptly increased to 0.023 l/g dry wt. when exposure increased to 106 μM U.

Liver concentrations of U in pH exposure series are shown in Figure 6. Liver and gill accumulation of U were significantly correlated (Pearson correlation coefficient 0.92, $p < 0.001$). The mean liver:gill U ratio was 0.061, which dropped to 0.014 when all control exposures were excluded.

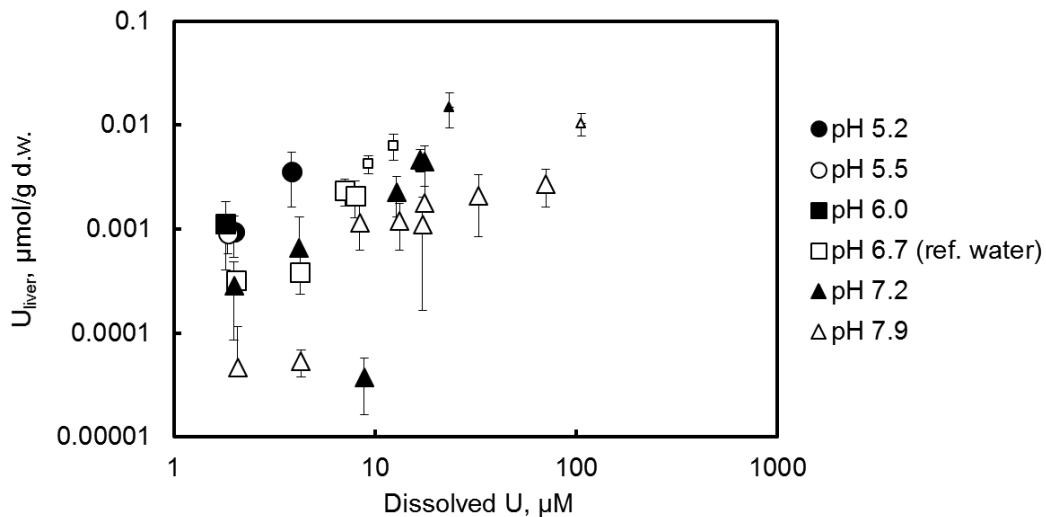


Figure 6. Relationship between U in solution and liver–accumulated U for *S. salar* in 96h acute exposures. Data are for all exposures with varying nominal pH. Large points represent exposures with no mortality, small point represent exposures with partial mortality. Values are means of up to seven replicates, error bars represent ± 1 standard deviation.

4.4.2 *U* accumulation modelling: *Lemna minor* and *Salmo salar*

Gill accumulation of U on *S. salar* was modelled using only data for those exposures where no mortality was observed.

To provide a coherent picture of accumulation across U doses and water compositions, we calculated for each exposure the ratio of accumulated U (mol/g dry weight tissue) to the UO_2^{2+} activity (mol/l) computed from the exposure medium composition using WHAM7. This ratio, which we denote Θ , provides an indication of the local “binding strength” of the tissue for U.

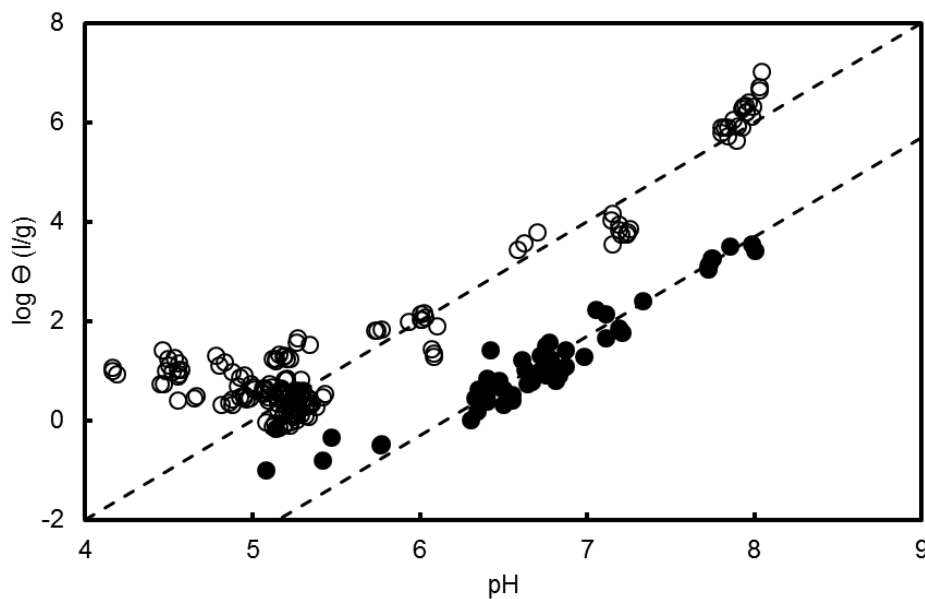


Figure 7. Plot of Θ against pH for exposures of *L. minor* (open symbols) and *S. salar* (closed symbols). Accumulation is to whole tissue for *L. minor* and to the gill for *S. salar*. The dashed lines have slopes of two and are for guidance to illustrate the Θ –pH trend.

Figure 7 plots $\log \Theta$ for *L. minor* and *S. salar* tissue accumulation against the exposure medium pH. The plot shows that a line with a slope of two follows the trend between $\log \Theta$ and pH well down to pH ~5 (*L. minor*) and pH ~6 (*S. salar*). Below these pHs the trends in $\log \Theta$ versus pH are weak.

4.4.3 *Modelling: one-site model*

Initially, we explored the modelling of the trends in Figure 7 using a single site BLM with the reactions



which results in this expression for the accumulated U, $\{\text{UO}_2\text{-S}\}$ (mol/g dry wt.):

$$\{\text{UO}_2\text{-S}\} = \{\text{S}\} \cdot f_{\text{S,UO}_2}; \quad f_{\text{S,UO}_2} = \frac{K_{\text{UO}_2} a_{\text{UO}_2^{2+}}}{1 + K_{\text{UO}_2} a_{\text{UO}_2^{2+}} + K_{\text{H}} a_{\text{H}^+}}$$

where $f_{\text{S,UO}_2}$ is the fractional occupancy of sites by U, and $a_{\text{UO}_2^{2+}}$ and a_{H^+} are the solution activities of UO_2^{2+} and H^+ , respectively. The parameters requiring fitting are $\{\text{S}\}$, the total concentration of binding sites, and the binding constants K_{UO_2} and K_{H} . However, fitting this model showed that it closely reproduced the variability in Θ with pH only when the total site density was such $\{\text{UO}_2\text{-S}\} \sim \{\text{S}\}$ except above pH7.5 – thus it could not satisfactorily reproduce the trends in accumulation. In order to make fitting using a single site feasible, it was clearly necessary to relax the assumption that only the free UO_2^{2+} ion could bind to the

biotic ligand. Therefore, we allowed the possibility that the U(VI) species UO_2OH^+ , $\text{UO}_2(\text{OH})_2$ and UO_2CO_3 could also bind to the biotic ligand. Since the model was intended to describe the variations in U(VI) uptake across all the studied variations in exposure medium chemistry, we also allowed the binding of Na^+ , Mg^{2+} , K^+ and Ca^{2+} to the biotic ligand.

Table 4. Outcome of stepwise fitting of binding constants, single site accumulation BLM for *L. minor*. At each stage the bolded row shows the model providing the most significant improvement over the previous best fit. ** = $p < 0.01$, * = $p < 0.001$, n.s. = not significant.**

Binding ion(s)	SOS in log(tissue U, $\mu\text{mol/g d.w.}$)	Significance
UO_2^{2+}	637.0	–
Two binding ions		
UO_2^{2+} UO_2OH^+	188.0	***
UO_2^{2+} $\text{UO}_2(\text{OH})_2/\text{UO}_2\text{CO}_3$	37.9	***
UO_2^{2+} H^+	188.0	***
UO_2^{2+} Na^+	637.0	n.s.
UO_2^{2+} Mg^{2+}	632.2	n.s.
UO_2^{2+} K^+	636.3	n.s.
UO_2^{2+} Ca^{2+}	601.0	**
Outcome: test $\text{UO}_2^{2+} + \text{UO}_2(\text{OH})_2/\text{UO}_2\text{CO}_3 + \text{one other.}$		
Three binding ions		
UO_2^{2+} $\text{UO}_2(\text{OH})_2/\text{UO}_2\text{CO}_3$ UO_2OH^+	37.9	n.s.
UO_2^{2+} $\text{UO}_2(\text{OH})_2/\text{UO}_2\text{CO}_3$ H^+	37.9	n.s.
UO_2^{2+} $\text{UO}_2(\text{OH})_2/\text{UO}_2\text{CO}_3$ Na^+	37.9	n.s.
UO_2^{2+} $\text{UO}_2(\text{OH})_2/\text{UO}_2\text{CO}_3$ Mg^{2+}	37.6	n.s.
UO_2^{2+} $\text{UO}_2(\text{OH})_2/\text{UO}_2\text{CO}_3$ K^+	37.9	n.s.
UO_2^{2+} $\text{UO}_2(\text{OH})_2/\text{UO}_2\text{CO}_3$ Ca^{2+}	26.9	***
Outcome: test $\text{UO}_2^{2+} + \text{UO}_2(\text{OH})_2/\text{UO}_2\text{CO}_3 + \text{Ca}^{2+} + \text{one other.}$		
Four binding species		
UO_2^{2+} $\text{UO}_2(\text{OH})_2/\text{UO}_2\text{CO}_3$ Ca^{2+} UO_2OH^+	26.9	n.s.
UO_2^{2+} $\text{UO}_2(\text{OH})_2/\text{UO}_2\text{CO}_3$ Ca^{2+} H^+	26.9	n.s.
UO_2^{2+} $\text{UO}_2(\text{OH})_2/\text{UO}_2\text{CO}_3$ Ca^{2+} Na^+	26.9	n.s.
UO_2^{2+} $\text{UO}_2(\text{OH})_2/\text{UO}_2\text{CO}_3$ Ca^{2+} Mg^{2+}	25.8	**
UO_2^{2+} $\text{UO}_2(\text{OH})_2/\text{UO}_2\text{CO}_3$ Ca^{2+} K^+	26.9	n.s.
Outcome: test $\text{UO}_2^{2+} + \text{UO}_2(\text{OH})_2/\text{UO}_2\text{CO}_3 + \text{Ca}^{2+} + \text{Mg}^{2+} + \text{one other.}$		
Five binding species		
UO_2^{2+} $\text{UO}_2(\text{OH})_2/\text{UO}_2\text{CO}_3$ Ca^{2+} Mg^{2+} UO_2OH^+	25.8	n.s.
UO_2^{2+} $\text{UO}_2(\text{OH})_2/\text{UO}_2\text{CO}_3$ Ca^{2+} Mg^{2+} H^+	25.8	n.s.
UO_2^{2+} $\text{UO}_2(\text{OH})_2/\text{UO}_2\text{CO}_3$ Ca^{2+} Mg^{2+} Na^+	25.8	n.s.
UO_2^{2+} $\text{UO}_2(\text{OH})_2/\text{UO}_2\text{CO}_3$ Ca^{2+} Mg^{2+} K^+	25.8	n.s.
Outcome: no further improvement in model fit		
Best model is $\text{UO}_2^{2+} + \text{UO}_2(\text{OH})_2/\text{UO}_2\text{CO}_3 + \text{Ca}^{2+} + \text{Mg}^{2+}$		

Fitting of binding constants was done by stepwise testing of the statistical significance of adding terms for the influence of U(VI) species and competing cations. An initial fit was done assuming only UO_2^{2+} to bind, then the influence of additional ions (UO_2OH^+ , $\text{UO}_2(\text{OH})_2$, UO_2CO_3 , H^+ , Na^+ , Mg^{2+} , K^+ , Ca^{2+}) was assessed in turn by fitting the model allowing each ion to bind and testing the significance of the fit using χ^2 testing (Jonker et al., 2005). Assuming any of the potentially competing ions to significantly improve the model, the ion giving the greatest improvement was added to the model and the remaining ions then tested in turn again. This process was repeated until either no more significant improvements to the fit could be made, or until all the competing ions considered were included in the model. Exploratory calculations showed that optimising the site density simultaneously with the binding constants sometimes produced spurious results, such as the optimal density being smaller than the highest accumulated U, or, for *L. minor*, being unrealistically large ($> 10^4$ $\mu\text{mol/g d.w.}$). Therefore, all the fitting was done with site densities of 10^3 $\mu\text{mol/g d.w.}$ and 10 $\mu\text{mol/g d.w}$ for *L. minor* and *S.salar* respectively.

For *L. minor*, a single binding constant was used to describe the binding of $\text{UO}_2(\text{OH})_2$ and UO_2CO_3 . This is because the speciation was done assuming a fixed partial pressure of CO_2 ($p\text{CO}_2$), which results in a perfect correlation between the activities of the $\text{UO}_2(\text{OH})_2$ and UO_2CO_3 species and hence no possibility of robustly deriving separate binding constants for them.

Table 5. Outcome of stepwise fitting of binding constants, single site accumulation BLM for *S. salar*. At each stage the bolded row shows the model providing the most significant improvement over the previous best fit. * = $p < 0.001$, n.s. = not significant.**

Binding ion(s)	SOS in log(gill U, $\mu\text{mol/g d.w.}$)	Significance
UO_2^{2+}	56.7	–
Two binding ions		
UO_2^{2+} UO_2OH^+	16.6	***
UO_2^{2+} $\text{UO}_2(\text{OH})_2$	4.17	***
UO_2^{2+} UO_2CO_3	4.49	***
UO_2^{2+} H^+	15.6	***
UO_2^{2+} Na^+	56.7	n.s.
UO_2^{2+} Mg^{2+}	53.8	n.s.
UO_2^{2+} K^+	56.7	n.s.
UO_2^{2+} Ca^{2+}	53.7	n.s.
Outcome: test $\text{UO}_2 + \text{UO}_2(\text{OH})_2 + \text{one other.}$		
Three binding ions		
UO_2^{2+} $\text{UO}_2(\text{OH})_2$ UO_2OH	4.17	n.s.
UO_2^{2+} $\text{UO}_2(\text{OH})_2$ UO_2CO_3	4.07	n.s.
UO_2^{2+} $\text{UO}_2(\text{OH})_2$ H^+	4.16	n.s.
UO_2^{2+} $\text{UO}_2(\text{OH})_2$ Na^+	4.17	n.s.
UO_2^{2+} $\text{UO}_2(\text{OH})_2$ Mg^{2+}	4.14	n.s.
UO_2^{2+} $\text{UO}_2(\text{OH})_2$ K^+	4.17	n.s.
UO_2^{2+} $\text{UO}_2(\text{OH})_2$ Ca^{2+}	4.17	n.s.
Outcome: No further improvement in fit.		
Best model is $\text{UO}_2 + \text{UO}_2(\text{OH})_2$.		

The model fitting outcomes for *S. salar* and *L. minor* are shown in Table 4 and Table 5 respectively. In both cases the best fit is obtained allowing $\text{UO}_2(\text{OH})_2$ (and UO_2CO_3 in the case of *L. minor*) to bind alongside UO_2^{2+} . In the case of *S. salar* invoking competing major ions does not improve the fit – the optimal model has only U(VI) species binding. In the case of *L. minor* competition from Mg^{2+} and Ca^{2+} is required for optimal fit.

Table 6. Outcome of stepwise fitting of binding constants, constrained single site accumulation BLM for *L. minor*. At each stage the bolded row shows the model providing the most significant improvement over the previous best fit. ** = $p < 0.01$, * = $p < 0.001$, n.s. = not significant.**

Binding ion(s)	SOS in log(tissue U, $\mu\text{mol/g}$ d.w.)	Significance
$\text{UO}_2^{2+}/\text{UO}_2\text{OH}^+$	232.7	–
Two binding ions		
$\text{UO}_2^{2+}/\text{UO}_2\text{OH}^+$ $\text{UO}_2(\text{OH})_2/\text{UO}_2\text{CO}_3$	42.1	***
$\text{UO}_2^{2+}/\text{UO}_2\text{OH}^+$ H^+	62.5	***
$\text{UO}_2^{2+}/\text{UO}_2\text{OH}^+$ Na^+	232.7	n.s.
$\text{UO}_2^{2+}/\text{UO}_2\text{OH}^+$ Mg^{2+}	230.2	n.s.
$\text{UO}_2^{2+}/\text{UO}_2\text{OH}^+$ K^+	232.7	n.s.
$\text{UO}_2^{2+}/\text{UO}_2\text{OH}^+$ Ca^{2+}	208.3	***
Outcome: test $\text{UO}_2^{2+}/\text{UO}_2\text{OH}^+ + \text{UO}_2(\text{OH})_2/\text{UO}_2\text{CO}_3 + \text{one other}$.		
Three binding ions		
$\text{UO}_2^{2+}/\text{UO}_2\text{OH}^+$ $\text{UO}_2(\text{OH})_2/\text{UO}_2\text{CO}_3$ H^+	42.1	n.s.
$\text{UO}_2^{2+}/\text{UO}_2\text{OH}^+$ $\text{UO}_2(\text{OH})_2/\text{UO}_2\text{CO}_3$ Na^+	42.1	n.s.
$\text{UO}_2^{2+}/\text{UO}_2\text{OH}^+$ $\text{UO}_2(\text{OH})_2/\text{UO}_2\text{CO}_3$ Mg^{2+}	41.7	n.s.
$\text{UO}_2^{2+}/\text{UO}_2\text{OH}^+$ $\text{UO}_2(\text{OH})_2/\text{UO}_2\text{CO}_3$ K^+	42.1	n.s.
$\text{UO}_2^{2+}/\text{UO}_2\text{OH}^+$ $\text{UO}_2(\text{OH})_2/\text{UO}_2\text{CO}_3$ Ca^{2+}	30.1	***
Outcome: test $\text{UO}_2^{2+}/\text{UO}_2\text{OH}^+ + \text{UO}_2(\text{OH})_2/\text{UO}_2\text{CO}_3 + \text{Ca}^{2+} + \text{one other}$.		
Four binding species		
$\text{UO}_2^{2+}/\text{UO}_2\text{OH}^+$ $\text{UO}_2(\text{OH})_2/\text{UO}_2\text{CO}_3$ Ca^{2+} H^+	30.1	n.s.
$\text{UO}_2^{2+}/\text{UO}_2\text{OH}^+$ $\text{UO}_2(\text{OH})_2/\text{UO}_2\text{CO}_3$ Ca^{2+} Na^+	30.1	n.s.
$\text{UO}_2^{2+}/\text{UO}_2\text{OH}^+$ $\text{UO}_2(\text{OH})_2/\text{UO}_2\text{CO}_3$ Ca^{2+} Mg^{2+}	28.8	**
$\text{UO}_2^{2+}/\text{UO}_2\text{OH}^+$ $\text{UO}_2(\text{OH})_2/\text{UO}_2\text{CO}_3$ Ca^{2+} K^+	30.1	n.s.
Outcome: test $\text{UO}_2^{2+}/\text{UO}_2\text{OH}^+ + \text{UO}_2(\text{OH})_2/\text{UO}_2\text{CO}_3 + \text{Ca}^{2+} + \text{Mg}^{2+} + \text{one other}$.		
Five binding species		
$\text{UO}_2^{2+}/\text{UO}_2\text{OH}^+$ $\text{UO}_2(\text{OH})_2/\text{UO}_2\text{CO}_3$ Ca^{2+} Mg^{2+} H^+	28.8	n.s.
$\text{UO}_2^{2+}/\text{UO}_2\text{OH}^+$ $\text{UO}_2(\text{OH})_2/\text{UO}_2\text{CO}_3$ Ca^{2+} Mg^{2+} Na^+	28.8	n.s.
$\text{UO}_2^{2+}/\text{UO}_2\text{OH}^+$ $\text{UO}_2(\text{OH})_2/\text{UO}_2\text{CO}_3$ Ca^{2+} Mg^{2+} K^+	28.8	n.s.
Outcome: no further improvement in model fit Best model is $\text{UO}_2^{2+}/\text{UO}_2\text{OH}^+ + \text{UO}_2(\text{OH})_2/\text{UO}_2\text{CO}_3 + \text{Ca}^{2+} + \text{Mg}^{2+}$		

In both cases the optimised model had UO_2^{2+} and $\text{UO}_2(\text{OH})_2$ binding, but not UO_2OH^+ . This was deemed somewhat unrealistic, so the fitting was re-run forcing UO_2OH^+ to bind, with the same log K as UO_2^{2+} . We term this model ‘constrained’ as unopposed to the ‘unconstrained’ model allowing the optimal fit without restricting which species may bind. Fitting results for the ‘constrained’ model are shown in Table 6 and Table 7. For both organisms the optimal

competing ions were the same as found previously. The optimal fits are slightly, but not excessively, poorer than for the corresponding ‘unconstrained’ model.

Table 7. Outcome of stepwise fitting of binding constants, constrained single site accumulation BLM for *S. salar*. At each stage the bolded row shows the model providing the most significant improvement over the previous best fit. * = $p < 0.05$, * = $p < 0.001$, n.s. = not significant ($p > 0.05$).**

Binding ion(s)	SOS in log(gill U, $\mu\text{mol/g d.w.}$)	Significance
$\text{UO}_2^{2+}/\text{UO}_2\text{OH}^+$	20.8	–
Two binding ions		
$\text{UO}_2^{2+}/\text{UO}_2\text{OH}^+$ $\text{UO}_2(\text{OH})_2$	4.37	***
$\text{UO}_2^{2+}/\text{UO}_2\text{OH}^+$ UO_2CO_3	4.81	***
$\text{UO}_2^{2+}/\text{UO}_2\text{OH}^+$ H^+	6.27	***
$\text{UO}_2^{2+}/\text{UO}_2\text{OH}^+$ Na^+	19.85	n.s.
$\text{UO}_2^{2+}/\text{UO}_2\text{OH}^+$ Mg^{2+}	19.02	*
$\text{UO}_2^{2+}/\text{UO}_2\text{OH}^+$ K^+	19.85	n.s.
$\text{UO}_2^{2+}/\text{UO}_2\text{OH}^+$ Ca^{2+}	19.44	n.s.
Outcome: test $\text{UO}_2/\text{UO}_2\text{OH}^+ + \text{UO}_2(\text{OH})_2 + \text{one other}$		
Three binding ions		
$\text{UO}_2^{2+}/\text{UO}_2\text{OH}^+$ $\text{UO}_2(\text{OH})_2$ UO_2CO_3	4.37	n.s.
$\text{UO}_2^{2+}/\text{UO}_2\text{OH}^+$ $\text{UO}_2(\text{OH})_2$ H^+	4.37	n.s.
$\text{UO}_2^{2+}/\text{UO}_2\text{OH}^+$ $\text{UO}_2(\text{OH})_2$ Na^+	4.37	n.s.
$\text{UO}_2^{2+}/\text{UO}_2\text{OH}^+$ $\text{UO}_2(\text{OH})_2$ Mg^{2+}	4.30	n.s.
$\text{UO}_2^{2+}/\text{UO}_2\text{OH}^+$ $\text{UO}_2(\text{OH})_2$ K^+	4.37	n.s.
$\text{UO}_2^{2+}/\text{UO}_2\text{OH}^+$ $\text{UO}_2(\text{OH})_2$ Ca^{2+}	4.37	n.s.
Outcome: No further improvement in fit.		
Best model is $\text{UO}_2/\text{UO}_2\text{OH}^+ + \text{UO}_2(\text{OH})_2$		

Fitting accumulation BLMs allowing a range of U(VI) species to bind to the biotic ligand produced good fits to the observed U accumulation (Table 8; Figure 8). The clearest difference between the models is the presence of significant competition from Mg^{2+} and Ca^{2+} for accumulation by *L. minor*, which is not found for *S. salar*. Forcing UO_2OH^+ to bind (the constrained model) did not produce great differences in the optimised binding constants. For *L. minor* the optimal fit had slightly higher log *K* for $\text{UO}_2^{2+}/\text{UO}_2\text{OH}^+$ and $\text{UO}_2(\text{OH})_2/\text{UO}_2\text{CO}_3$, which was compensated for by higher optimal log *K*s for Mg^{2+} and Ca^{2+} . For *S. salar* the log *K*s of the constrained model are slightly lower than for the unconstrained model, the optimal fit being achieved due to having more U(VI) species able to accumulate.

Table 8. Optimised parameters and error terms for the unconstrained and constrained single-site accumulation BLMs, *L. minor* and *S. salar*.

	<i>L. minor</i>		<i>S. salar</i>	
	Optimised log <i>K</i>		Optimised log <i>K</i>	
	unconstrained	constrained	unconstrained	constrained
{S}, µmol/g	10 ³	10 ³	10	10
UO ₂ ²⁺	4.24	4.25	4.40	4.25
UO ₂ OH ⁺	–	(4.25) ^b	–	(4.25) ^b
UO ₂ (OH) ₂	5.74	5.90	5.61	5.56
UO ₂ CO ₃	(5.74) ^c	(5.90) ^c	–	–
H ⁺	–	–	–	–
Na ⁺	–	–	–	–
Mg ²⁺	2.96	3.20	–	–
K ⁺	–	–	–	–
Ca ²⁺	3.10	3.30	–	–
RMSE ^a in log(accumulated U, µmol/g d.w.)	0.38	0.40	0.28	0.29

^a Root mean squared error.

^b Forced equal to the log *K* for UO₂²⁺.

^c Forced equal to the log *K* for UO₂(OH)₂.

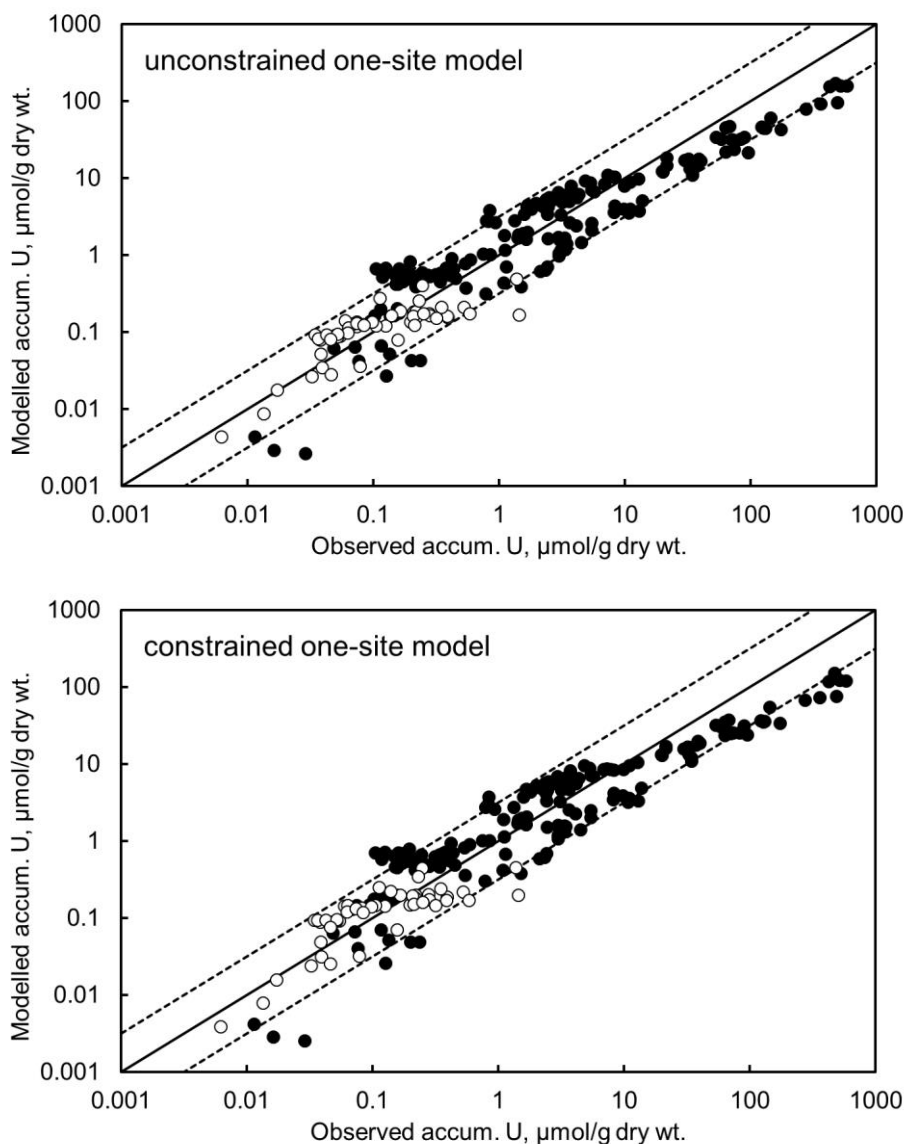
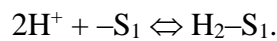


Figure 8. Observed and modelled U accumulation on *L. minor* (closed points) and on gills of *S. salar* (open points) using the unconstrained (top) and constrained (bottom) one-site BLM. The solid line is the 1:1 line and the dotted lines indicate a difference of ± 0.5 orders of magnitude from the 1:1 correspondence.

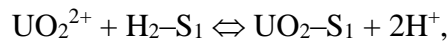
4.4.4 *Modelling: two-site model*

The one-site models described the U accumulation well by postulating that multiple U(VI) species may bind to the biotic ligand. However, in no case did H^+ emerge as a significant competing ion for U(VI) binding. This is somewhat unrealistic, since H^+ is an important competitor for the binding of U(VI) and other cations to organic functional groups. A

possibility is that the need to allow multiple U(VI) species to bind in order to explain binding to single biotic ligand masks the effect of H⁺ competition, since the UO₂OH⁺ and UO₂(OH)₂ ion activities are functions of the UO₂²⁺ and H⁺ activities. Therefore, we developed an alternative BLM formulation focused on allowing only UO₂²⁺ to bind, and forcing the pH dependence of accumulation to be described by H⁺ competition. In order to account for pH dependence, a two-site BLM was required. The first site (Site 1) simulates UO₂²⁺ binding in the pH range where the variation of log Θ with pH (Figure 7) has a slope of approximately two. Initially two reactions were postulated:



However, fitting this model suggested that the binding strengths of both UO₂²⁺ and H⁺ needed to be sufficiently strong that the concentration of unoccupied sites (-S₁) would be negligible, and therefore the binding was re-formulated as a single exchange reaction of UO₂²⁺ with two protons:



which can be described by a single exchange constant, K_{exch} :

$$K_{\text{exch}} = \frac{\{\text{UO}_2-\text{S}_1\} \cdot a_{\text{H}^+}^2}{\{\text{H}_2-\text{S}_1\} \cdot a_{\text{UO}_2^{2+}}}.$$

The bound U(VI) concentration is then given by

$$\{\text{UO}_2-\text{S}_1\} = \{\text{S}_1\} \cdot f_{\text{S}_1, \text{UO}_2}; \quad f_{\text{S}_1, \text{UO}_2} = \frac{K_{\text{exch}} a_{\text{UO}_2^{2+}}}{K_{\text{exch}} a_{\text{UO}_2^{2+}} + a_{\text{H}^+}^2}$$

The second site, denoted site 2, was formulated as a ‘conventional’ biotic ligand allowing 1:1 binding of UO₂²⁺ and competing ions (H⁺, Na⁺, Mg²⁺, K⁺, Ca²⁺, Cd²⁺) as required:

$$\{\text{UO}_2-\text{S}_2\} = \{\text{S}_2\} \cdot f_{\text{S}_2, \text{UO}_2}; \quad f_{\text{S}_2, \text{UO}_2} = \frac{K_{\text{UO}_2} a_{\text{UO}_2^{2+}}}{1 + K_{\text{UO}_2} a_{\text{UO}_2^{2+}} + \sum_1^i K_{\text{X},i} a_{\text{X},i}}$$

where X,_i is a competitively binding cation. The total predicted accumulated U(VI) is then simply the sum of {UO₂-S₁} and {UO₂-S₂}.

Model fitting for each organism then entailed deriving parameters for the exchange reaction at Site 1, the binding constants for Site 2, and the total site densities for both sites. Exploratory modelling suggested that a reasonable value for K_{exch} was 10^{-6.5}. Fixing the exchange constant in this way allowed the site density {S₁} to be fitted independently. Fitted values of {S₁} were 235 μmol/g dry wt. for *L. minor* and 1.40 μmol/g dry wt. for *S. salar*. Independent determination of the densities of Site 2 was not possible given the relatively restricted pH range over which the site was the major binder of U(VI). Therefore, for pragmatic reasons we

forced $\{S_2\}$ equal to $\{S_1\}$ for both organisms. Fitting of binding constants for Site 2 on *L. minor* was done by the stepwise testing method previously described for the one-site BLM.

Fitting results for *L. minor* are shown in Table 9. The ions Mg^{2+} and Ca^{2+} were shown to need including in the Site 2 model to provide the optimal fit to the data.

Fitting of competing ion constants for Site 2 on *S. salar* proved challenging, since the number of points for which Site 2 was important was relatively low (of the total 109 points, only six were at $pH < 6$). Therefore, a pragmatic decision was made to fix the binding constants for Mg^{2+} and Ca^{2+} equal to those for *L. minor*. A small improvement to the fit was then obtained by optimising the binding constant for H^+ .

Table 9. Outcome of stepwise fitting of binding constants for competing ions, two-site accumulation model for *L. minor*. Each row shows a test of a combination of binding species, the sum of squares (SOS) error and the significance of the fit in comparison with the reduced model, calculated by chi-squared testing (Jonker et al., 2005) using the previous best fit as the baseline comparison. At each stage the bolded row shows the model providing the most significant improvement over the previous best fit. * = $p < 0.001$, ** = $p < 0.01$, n.s. = not significant.**

Competing ion(s)	SOS error in log U_{tissue}	Significance
No competition	39.62	–
One competing ion		
<i>H</i>	39.62	n.s.
<i>Na</i>	39.43	n.s.
Mg	36.96	***
<i>K</i>	36.92	n.s.
Ca	31.76	***
Outcome: test Ca + one other		
Two competing ions		
<i>H</i> <i>Ca</i>	31.76	n.s.
<i>Na</i> <i>Ca</i>	31.30	n.s.
Mg Ca	30.24	**
<i>K</i> <i>Ca</i>	31.60	n.s.
Outcome: test Mg Ca + one other		
Three competing ions		
<i>H</i> <i>Mg</i> <i>Ca</i>	30.24	n.s.
<i>Na</i> <i>Mg</i> <i>Ca</i>	30.13	n.s.
<i>Mg</i> <i>K</i> <i>Ca</i>	30.24	n.s.
Outcome: no further testing		

Modelled accumulation is compared for both organisms in Figure 9. Accumulated U on *L. minor*, which ranges from $2.7-1.38 \times 10^5$ $\mu\text{g/g}$ dry wt., was predicted largely to within half an order of magnitude (141 of 182 points) and almost entirely within an order of magnitude (181

of 182 points). Accumulation on *S. salar* gills was predicted almost entirely to within half an order of magnitude (50 of 53 points) and entirely to within one order of magnitude.

The accumulation model parameters are summarised in Table 10.

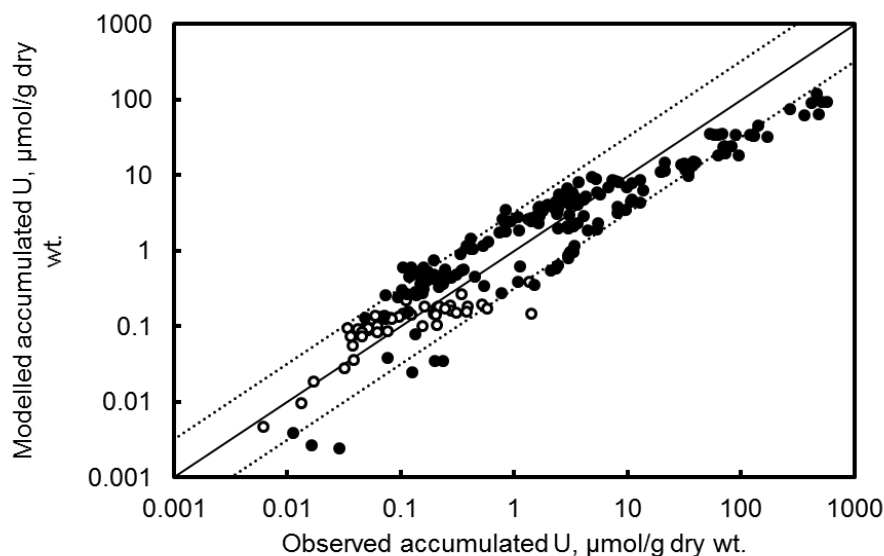


Figure 9. Observed and modelled U accumulation on *L. minor* (closed points) and on gills of *Salmo salar* (open points) using the two-site model. The solid line is the 1:1 line and the dotted lines indicate a difference of ± 0.5 orders of magnitude from the 1:1 correspondence.

Table 10. Parameters of the two-site U accumulation model for *L. minor* and *S. salar*.

Parameter	<i>L. minor</i>	<i>S. salar</i>	Comments
Site 1			
{S ₁ } (μmol/g)	234	1.41	Optimised in conjunction with log K_{exch} .
log K_{exch}	-6.5	-6.5	Optimised in conjunction with {S ₁ }.
Site 2			
{S ₂ } (μmol/g)	234	1.41	Forced to equal {S ₁ }.
log K_{UO_2}	8.02	8.02	Optimised for <i>L. minor</i> , fixed for <i>S. salar</i> .
log K_{H}	–	7.74	Optimised for <i>S. salar</i> .
log K_{Mg}	6.46	6.46	Optimised for <i>L. minor</i> , fixed for <i>S. salar</i> .
log K_{Ca}	6.28	6.28	Optimised for <i>L. minor</i> , fixed for <i>S. salar</i> .
RMSE	0.51	0.28	Root mean squared error in log(accumulated U, μmol/g)

For *L. minor* the two-site model provides an inferior fit to either the constrained or unconstrained one-site models. Comparison of the fits shows that while all the models underestimate accumulation at higher values (>~10 µmol/g d.w.), this underestimation is smaller for both the one-site models than for the two-site model. For *S. salar*, there is little difference in fit among any of the models.

4.4.5 *U* toxicity modelling: *Lemna minor* and *Salmo salar*

Extension of the accumulation BLMs for *L. minor* and *S. salar* to toxic effects entailed prediction of accumulation for all exposures and fitting of a dose–response model to relate prediction and accumulation and effect. For both organisms we describe effect (growth inhibition, mortality) as increasing with increasing dose to a maximum of 100%. The expression for this response is then

$$\text{response}(\% \text{ of control}) = 100 - \frac{100}{1 + \left(\frac{\{UO_2 - S\}}{\{UO_2 - S\}_{L(E)C50}} \right)^{\beta_U}}$$

where $\{UO_2 - S\}$ is the predicted accumulation, $\{UO_2 - S\}_{L(E)C50}$ is the accumulation causing an effect of 50% relative to the control and β_U is a slope term.

Toxicity was modelled based on the predictions of all three U accumulation models. Parameters and error terms are shown in Table 10. For *L. minor* the two-site model provides the best fit, despite the fact that the corresponding accumulation model gives the poorest fit.

Table 11. Toxicity model parameters for *L. minor* and *S. salar*.

<i>L. minor</i>				
Model	one-site unconstrained	one-site constrained	two-site	
$\{UO_2 - S\}_{L(E)C50}$ (µmol/g d.w.)	23.8	21.1	20.7	
β_U	1.10	1.18	1.20	
RMSE in response	19.0	20.3	12.5	
<i>S. salar</i>				
Model	one-site unconstrained	one-site constrained	two-site	two-site optimising log K_H
$\{UO_2 - S\}_{L(E)C50}$ (µmol/g d.w.)	0.21	0.23	0.20	0.20
β_U	15.1	11.6	20.4	26.6
RMSE in response	20.1	21.6	24.3	14.6

Fitting the two-site model to *S.salar* initially produced overestimation of effects at low pH. Allowing optimisation of $\log K_H$ alongside $\{UO_2-S\}_{L(E)C50}$ and β gave a significantly improved fit ($p < 0.001$ by χ^2 test). The optimised value of $\log K_H$ was 8.53, providing stronger competition for UO_2^{2+} due to H^+ than was predicted by fixing the parameters of the accumulation model. Figure 10 and Figure 11 show the relationships between the predicted accumulated U and the observed and modelled effects for the two-site models.

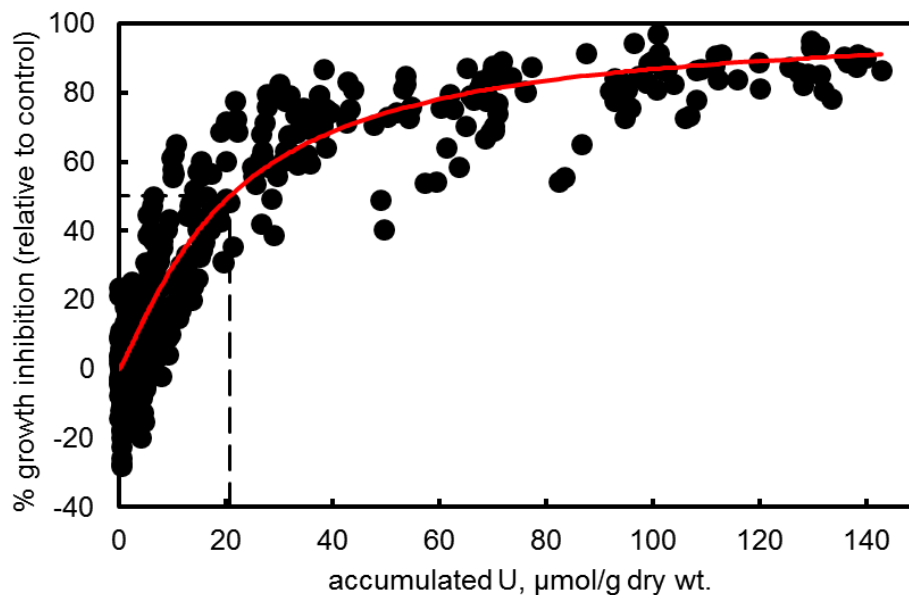


Figure 10. Observed and modelled growth inhibition of *L. minor* in response to U accumulation, plotted against modelled U accumulation using the two-site model. The dashed line marks the $\{UO_2-S\}_{L(E)C50}$.

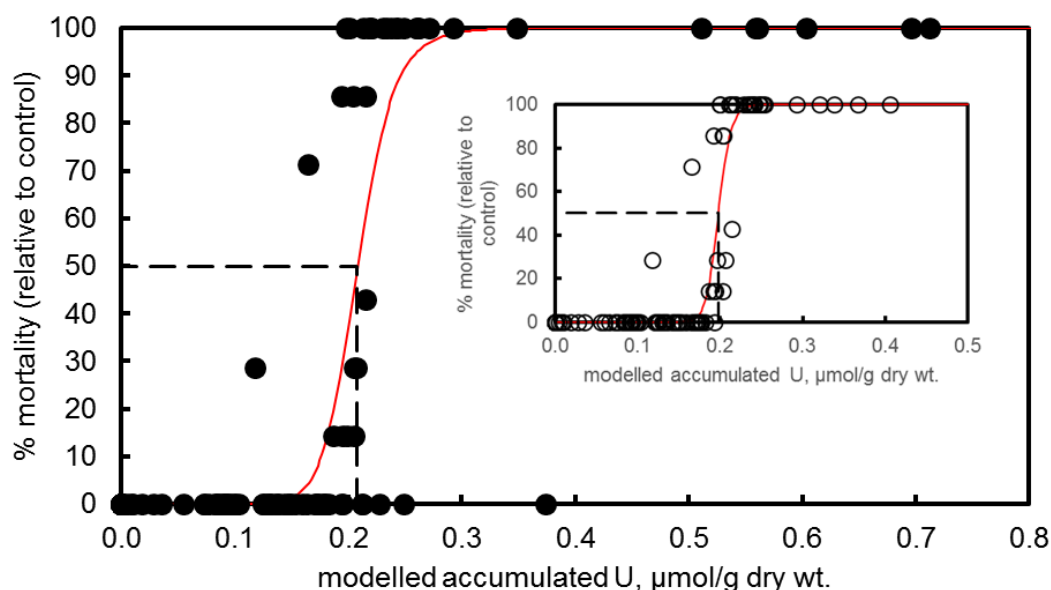


Figure 11. Observed and modelled mortality of *S. salar* in response to U accumulation, plotted against modelled U accumulation, using the two-site model. The dashed line marks the $\{UO_2-S\}_{L(E)C50}$. The inset chart shows the improved fit obtained by allowing $\log K_H$ to be adjusted.

The combined accumulation–toxicity models can be used to predict the relationship between exposure dissolved U and effect for individual series of exposures. Figure 12, Figure 13 and Figure 14 present such relationships each exposure series for *L. minor*, for the two-site model. Corresponding plots for the one-site models are presented in Annex 2. Regardless of the type of accumulation model, toxicity modelling reproduces well the trends in effect with increasing U(VI) dose, and also reproduces well the influence of pH on the response. The effect is overestimated somewhat, by all the models, in the pH6 series, which is mostly likely due a combination of a shift in pH with increasing U(VI), observed during this exposure, and the sensitivity of the model to pH as a variable. The models also underestimate effect somewhat at the highest concentrations of Mg and Ca (HMg and HCa series).

Figure 15, Figure 16 and Figure 17 show the modelled response of *S. salar* to U across all the exposure series, using the two-site toxicity model. The corresponding modelled responses due to the one-site models are shown in Annex 3. The two–site BLM reproduces the effect of pH on toxicity reasonably well (Figure 15) although if additional optimisation of $\log K_H$ is not done the effects are somewhat overestimated at the three lowest pH values, where binding of UO_2^{2+} to Site 2 dominates uptake and toxicity. The unconstrained one-site model performs the most poorly (Table 11) which is likely related to the relatively low value of the best fit slope of the dose–response curve (Figure A3-1, Annex 3).

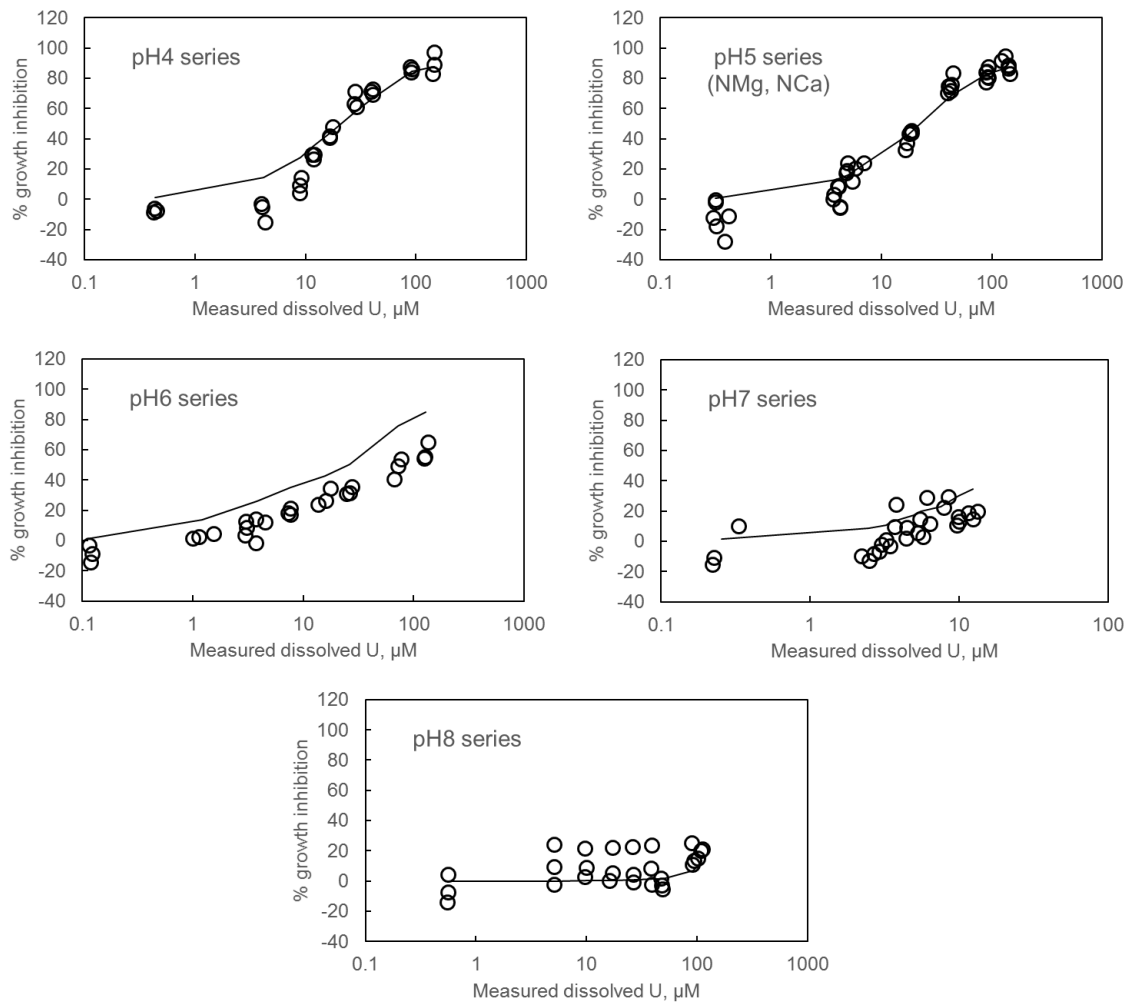


Figure 12. Observed and modelled growth inhibition of *L. minor* in the pH series of U exposures, plotted against the measured dissolved U (0.22µm filtered) in the exposures.

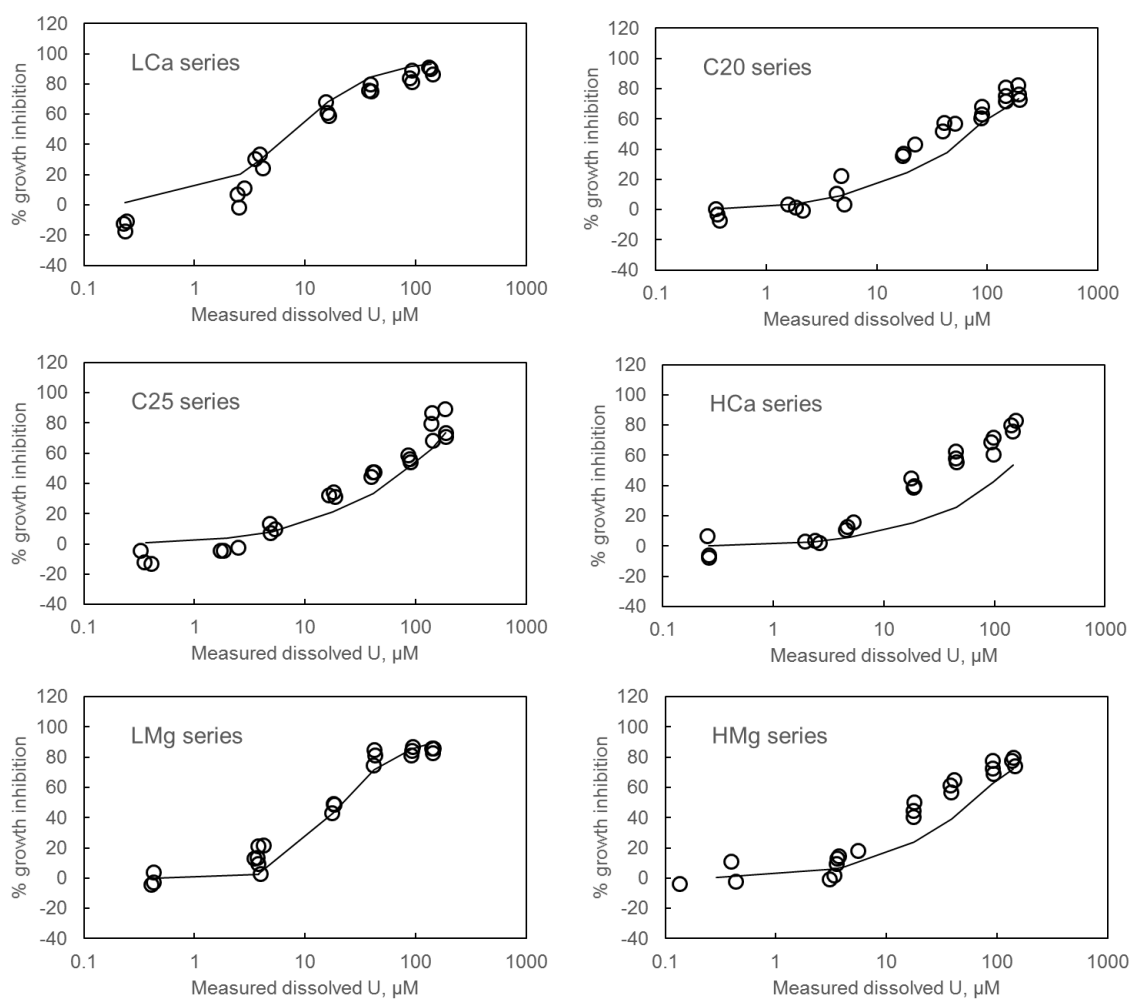


Figure 13. Observed and modelled growth inhibition of *L. minor* in the Ca and Mg series of U exposures, plotted against the measured dissolved U (0.22µm filtered) in the exposures.

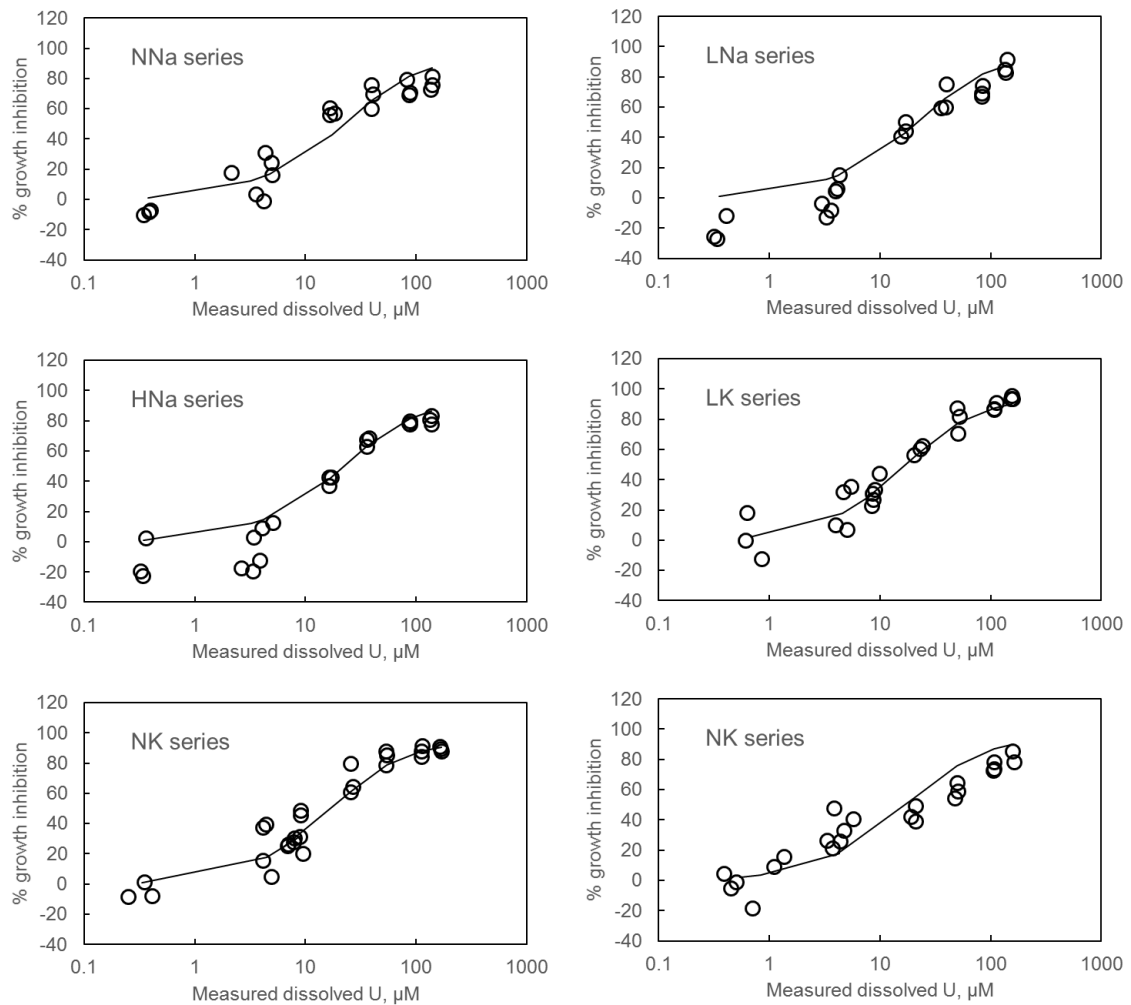


Figure 14. Observed and modelled growth inhibition of *L. minor* in the Na and K series of U exposures, plotted against the measured dissolved U (0.22μm filtered) in the exposures.

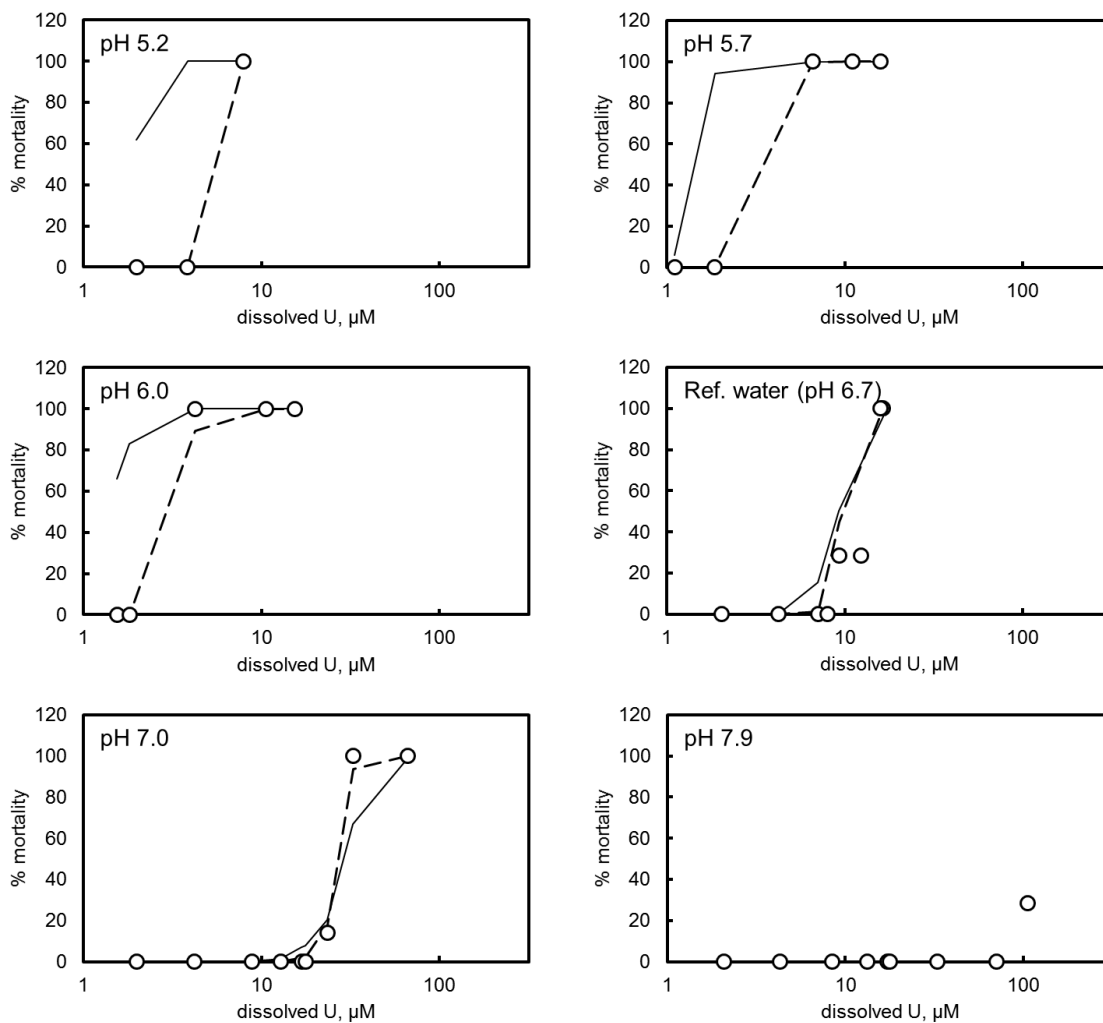


Figure 15. Observed and modelled mortality of *S. salar* in the pH series of U exposures, plotted against the measured dissolved U (0.45µm filtered). Solid lines obtained by optimisation of $\{UO_2-S\}_{L(E)C50}$ and β , dashed lines obtained by additional optimisation of $\log K_H$

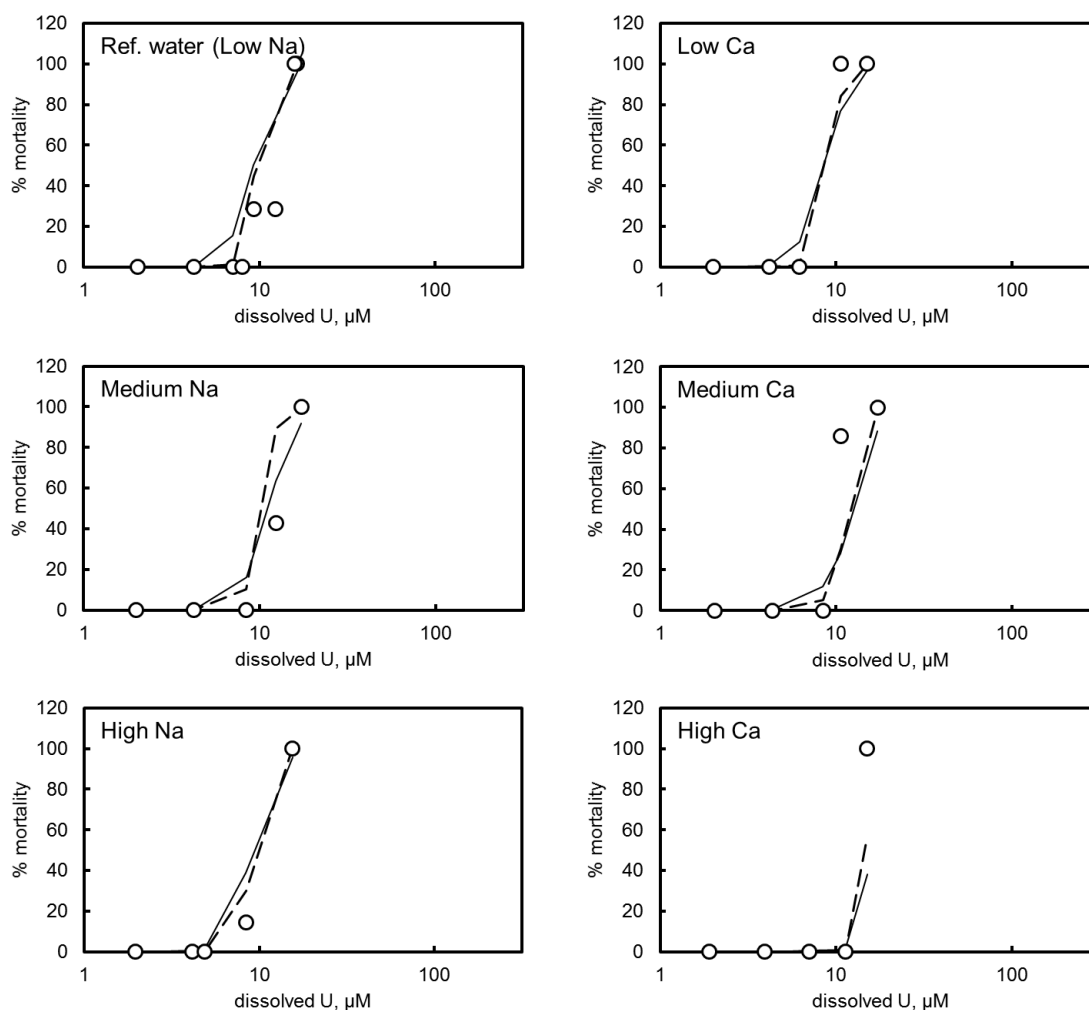


Figure 16. Observed and modelled mortality of *S. salar* in the Na and K series of U exposures, plotted against the measured dissolved U (0.45µm filtered). Solid lines obtained by optimisation of $\{UO_2-S\}_{L(E)C50}$ and β , dashed lines obtained by additional optimisation of $\log K_H$.

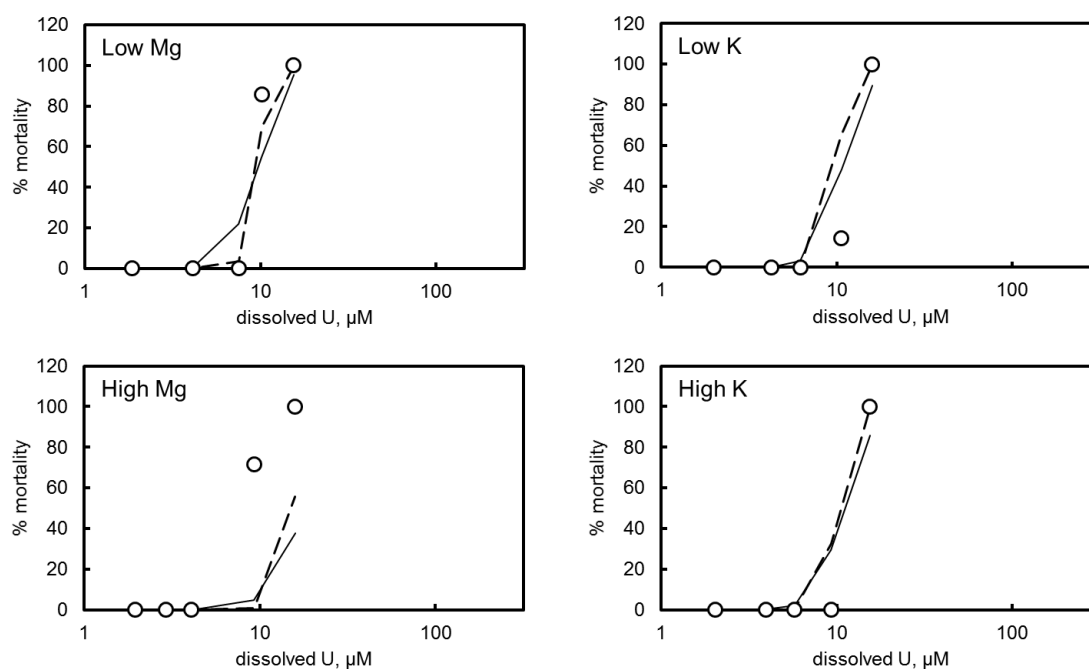


Figure 17. Observed and modelled mortality of *S. salar* in the Mg and K series of U exposures, plotted against the measured dissolved U (0.45µm filtered). Solid lines obtained by optimisation of $\{UO_2-S\}_{L(E)C50}$ and β , dashed lines obtained by additional optimisation of $\log K_H$

4.4.6 *U toxicity modelling: Daphnia magna*

Measurements of U accumulation were not made for *D. magna*. Therefore BLM fitting was done directly to the toxicity data. In this case it was not necessary to define a total site density, as fitting could be done by taking the fractional occupancy of sites by UO_2 as a measure of dose. So the dose-response model was adjusted to make the dose the fractional occupancy of sites by $U(VI)$, f_{S,UO_2} :

$$\text{response(\% of control)} = 100 - \frac{100}{1 + \left(\frac{f_{S,UO_2}}{f_{S,UO_2,L(E)C50}} \right)^{\beta_U}}$$

where f_{S,UO_2} is the fractional occupancy of sites computed by whatever binding model formulation is applied and $f_{S,UO_2,L(E)C50}$ is the fractional occupancy at the $L(E)C50$. Given the strong pH dependence of $U(VI)$ uptake for *L. minor* and *S. salar* and the insight gained by plotting Θ , the “local binding strength”, against pH, we first examined the trends in toxicity across the pH series. This was done by calculating the $LC50$ for each dose–response curve in the pH series as the free UO_2^{2+} activity ($LC50_{UO_2^{2+}}$) and then plotting $\log(1/LC50_{UO_2^{2+}})$ against pH. Since at a constant level of effect the loading of sites with UO_2 should also be constant, the trend in this plot is expected to be similar to a trend in $\log \Theta$ against pH and thus to provide similar insights for model formulation.

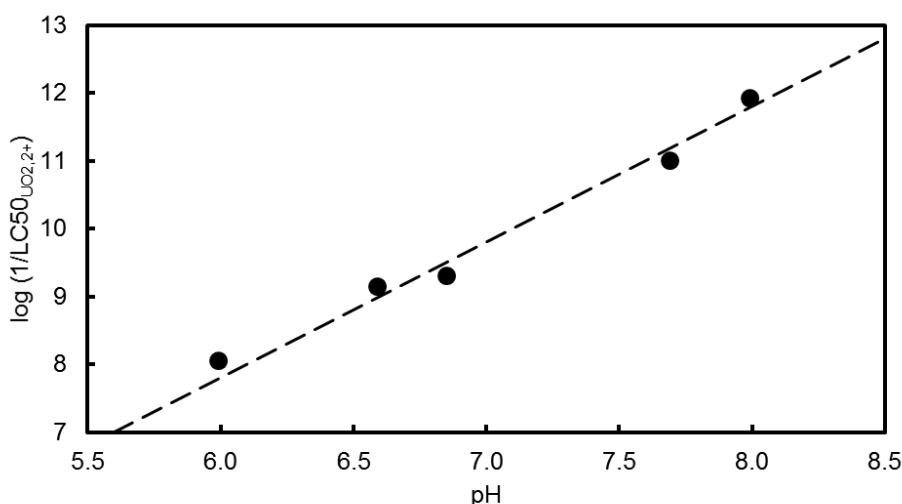


Figure 18. Plot of the logged inverse of the LC50s for the pH series of *D. magna* exposures, against the exposure pH. The dashed reference line has a slope of two.

Figure 18 shows the plot of $\log(1/LC50_{UO_2,2+})$ against pH. The slope of the relationship was sufficiently close to two to suggest that the two-site model formulation was appropriate. Such a model was thus constructed and applied. As with the *L. minor* and *S. salar* models, $\log K_{exch}$ for Site 1 was fixed to -6.5 on the basis of theory, and the relative concentrations of Site 1 and Site 2 were fixed to be equal. The constant for UO_2^{2+} binding to Site 2 was constrained to the value used for the other organisms (Table 10). Binding constants for H^+ , Na^+ , Mg^{2+} and Ca^{2+} at Site 2 were fitted by the stepwise procedure used for *L. minor*, together with the dose-response slope β and $f_{S,UO_2,L(E)C50}$. A reasonable final fit was obtained, with all the competing ions predicted to be required. However, the model did not predict the pH series well, overestimating toxicity at the low end of the pH range and underestimating it at the high end (Figure A5-1, Annex 5). Re-fitting without H^+ binding at Site 2 produced a poorer fit. Therefore, it was decided to attempt fitting only with the one-site model, allowing UO_2OH^+ , $UO_2(OH)_2$ and UO_2CO_3 to bind if it significantly improved the fit. The expression for the fractional occupancy of sites was:

$$f_{S,UO_2} = \frac{K_{UO_2}a_{UO_2,2+} + \sum_1^i K_{UO_2L,i}a_{UO_2L,i}}{1 + K_{UO_2}a_{UO_2,2+} + \sum_1^i K_{UO_2L,i}a_{UO_2L,i} + \sum_1^j K_{X,j}a_{X,j}}$$

where K_{UO_2} is the binding constant for the uranyl free ion, $a_{UO_2,2+}$ is the activity of the uranyl free ion, $K_{UO_2L,i}$ and $a_{UO_2L,i}$ are respectively the binding constant and activity for a binding U(VI) complex, and $K_{X,j}$ and $a_{X,j}$ are respectively the binding constant and activity for a competing ion.

The optimal set of binding constants was obtained by stepwise fitting. It was found that all the U(VI) species considered, and all the competing ions (Na^+ , Mg^{2+} and Ca^{2+}) made statistically

significant ($p < 0.05$) contributions to the fit. The optimal binding constants are listed in Table 12, and the outcome of the stepwise fitting procedure in Table 13.

Table 12. BLM binding constants for acute uranyl toxicity to *Daphnia magna*.

Binding species	log K
UO_2^{2+}	10.6
UO_2OH^+	9.1
$\text{UO}_2(\text{OH})_2^0$	7.9
UO_2CO_3	8.6
H^+	9.5
Na^+	4.3
Mg^{2+}	5.2
Ca^{2+}	5.5

Observed and modelled dose–response curves for *D. magna* are shown in Figures 19-22 for the pH, Na, Mg and Ca series exposures respectively. The model reproduces the key trend in toxicity against pH well, although effects are somewhat underestimated in the pH 6.5 series. The smaller variability in effect due to changes in medium Na, Mg and Ca concentrations are reproduced well, with the trend against Mg reproduced best. There is a tendency to underestimate effect at the lowest Na concentrations and to either overestimate or underestimate at some of the Ca concentrations.

Table 13. Outcome of stepwise fitting of binding constants, single site toxicity model for *D. magna*. Each row shows a test of a combination of binding species, the sum of squares error (SOS) and the significance of the fit in comparison with the reduced model, calculated by chi-squared testing (Jonker et al., 2005) using the previous best fit as the baseline comparison. At each stage the bolded row shows the model providing the most significant improvement over the previous best fit. * = $p < 0.001$, n.s. = not significant. Table is continued overleaf.**

Binding ion(s)	SOS in % mortality	Significance
UO_2^{2+}	1.65×10^6	–
Two binding ions		
UO_2^{2+} UO_2OH^+	1.35×10^6	***
UO_2^{2+} $UO_2(OH)_2$	9.15×10^5	***
UO_2^{2+} UO_2CO_3	1.21×10^6	***
UO_2^{2+} H^+	1.48×10^6	n.s.
UO_2^{2+} Na^+	1.65×10^6	***
UO_2^{2+} Mg^{2+}	1.58×10^6	n.s.
UO_2^{2+} Ca^{2+}	1.65×10^6	***
Outcome: test UO_2^{2+} $UO_2(OH)_2$ + one other		
Three binding ions		
UO_2^{2+} $UO_2(OH)_2$ UO_2OH^+	9.15×10^5	n.s.
UO_2^{2+} $UO_2(OH)_2$ UO_2CO_3	9.15×10^5	n.s.
UO_2^{2+} $UO_2(OH)_2$ H^+	8.87×10^5	***
UO_2^{2+} $UO_2(OH)_2$ Na^+	9.15×10^5	n.s.
UO_2^{2+} $UO_2(OH)_2$ Mg^{2+}	7.50×10^5	***
UO_2^{2+} $UO_2(OH)_2$ Ca^{2+}	8.30×10^5	***
Outcome: test UO_2^{2+} $UO_2(OH)_2$ Mg^{2+} + one other		

[contd.]

Table 13. [continued].

Binding ion(s)	SOS in % mortality	Significance
Four binding ions		
UO_2^{2+} $UO_2(OH)_2$ Mg^{2+} UO_2OH^+	7.50×10^5	<i>n.s.</i>
UO_2^{2+} $UO_2(OH)_2$ Mg^{2+} UO_2CO_3	7.50×10^5	<i>n.s.</i>
UO_2^{2+} $UO_2(OH)_2$ Mg^{2+} H^+	7.09×10^5	***
UO_2^{2+} $UO_2(OH)_2$ Mg^{2+} Na^+	7.47×10^5	<i>n.s.</i>
UO_2^{2+} $UO_2(OH)_2$ Mg^{2+} Ca^{2+}	6.25×10^5	***
Outcome: test UO_2 $UO_2(OH)_2$ Mg Ca + one other		
Five binding ions		
UO_2^{2+} $UO_2(OH)_2$ Mg^{2+} Ca^{2+} UO_2OH^+	6.25×10^5	<i>n.s.</i>
UO_2^{2+} $UO_2(OH)_2$ Mg^{2+} Ca^{2+} UO_2CO_3	6.25×10^5	<i>n.s.</i>
UO_2^{2+} $UO_2(OH)_2$ Mg^{2+} Ca^{2+} H^+	5.80×10^5	***
UO_2^{2+} $UO_2(OH)_2$ Mg^{2+} Ca^{2+} Na^+	6.12×10^5	***
Outcome: test UO_2 $UO_2(OH)_2$ Mg Ca H + one other		
Six binding ions		
UO_2^{2+} $UO_2(OH)_2$ Mg^{2+} Ca^{2+} H^+ UO_2OH^+	5.55×10^5	***
UO_2^{2+} $UO_2(OH)_2$ Mg^{2+} Ca^{2+} H^+ UO_2CO_3	5.68×10^5	***
UO_2^{2+} $UO_2(OH)_2$ Mg^{2+} Ca^{2+} H^+ Na^+	5.47×10^5	***
Outcome: test UO_2^{2+} $UO_2(OH)_2$ Mg^{2+} Ca^{2+} H^+ Na^+ + one other		
Seven binding ions		
UO_2^{2+} $UO_2(OH)_2$ Mg^{2+} Ca^{2+} H^+ Na^+ UO_2OH^+	5.21×10^5	***
UO_2^{2+} $UO_2(OH)_2$ Mg Ca^{2+} H^+ Na^+ UO_2CO_3	5.18×10^5	***
Outcome: test UO_2^{2+} $UO_2(OH)_2$ Mg^{2+} Ca^{2+} H^+ Na^+ UO_2CO_3 + UO_2OH^+		
Eight binding ions		
UO_2^{2+} $UO_2(OH)_2$ Mg^{2+} Ca^{2+} H^+ Na^+ UO_2CO_3 UO_2OH^+	4.93×10^5	***
Outcome: testing complete. All tested binding ions in final model.		

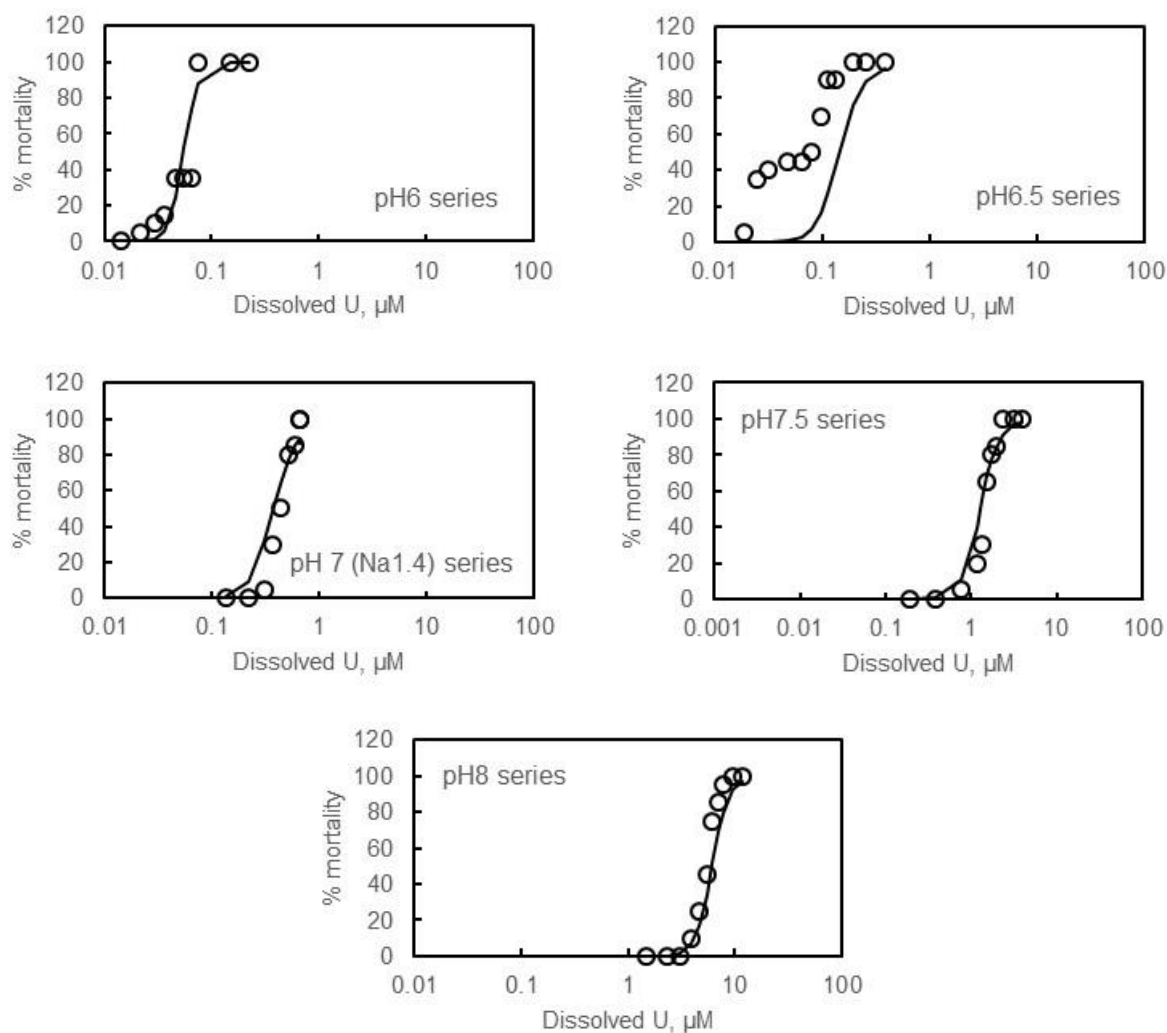


Figure 19. Observed and modelled mortality of *D. magna* in the pH series of U exposures, plotted against the measured dissolved U (0.45µm filtered).

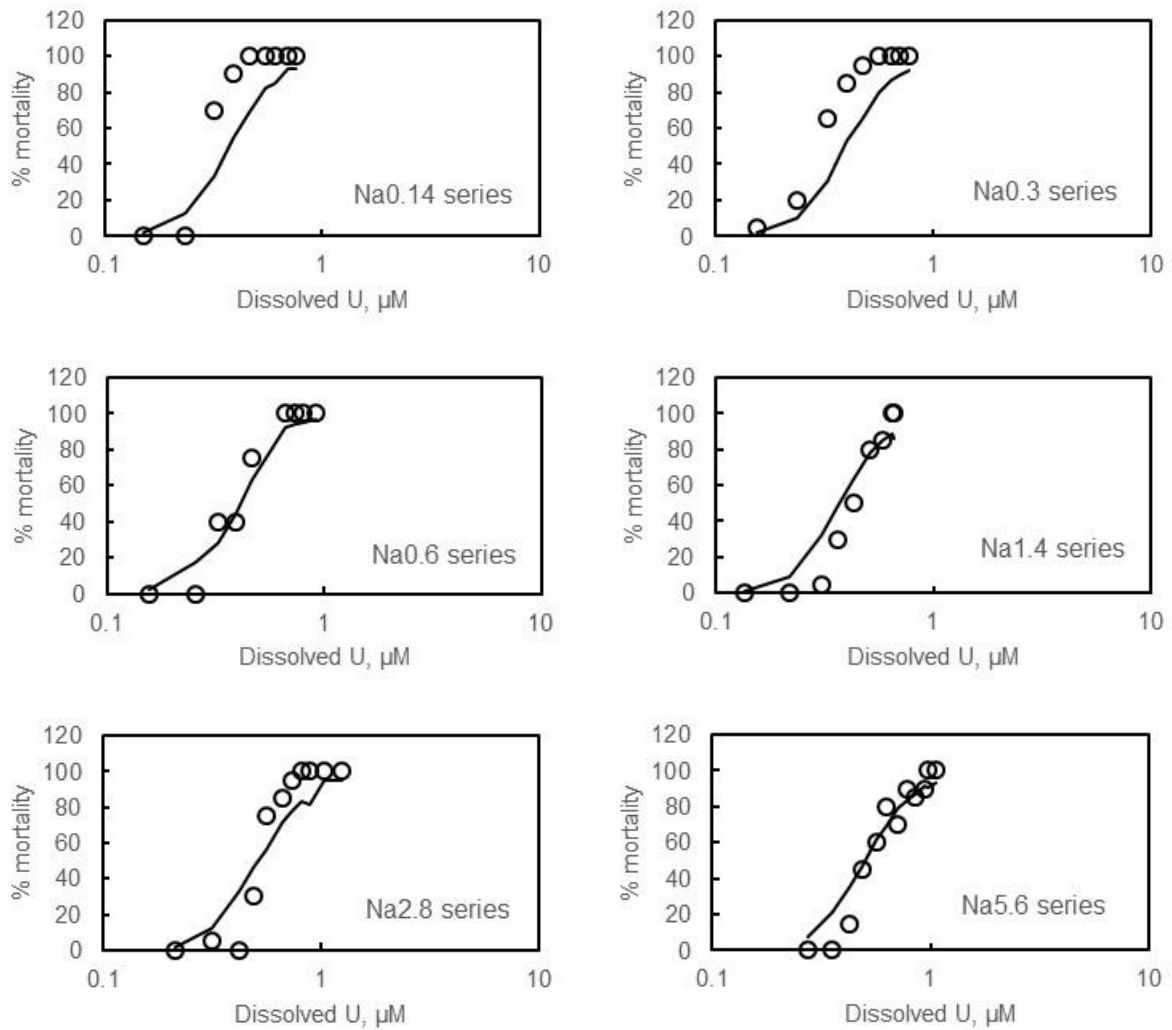


Figure 20. Observed and modelled mortality of *D. magna* in the Na series of U exposures, plotted against the measured dissolved U (0.45µm filtered).

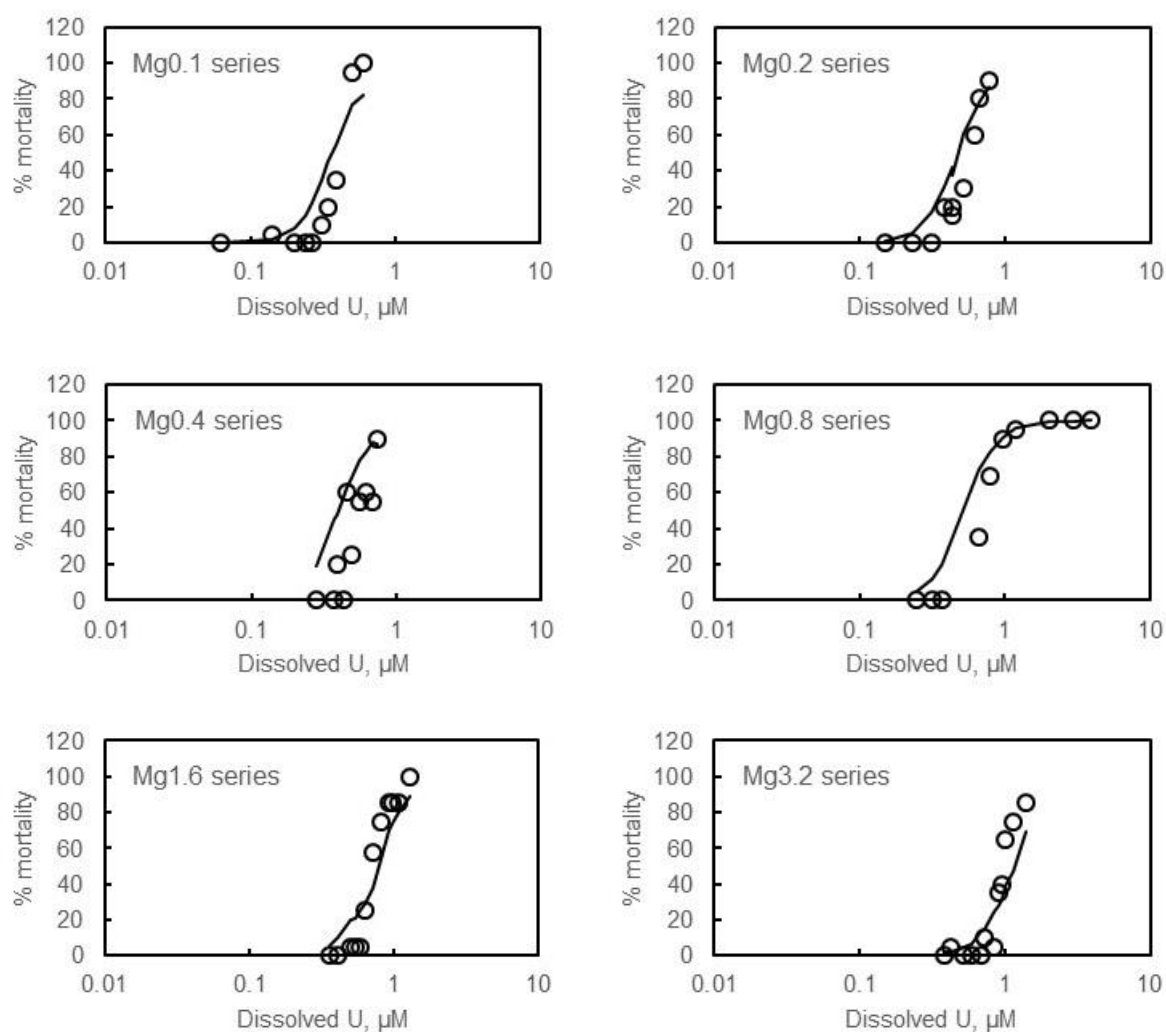


Figure 21. Observed and modelled mortality of *D. magna* in the Mg series of U exposures, plotted against the measured dissolved U (0.45µm filtered).

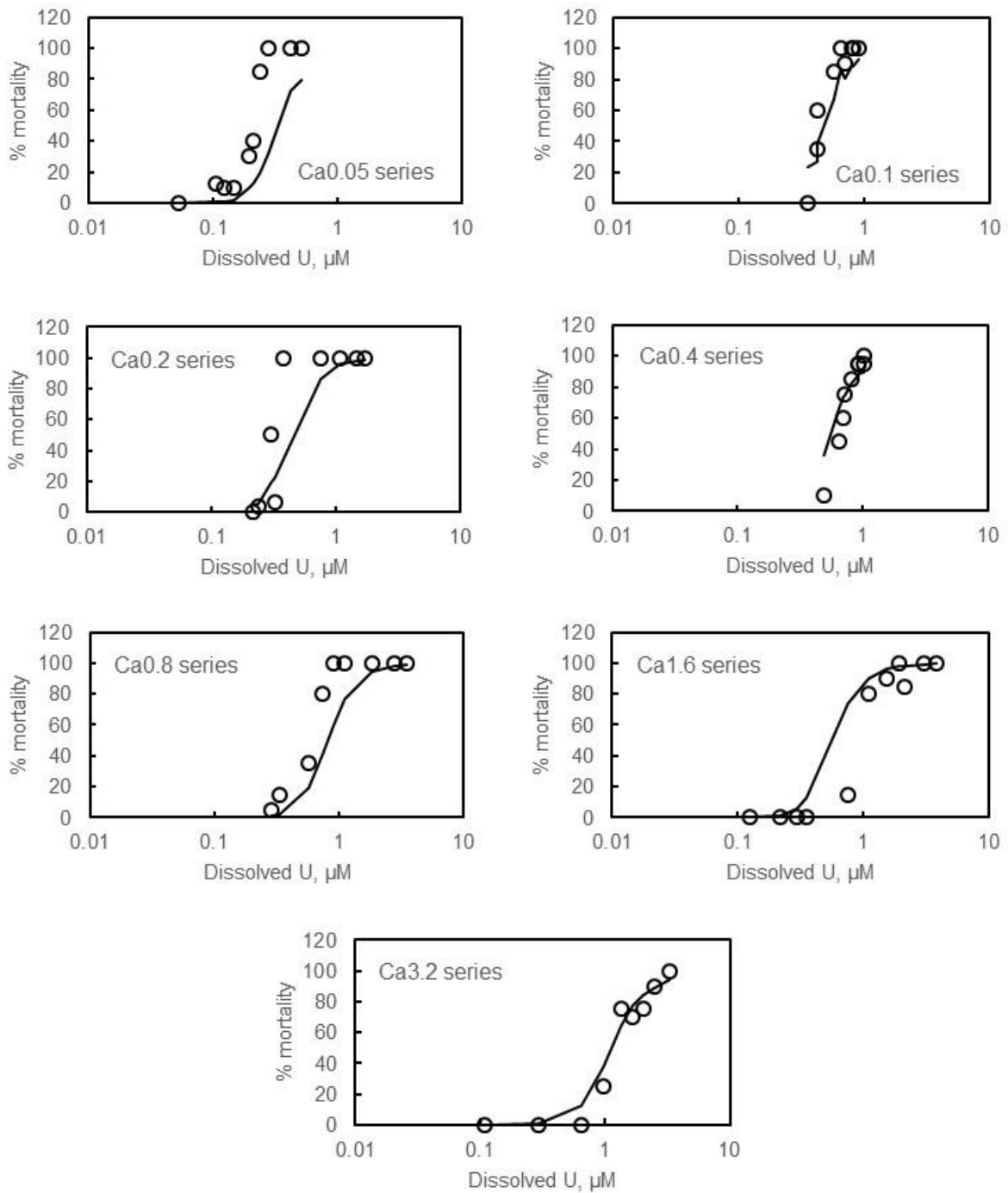


Figure 22. Observed and modelled mortality of *D. magna* in the Ca series of U exposures, plotted against the measured dissolved U (0.45µm filtered).

5 Modelling mixture accumulation and toxicity

Past work on applying BLMs to mixtures has had to confront the issue of model choice. Most of the studies carried out have assumed the potentially toxic species to bind at the same biotic ligand along with competing ions, and thus to potentially directly affect each other's uptake (e.g. Hatano and Shoji, 2008; Kamo and Nagai, 2008; Iwasaki et al., 2015). Other authors have employed a multi-site BLM, allowing potentially toxic metal ions to compete for binding at all sites but allowing binding to one site per metal to result in toxicity (Santore and Ryan, 2015). Any such approach is of necessity a simplification of the reality of metal ion uptake by cells, since different ions may be initially taken up by different active or passive transport mechanisms (ion channels). For example, copper is known to be taken up via sodium and potassium ion channels (e.g. Lauren and McDonald, 1986) and cadmium via calcium channels (e.g. Verbost et al., 1989).

Extending the U(VI) BLMs developed to consider mixtures of U(VI) with other metals thus requires a pragmatic choice of mixture BLM to be made. In the formulation of this work it was originally envisaged that U(VI) accumulation and toxicity to the test species could be adequately described by a single site BLM, readily extendible to consideration of mixtures by assuming Cd^{2+} to bind at the same site as UO_2^{2+} and the other competing ions. In practice, the relative complexity of UO_2^{2+} interactions with *L. minor* and *S. salar* drove the derivation of alternative, two-site models for these species. Extending such models for mixtures requires assessment of how the other metal species may interact with UO_2^{2+} at either or both sites.

The two-site model for *L. minor* and *S. salar* comprises one site at which UO_2^{2+} and H^+ both bind very strongly, to the extent that their interactions can be described by a single exchange constant, and one site where UO_2^{2+} binds relatively weakly, in competition with Mg^{2+} and Ca^{2+} (and H^+ in the case of *S. salar*). In extending this BLM to U–Cd mixtures it was assumed that Cd^{2+} binding would occur only at the second site. Values of $\log K_{\text{Cd}}$ were fitted to accumulation data for Cd exposure only, then toxicity in the same exposure was modelled from predicted accumulation. When extending the one-site models, Cd was assumed to bind at the single site in competition with the U(VI) species and competing ions.

Following parameterisation for Cd, the mixture BLMs were applied predictively to the accumulation and toxicity data for U(VI)–Cd mixtures. The MIXTOX model framework was used to investigate the presence of any deviations of the predictions from additivity, using both the concentration addition (CA) and independent action (IA) reference models.

5.1 *Lemna minor*

5.1.1 Cadmium accumulation and toxicity

For the one-site model, the accumulation of Cd was simulated assuming it to bind at the single site:

$$\{Cd - S\} = \{Cd-S\}_{bkg} + \{S\} \cdot \frac{K_{Cd} a_{Cd^{2+}}}{1 + K_{Cd} a_{Cd^{2+}} + \sum_1^i K_{X_i} a_{X_i}}$$

where X_i is a binding ion (either a U(VI) species or a competing major ion) and K_{X_i} is its binding constant. The binding site density $\{S\}$ and the binding constants for other binding ions were fixed to the values derived from modelling the U only accumulation and model fitting was done by optimising the Cd binding constant, K_{Cd} , and the ‘background’ accumulated Cd, $\{Cd-S\}_{bkg}$.

In the case of the two-site model, the expression for accumulation at Site 2 was extended to allow binding of Cd:

$$\{Cd - S\} = \{Cd-S\}_{bkg} + \{S_2\} \cdot \frac{K_{Cd,2} a_{Cd^{2+}}}{1 + K_{Cd,2} a_{Cd^{2+}} + K_{Mg,2} a_{Mg^{2+}} + K_{Ca,2} a_{Ca^{2+}}}$$

The parameters derived from fitting to U accumulation data were maintained at their values, and the model was fitted by adjusting the binding constant for Cd and the background accumulated Cd.

The model results are shown in Figure 23. Allowing for the presence of ‘background’ tissue Cd, i.e. Cd present in the plants prior to exposure, produced a statistically superior fit ($p = 1.58 \times 10^{-6}$ for the unconstrained one-site model, 5.87×10^{-7} for the constrained one-site model, and 5.86×10^{-7} for the two-site model). The optimal $\log K_{Cd}$ for the one-site model was 2.80 for the unconstrained one-site model and 3.03 for the constrained one site model, and the optimal $\log K_{Cd,2}$ for the two-site model was 6.73. The optimal ‘background’ Cd, $\{Cd-S\}_{bkg}$, was $0.5 \mu\text{mol/g d.w.}$ for all the models.

Modelling Cd toxicity was done using a similar model structure as for U toxicity, but assuming the ‘background’ Cd to have no toxic effect:

$$\% \text{ growth inhibition} = 100 - \frac{100}{1 + \left(\frac{\{Cd - S\} - \{Cd - S\}_{bkg}}{\{Cd - S\}_{EC50}} \right)^{\beta_{Cd}}}$$

Optimisation produced $\beta_{Cd} = 0.60$ and $\{Cd-S\}_{EC50} = 2.57 \mu\text{mol/g d.w.}$ for the one-site model, and $\beta_{Cd} = 0.61$ and $\{Cd-S\}_{EC50} = 2.92 \mu\text{mol/g d.w.}$ for the two-site model. The latter parameter is the accumulated Cd above the background at the EC50. The modelling results are shown in **Figure 24**. Both the one-site and two-site models give similar fits (root mean squared error in % growth inhibition was 2.54 in both cases).

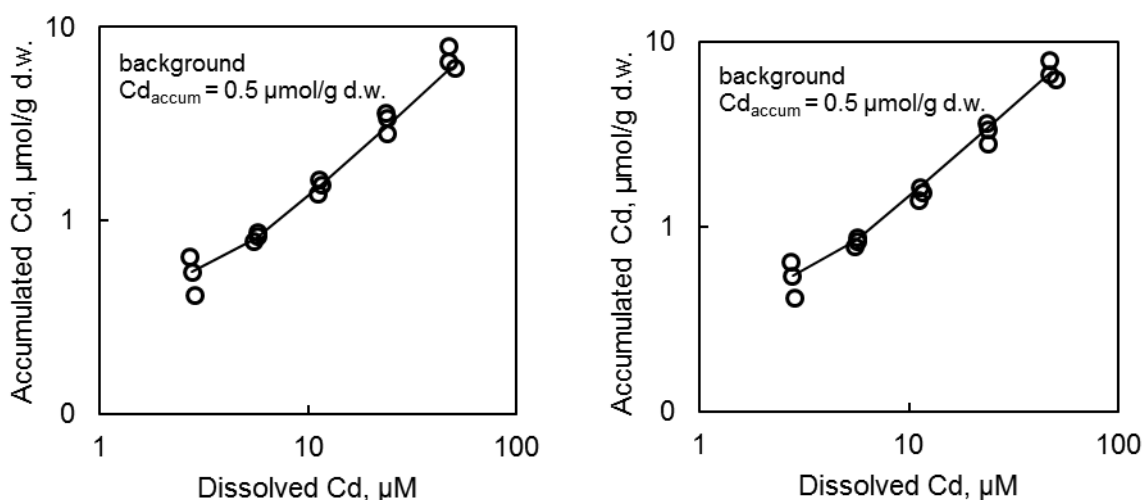


Figure 23. Observed and modelled accumulation of Cd by *L. minor* plotted against the dissolved Cd exposure concentration, for the one-site (left) and two-site (right) accumulation models.

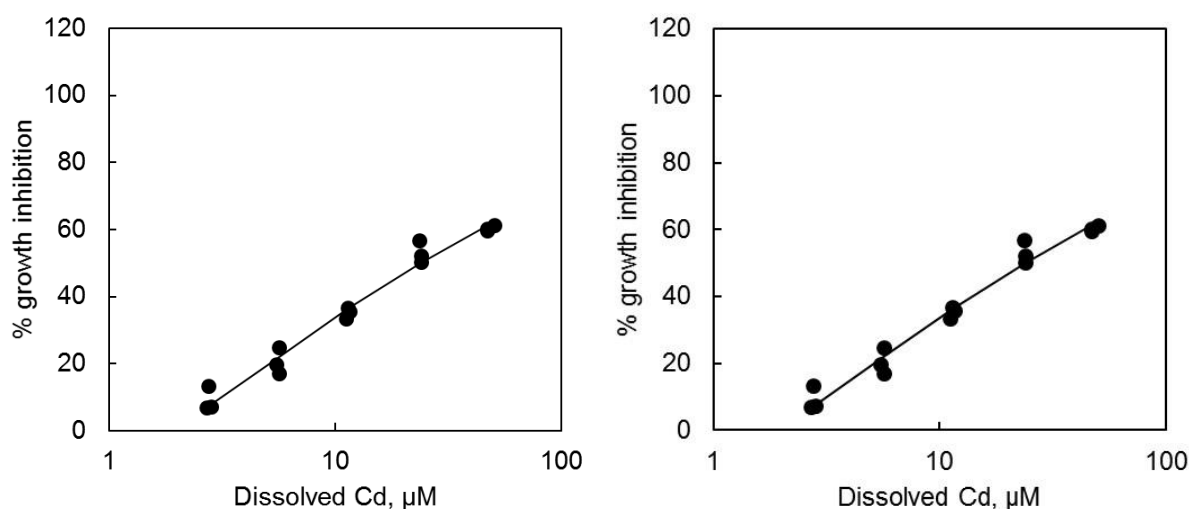


Figure 24. Observed and modelled growth inhibition in to Cd only exposure series of the mixture experiment, plotted against the exposure dissolved Cd, for the one-site (left) and two-site (right) accumulation models.

5.1.2 *Mixture accumulation*

Observed and predicted accumulation of U and Cd in the mixture exposures is shown in Figures 25-26 and compared with the results obtained by fitting to the single exposure accumulation data. In the case of U the predicted accumulation in the mixture exposures agrees well with the single exposure results, suggesting that U accumulation is not affected by the presence of Cd in the mixture exposures. In contrast, there is a clear influence of U on the

observed accumulation of Cd, which is not reproduced by the model. In a number of cases the observed Cd accumulation is below the ‘background’ accumulated Cd of 0.5 $\mu\text{mol/g d.w.}$.

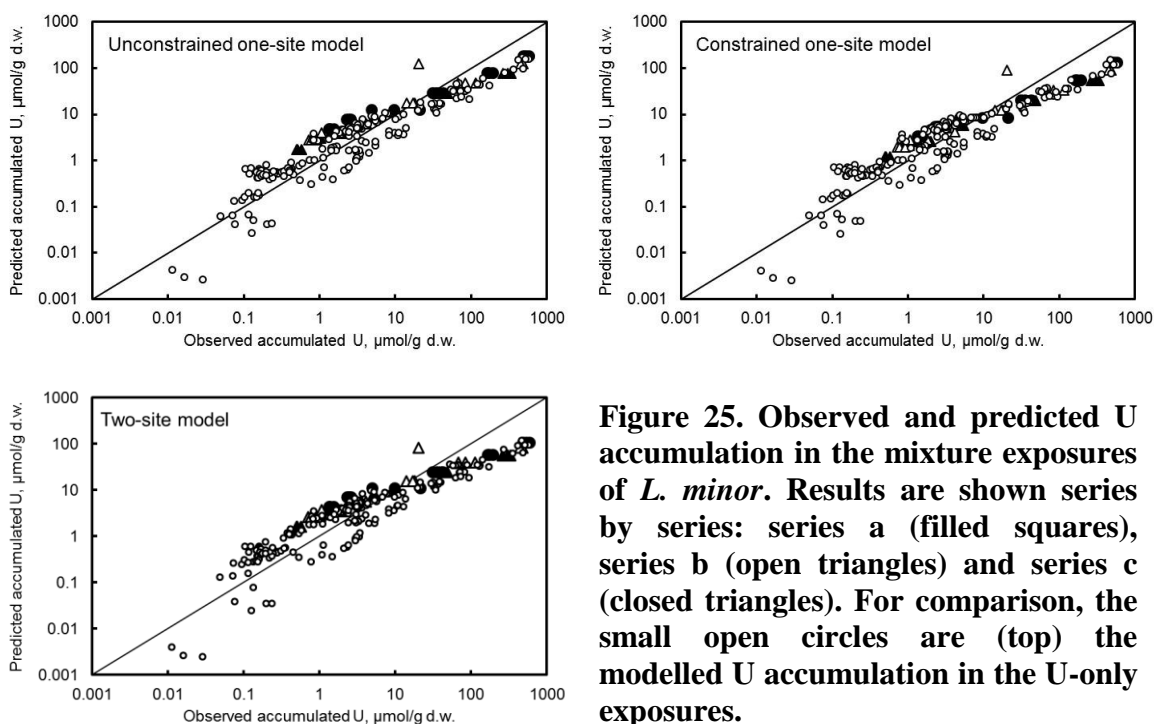


Figure 25. Observed and predicted U accumulation in the mixture exposures of *L. minor*. Results are shown series by series: series a (filled squares), series b (open triangles) and series c (closed triangles). For comparison, the small open circles are (top) the modelled U accumulation in the U-only exposures.

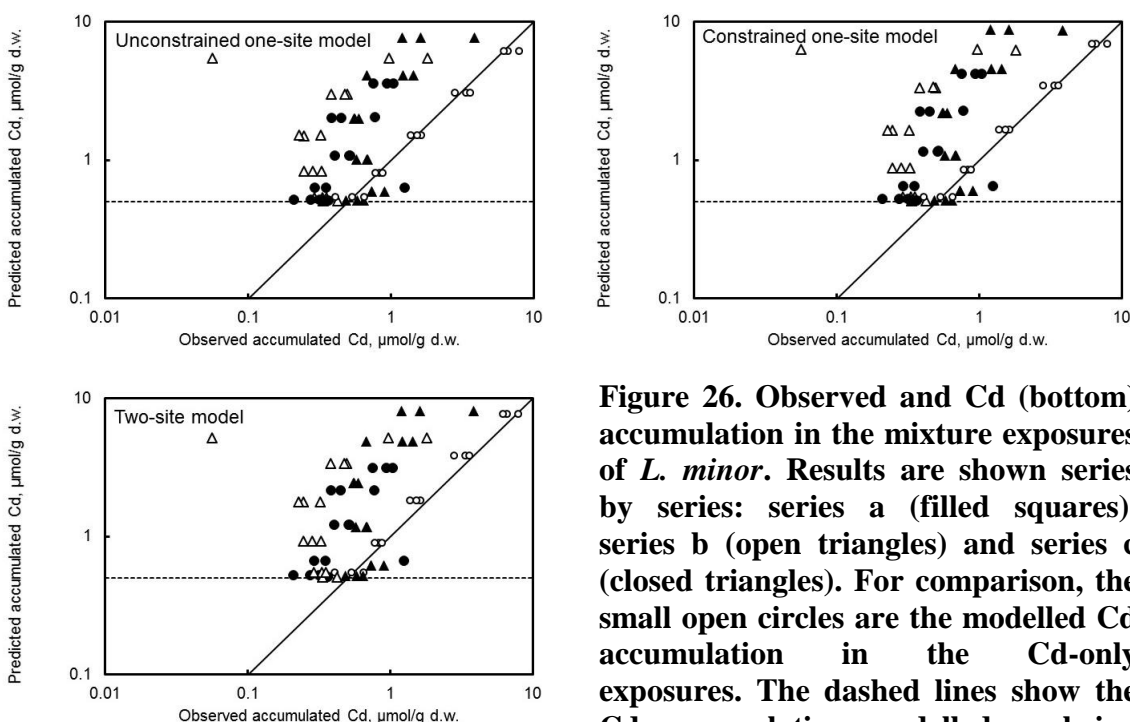


Figure 26. Observed and Cd (bottom) accumulation in the mixture exposures of *L. minor*. Results are shown series by series: series a (filled squares), series b (open triangles) and series c (closed triangles). For comparison, the small open circles are the modelled Cd accumulation in the Cd-only exposures. The dashed lines show the Cd accumulation modelled as being due to ‘background’ Cd in the tissues.

5.1.3 *Mixture toxicity*

The parameterised model was used to predict the toxic effect across the three series of U-Cd mixture exposures (a, b and c). The three series represent combined exposures varying the nominal concentrations of U and Cd at constant molar ratios of 3:1 (series a), 3:2 (series b) and 3:4 (series c). Predictions were made using both concentration addition (CA) and independent action (IA) as reference models.

Using the CA reference model, the expression for prediction of effect, assuming additivity, is

$$\frac{\{UO_2 - S\}}{\{UO_2 - S\}_{EC50} \left(\frac{Y_{mix}}{100 - Y_{mix}} \right)^{1/\beta_U}} + \frac{\{Cd - S\} - \{Cd - S\}_{bkg}}{\{Cd - S\}_{EC50} \left(\frac{Y_{mix}}{100 - Y_{mix}} \right)^{1/\beta_{Cd}}} = 1$$

and Y_{mix} is found by iteration (cf. Section 1.2.1), while for the IA reference model the expression is

$$\% \text{ growth inhibition} = 100 \cdot \left(1 - \frac{100}{\left[1 + \left(\frac{\{UO_2 - S\}}{\{UO_2 - S\}_{EC50}} \right)^{\beta_U} \right] \cdot \left[1 + \left(\frac{\{Cd - S\} - \{Cd - S\}_{bkg}}{\{Cd - S\}_{EC50}} \right)^{\beta_{Cd}} \right]} \right)$$

Table 14. Goodness-of-prediction and deviation modelling outcomes for predictions of combined U and Cd toxicity to *L. minor*.

Model	RMSE ^a (CA ^b)	RMSE (CA, S/A ^c)	a ^d	p ^e	RMSE (IA ^f)	RMSE (IA, S/A ^g)	a	p ^h
Unconstrained one-site	11.9	11.5	1.03	0.013	14.8	11.1	1.86	7.0 × 10 ⁻¹³
Constrained one-site	10.7	10.6	1.81	0.210	12.7	10.0	1.81	6.3 × 10 ⁻⁷
Two-site	9.4	8.8	1.07	0.047	12.0	7.7	1.81	6.4 × 10 ⁻⁷

^a root mean squared error in % growth inhibition.

^b concentration addition reference model.

^c concentration addition reference model with synergism/antagonism deviation function.

^d fitting parameter in synergism/antagonism deviation function.

^e p value for significance of CA, S/A model over CA model.

^f independent action reference model.

^g independent action reference model with synergism/antagonism deviation function.

^h p value for significance of IA, S/A model over IA model.

The model predictions are shown in Figure 27, Figure 28 and Figure 29, and measures of goodness-of-prediction as are presented in

Table 14. Generally, the two-site model gave the best effect predictions, and the concentration addition model performed better than did the independent action model. Significant ($p < 0.05$) deviation from the independent action reference model was shown for all three BLMs, and the unconstrained one-site and two-site models showed significant deviations from the concentration addition reference model. All the significant deviations from the reference models were antagonistic.

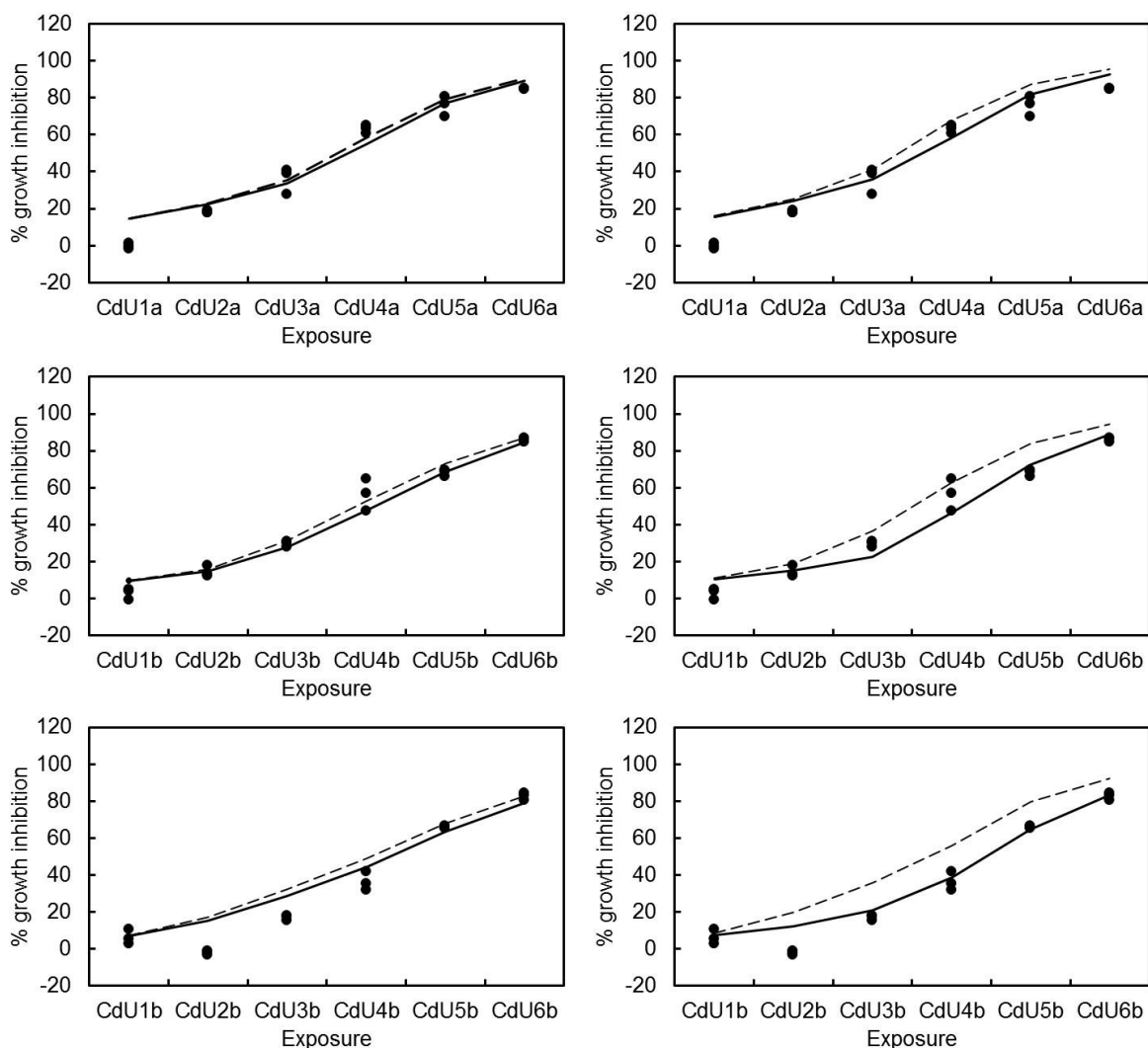


Figure 27. Predicted U-Cd mixture toxicity to *L. minor* using the unconstrained one-site model. Points are observed effects. The dashed lines show the prediction of effects according to the mixture BLM assuming additivity with the concentration addition reference model (left hand panes) and the independent action reference model (right hand panes). Solid lines show the fits obtained using the synergism/antagonism deviation model.

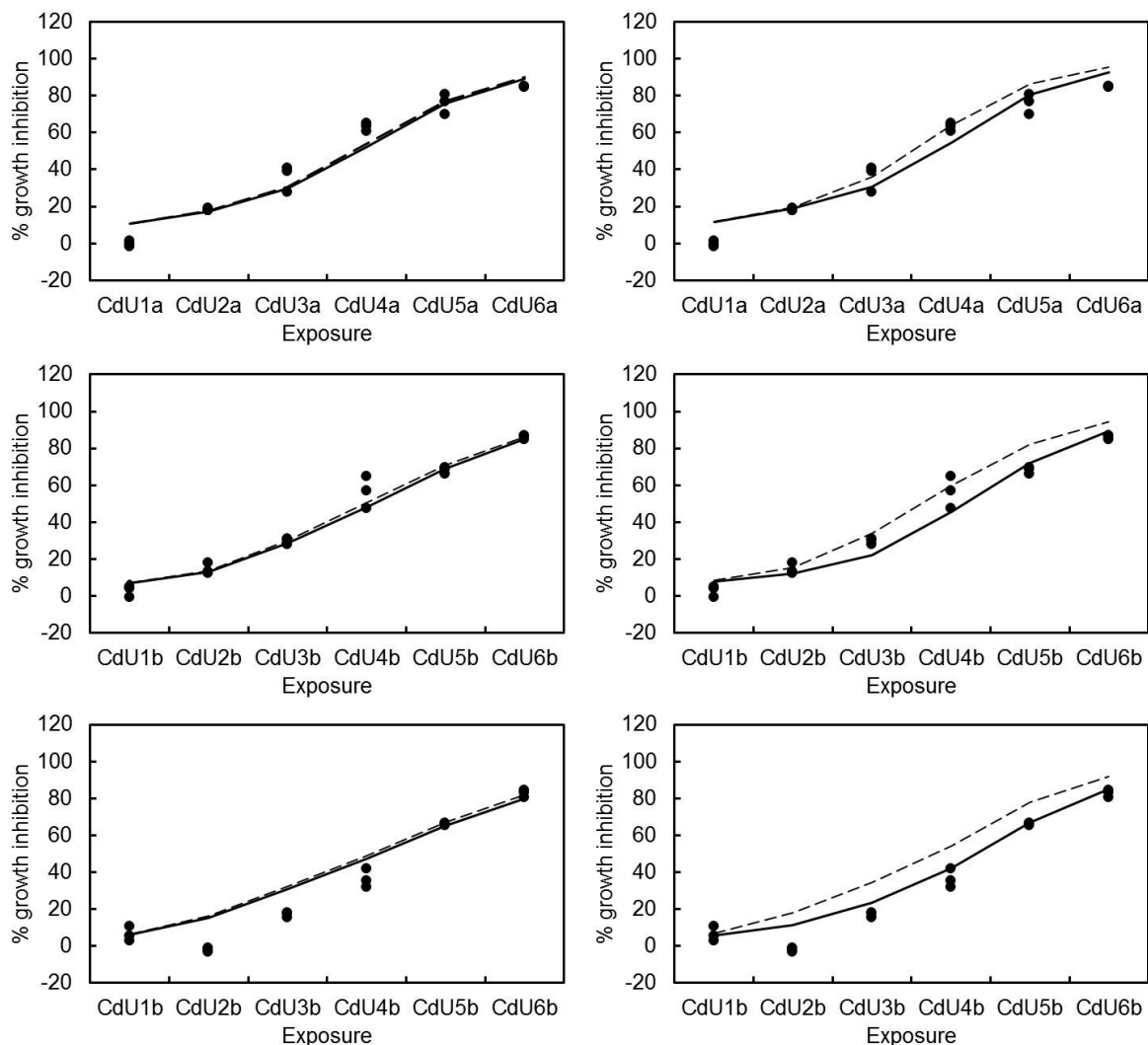


Figure 28. Predicted U-Cd mixture toxicity to *L. minor* using the constrained one-site model. Points are observed effects. The dashed lines show the prediction of effects according to the mixture BLM assuming additivity with the concentration addition reference model (left hand panes) and the independent action reference model (right hand panes). Solid lines show the fits obtained using the synergism/antagonism deviation model.

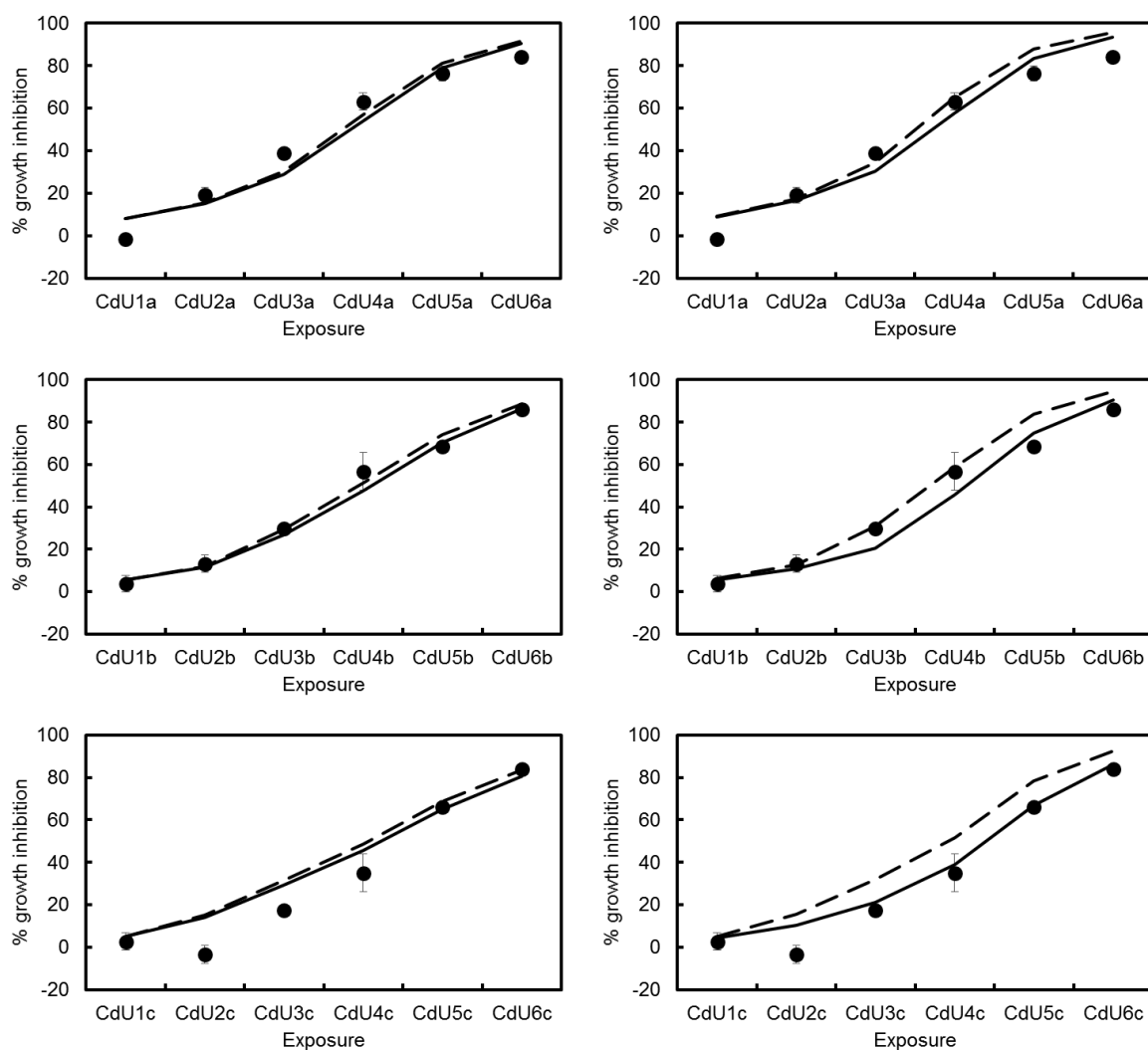


Figure 29. Predicted U-Cd mixture toxicity to *L. minor* using the two-site model. Points are observed effects. The dashed lines show the prediction of effects according to the mixture BLM assuming additivity with the concentration addition reference model (left hand panes) and the independent action reference model (right hand panes). Solid lines show the fits obtained using the synergism/antagonism deviation model.

5.2 *Salmo salar*

5.2.1 *Cadmium accumulation and toxicity*

The accumulation models were extended to describe Cd binding using the same approach as taken for *L. minor*. Because only U(VI) species bind in the unconstrained and constrained one-site models, the Cd accumulation parameters were the same for both models. The optimised $\log K_{Cd}$ was 5.80 and the optimal background Cd was 0.0038 $\mu\text{mol/g d.w.}$. For the two-site model, the optimal $\log K_{Cd,2}$ was 9.03 and the optimal background Cd was 0.0039

$\mu\text{mol/g}$. The goodness-of-fits were similar, with the root mean squared error in log (accumulated Cd) being 17.0 for the one-site model and 17.4 for the two-site model. The best fits to accumulation are shown in Figure 30.

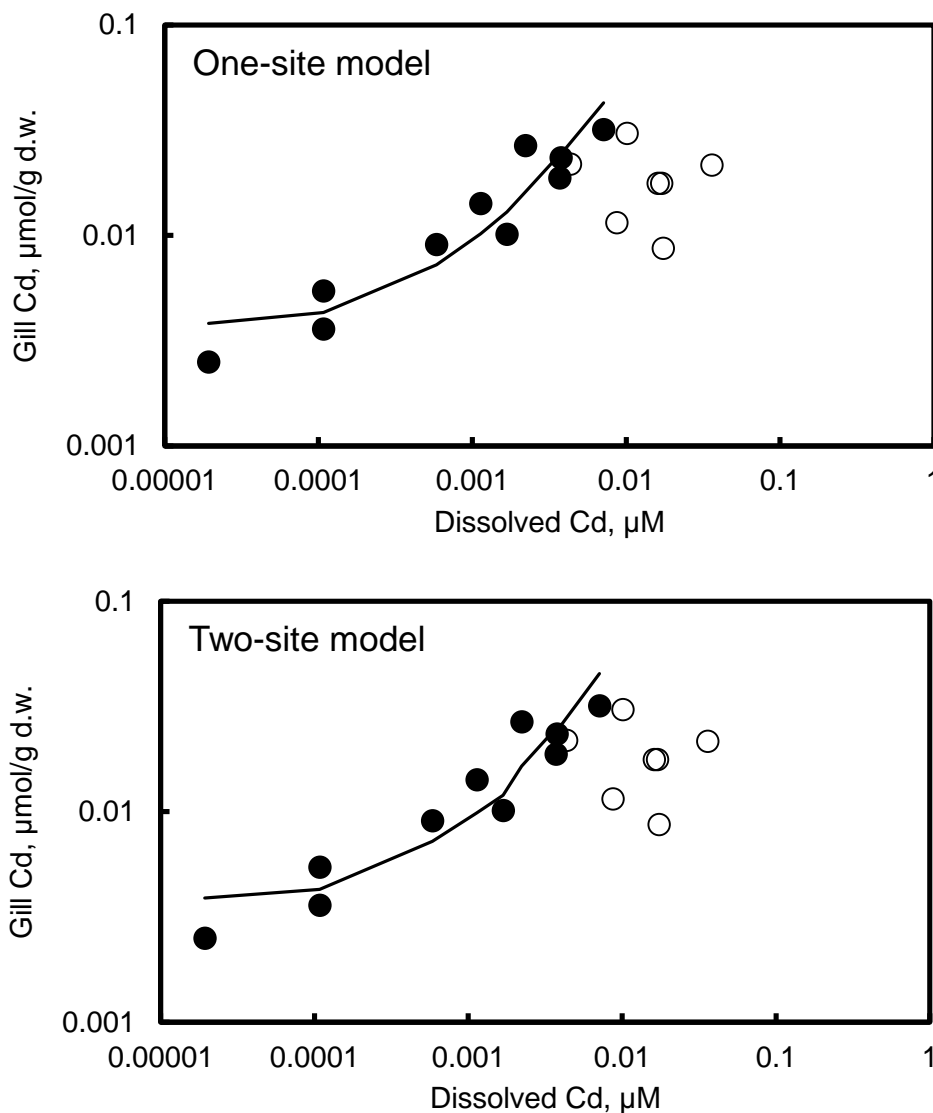


Figure 30. Observed and modelled accumulation of Cd on gills of *S. salar*, plotted against the dissolved Cd exposure concentration. Filled points are those from exposures with zero mortality and used for fitting. Open points are those from exposures with partial mortality, and not used for fitting.

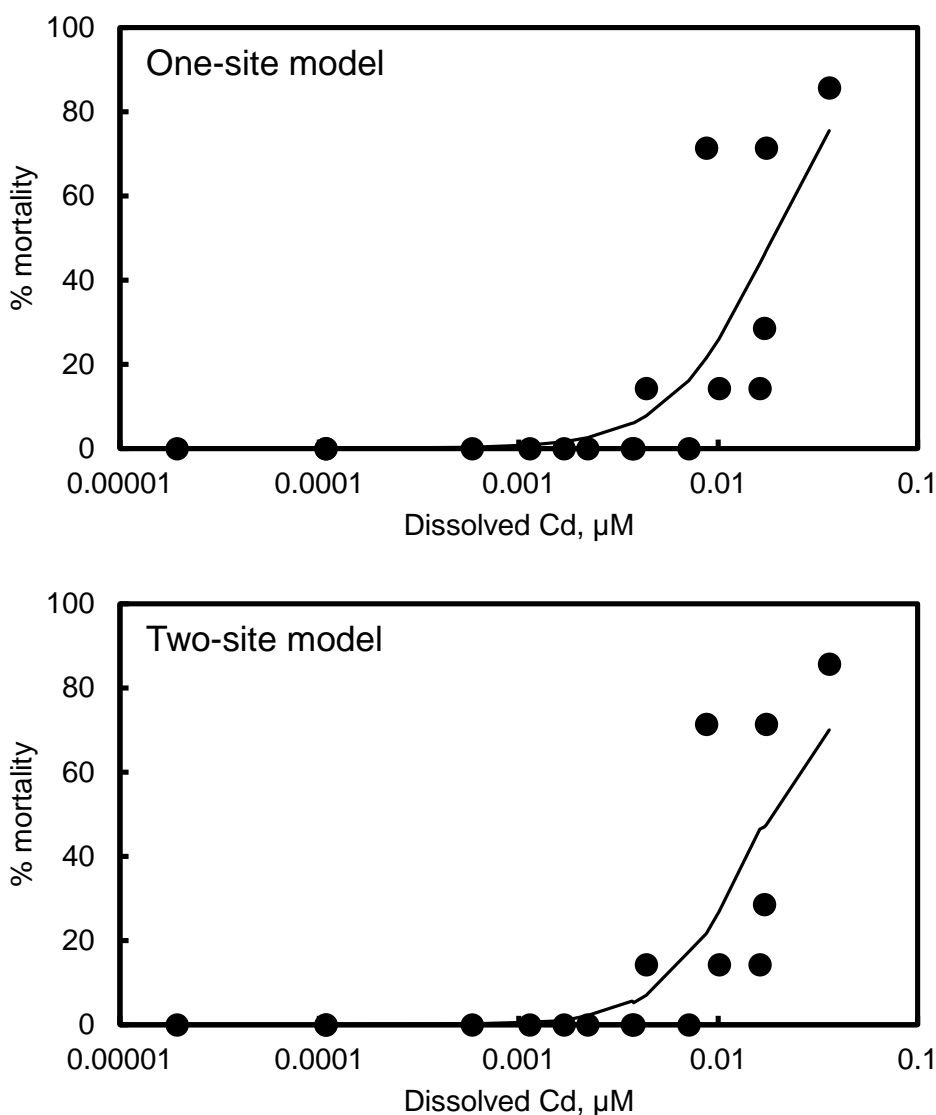


Figure 31. Observed and modelled toxicity of Cd to *S. salar*, plotted against the dissolved Cd exposure concentration.

Toxicity was modelled by applying the same dose-response model as was used for *L. minor*. Figure 31 shows the optimised relationship between the measured dissolved Cd in the exposure medium and the toxic response. The optimised $\{Cd-S\}_{EC50}$ values were 0.102 and 0.96 $\mu\text{mol/g d.w.}$ for the one-site and two-site models, respectively. The optimal β_{Cd} values were 1.72 and 1.87 respectively. The goodnesses-of-fit were similar, with the RMSE in % mortality being 17.0 for the one-site model and 17.6 for the two-site model.

5.2.2 Mixture accumulation

The parameterised model was applied predictively to the observed accumulation and effect in U–Cd mixtures. Figure 32 shows the observed and modelled accumulation of Cd on *S. salar*

gills for four exposure series where the nominal dissolved U was maintained constant and nominal dissolved Cd varied. The three alternative BLMs provide similar predictions of Cd accumulation in the presence of U, and all tend to overestimate Cd accumulation in mixed exposure with U. Predictions of U accumulation in the mixed exposures are shown in Figure 33. The three BLMs give very similar predictions of U accumulation in the presence of Cd. There is a tendency to underestimate U accumulation, however this is also seen in the fits to U only exposures and so does not imply that there is significant competition from Cd for U uptake.

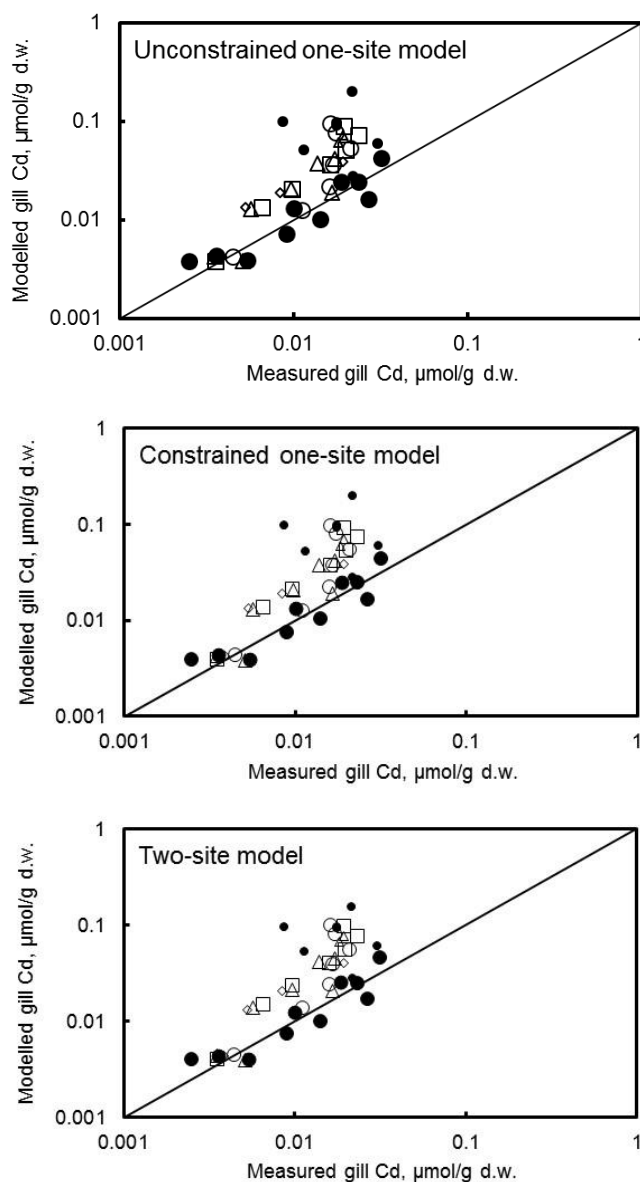


Figure 32. Observed and modelled accumulation of Cd on *S. salar* gills in the presence of varying concentrations of U and Cd in solution. Points represent Cd accumulation in the presence of the following nominal concentrations of dissolved U: open circles: 4.20 μM ; open squares: 8.40 μM ; open triangles: 9.87 μM ; open diamonds: 11.3 μM . Closed circles: exposures in the absence of U. Small points represent exposures with partial mortality.

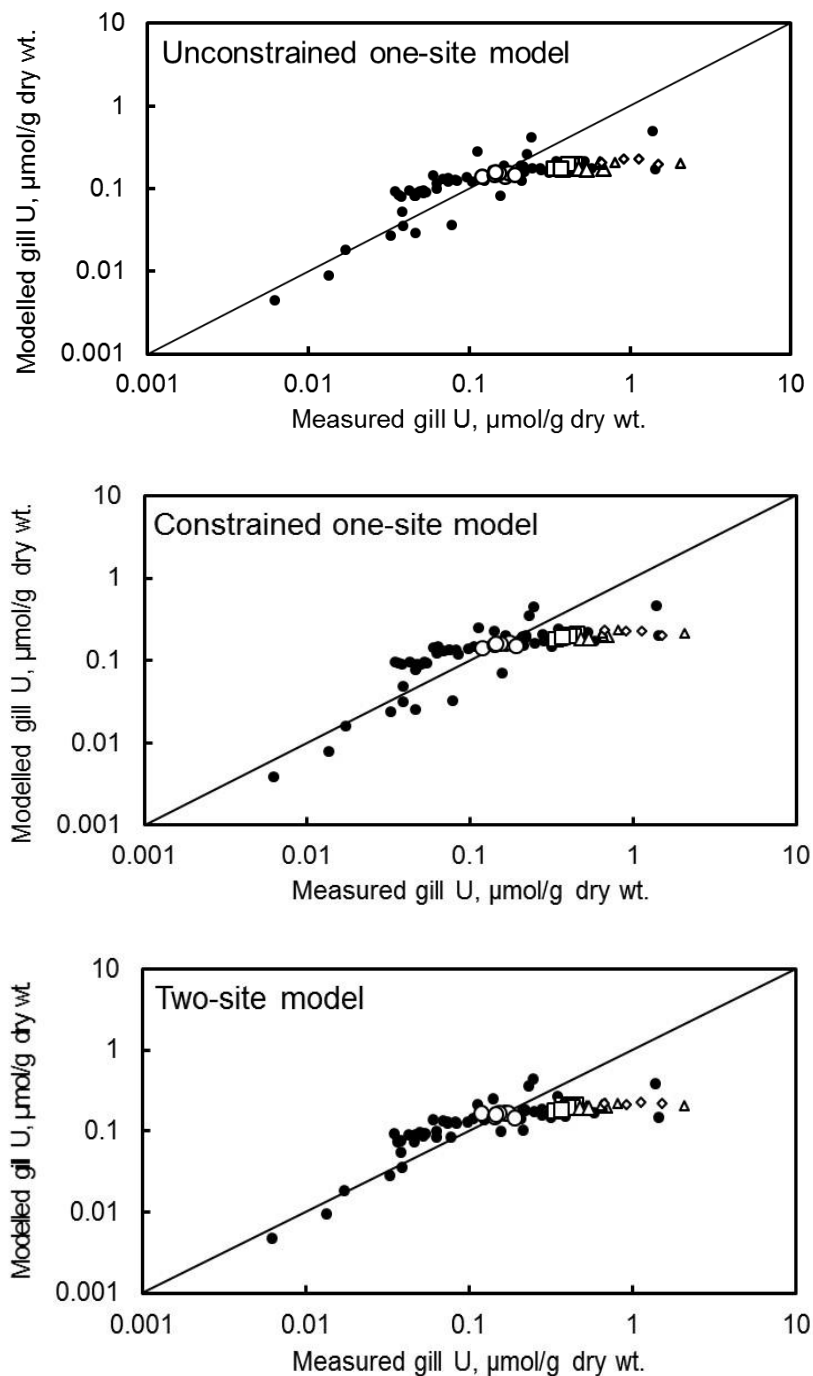


Figure 33. Observed and predicted U accumulation on *S. salar* gills in the presence of Cd. Points represent accumulation from solutions with different nominal dissolved U concentrations: open circles: 4.20 μM ; open squares: 8.40 μM ; open triangles: 9.87 μM ; open diamonds: 11.3 μM . Small points represent exposures with partial mortality. The closed circles are the modelled U accumulation in the U-only exposures.

5.2.3 *Mixture toxicity*

Consideration of mixture toxicity used the same expressions as for mixture toxicity of *L. minor* (Section 5.1.3). Table 15 shows the goodnesses-of-prediction for the application of the three BLMs to the mixture effect data. The unconstrained one-site model provides the closest predictions using either reference model (Figure 34 and Figure 35). Modelling overestimates mortality at the two lowest nominal U concentrations (4.20 and 8.40 μM) and overestimates it at the highest nominal concentration of 11.3 μM . Further figures, for the constrained one-site and two-site models, are in Annex 4.

Table 15. Goodness-of-prediction and deviation modelling outcomes for predictions of combined U and Cd toxicity to *S. salar*.

Model	RMSE ^a (CA ^b)	RMSE (CA, S/A ^c)	a ^d	p ^e	RMSE (IA ^f)	RMSE (IA, S/A ^g)	a	p ^h
Unconstrained one-site	52.4	29.6	2.70	1.5×10^{-8}	28.4	21.7	3.21	9.6×10^{-5}
Constrained one-site	49.3	29.7	2.61	9.8×10^{-8}	27.2	23.2	2.31	0.0030
Two-site	58.4	29.4	2.59	5.6×10^{-10}	32.7	24.1	4.88	3.6×10^{-5}

^a root mean squared error in % growth inhibition.

^b concentration addition reference model.

^c concentration addition reference model with synergism/antagonism deviation function.

^d fitting parameter in synergism/antagonism deviation function.

^e p value for significance of CA, S/A model over CA reference model.

^f independent action reference model.

^g independent action reference model with synergism/antagonism deviation function.

^h p value for significance of IA, S/A model over IA reference model.

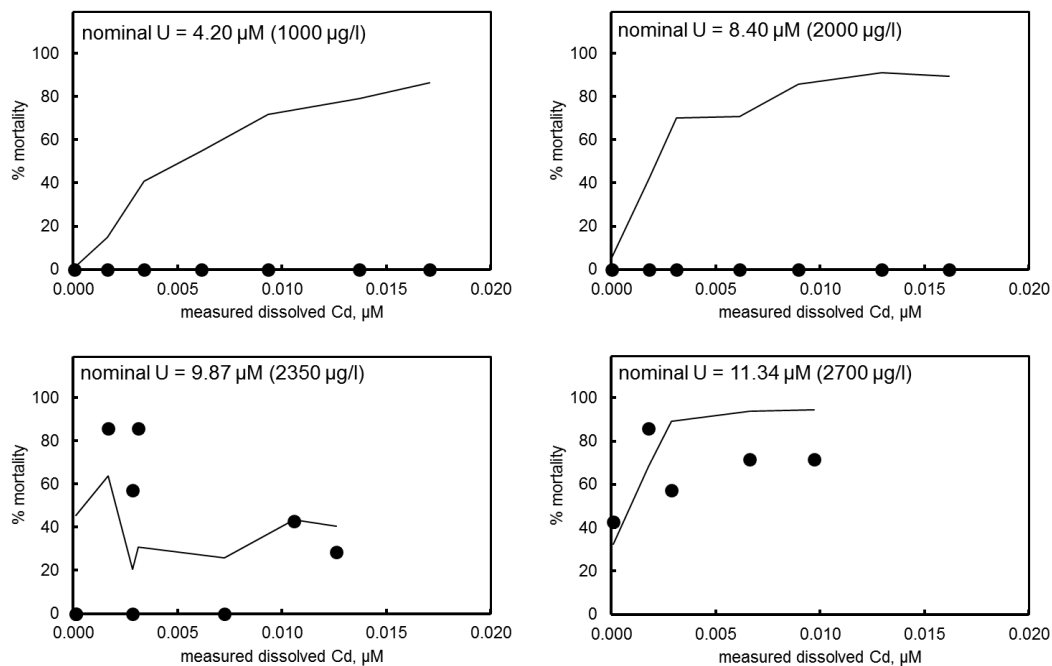


Figure 34. Modelled toxicity of U–Cd mixtures to *S. salar* using the unconstrained one-site BLM and concentration addition reference model . Data are presented in series where nominal dissolved U is constant and dissolved Cd is varied. Solid lines are the reference model predictions.

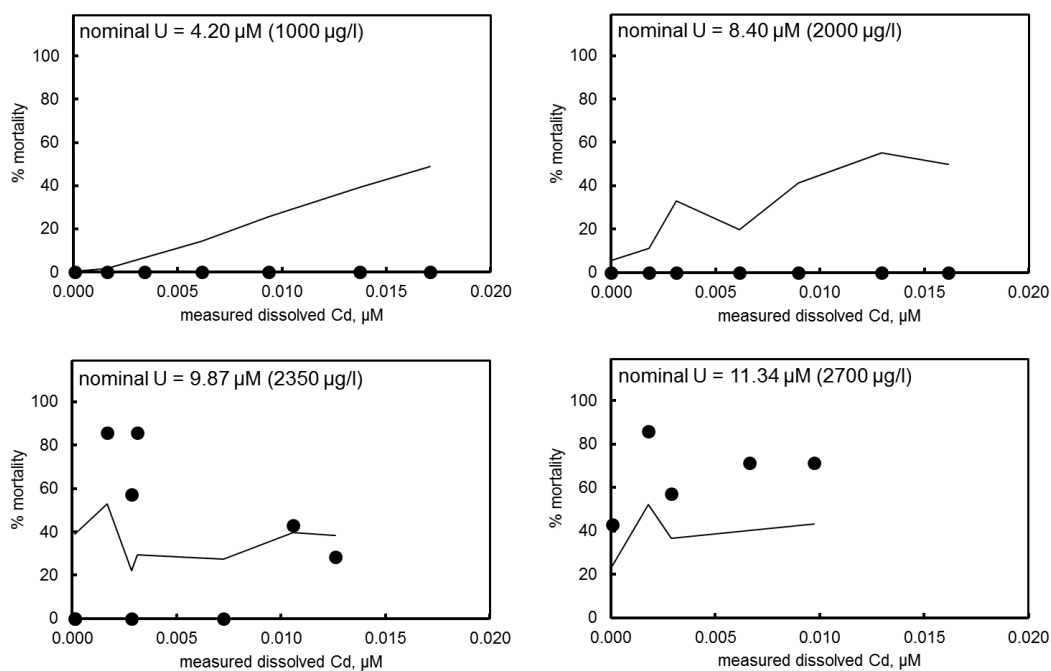


Figure 35. Modelled toxicity of U–Cd mixtures to *S. salar* using the unconstrained one-site BLM and independent action reference model . Data are presented in series where nominal dissolved U is constant and dissolved Cd is varied. Solid lines are the reference model predictions.

5.3 *Daphnia magna*

Modelling the mixture toxicity of *D. magna* presents specific issues due to the lack of accumulation data. In the cases of *L. minor* and *S. salar* it is possible to fit 50% lethal accumulation concentrations ($\mu\text{mol/g d.w.}$) for uranium and cadmium separately. The relative values of these parameters then behave as relative toxic potencies in mixture modelling. In the case of *D. magna* it is necessary instead to fit the relative potency of the bound species. In fitting the *D. magna* BLM for U(VI) alone, the fractional occupancy of the biotic ligand corresponding to a 50% effect on survival ($f_{\text{UO}_2\text{BL,L(E)C50}}$) was fixed for modelling to a value of 0.1. Similarly fixing the corresponding value for cadmium is not feasible since this would control the optimised biotic ligand binding constant in fitting to cadmium only exposure data, and thus determine the strength of competition between Cd and U(VI) at the biotic ligand. In order to avoid this, both the cadmium only and Cd-U(VI) data were fitted in a single step, adjusting the following parameters:

- $\log K_{\text{Cd}}$, the biotic ligand binding constant for Cd;
- $f_{\text{S,Cd,L(E)C50}}$, the fractional occupancy of the biotic ligand by cadmium alone resulting in a 50% effect;
- β_{Cd} , the slope of the cadmium dose–response curve.

All other BLM parameters were maintained at the values given in Table 12. Thus, in the CA and IA model expressions:

$$\frac{f_{S,UO2}}{f_{S,UO2,L(E)C50} \left(\frac{Y_{mix}}{Y_{max} - Y_{mix}} \right)^{1/\beta_U}} + \frac{f_{S,Cd}}{f_{S,Cd,L(E)C50} \left(\frac{Y_{mix}}{Y_{max} - Y_{mix}} \right)^{1/\beta_{Cd}}} = 1$$

and

$$Y_{mix} = 100 \cdot \left(1 - \frac{100}{\left[1 + \left(\frac{f_{S,UO2}}{f_{S,UO2,L(E)C50}} \right)^{\beta_U} \right] \cdot \left[1 + \left(\frac{f_{S,Cd}}{f_{S,Cd,L(E)C50}} \right)^{\beta_{Cd}} \right]} \right)$$

the fractional occupancy of the biotic ligand by Cd is given by

$$f_{S,Cd} = \frac{K_{Cd} a_{Cd,2+}}{1 + K_{Cd} a_{Cd,2+} + K_{UO2} a_{UO2,2+} + \sum_1^i K_{UO2L,i} a_{UO2L,i} + \sum_1^j K_{X,j} a_{X,j}}$$

where $a_{Cd,2+}$ is the solution activity of the Cd free ion and the other terms are as in the expression for U(VI) species binding (Section 4.4.6).

Separate fits were done using both the CA and IA reference models, and deviation functions were fitted to assess whether there was any significant residual synergism or antagonism predicted following fitting.

Fits are shown in Figure 36 and Figure 37 and fitting parameters are provided in

Table 16. The optimised CA reference model underestimated survival and including the synergism/antagonism deviation function produced a statistically better fit than the reference model ($p \chi^2 < 0.05$); in other words, obtaining the best possible fit optimising U–Cd competition could not account for all non-additive behaviour. The optimised IA reference model overestimated survival, and thus the synergism/antagonism model produced a statistically better fit than the reference model ($p \chi^2 < 0.05$). As with the CA reference model, obtaining the best possible fit optimising U–Cd competition at the biotic ligand did not completely account for non-additive behaviour.

In general the fits using the IA as reference model were inferior to those obtained using CA as reference. Notably, fitting to the IA reference model produced a slope of Cd dose–response clearly lower than that observed in the Cd only exposures (Figure 37, top) and did not predict

any % survival above approximately 60% in the varying ratio mixture exposure (Figure 37, bottom). Furthermore, the optimised $f_{CdBL,LC50}$ values are extremely low relative to those obtained using the CA reference model and suggest that bound Cd is around six orders of magnitude more potent than U(VI) for *D. magna*. In contrast, when using the CA models the fitted slopes were reasonably consistent regardless of the deviation function all the significant fitted models were able to reproduce the full range of % survival observed in the varying ratio mixture exposure series.

Table 16. Parameters for Cd BLM fitting and U(VI)–Cd mixture modelling for *D. magna*.

	CA ^b	CA_SA ^c	IA ^d	IA_SA ^e
$\log K_{Cd}$	5.53	5.40	1.89	1.85
$f_{CdBL,LC50}$	0.0013	0.00091	2.3×10^{-7}	2.5×10^{-7}
β_{Cd}	5.52	5.90	2.43	5.44
RMSE ^a	18.1	15.9	23.4	15.9
$p\chi^2$ ^f	—	5.0×10^{-11}	—	9.1×10^{-30}
a ^g	—	0.63	—	-5.18

^a root mean squared error in % mortality.

^b concentration addition reference model.

^c concentration addition reference model with synergism/antagonism deviation function.

^d independent action reference model.

^e independent action reference model with synergism/antagonism deviation function.

^f p value for significance of S/A model over reference model.

^g fitting parameter in synergism/antagonism deviation function.

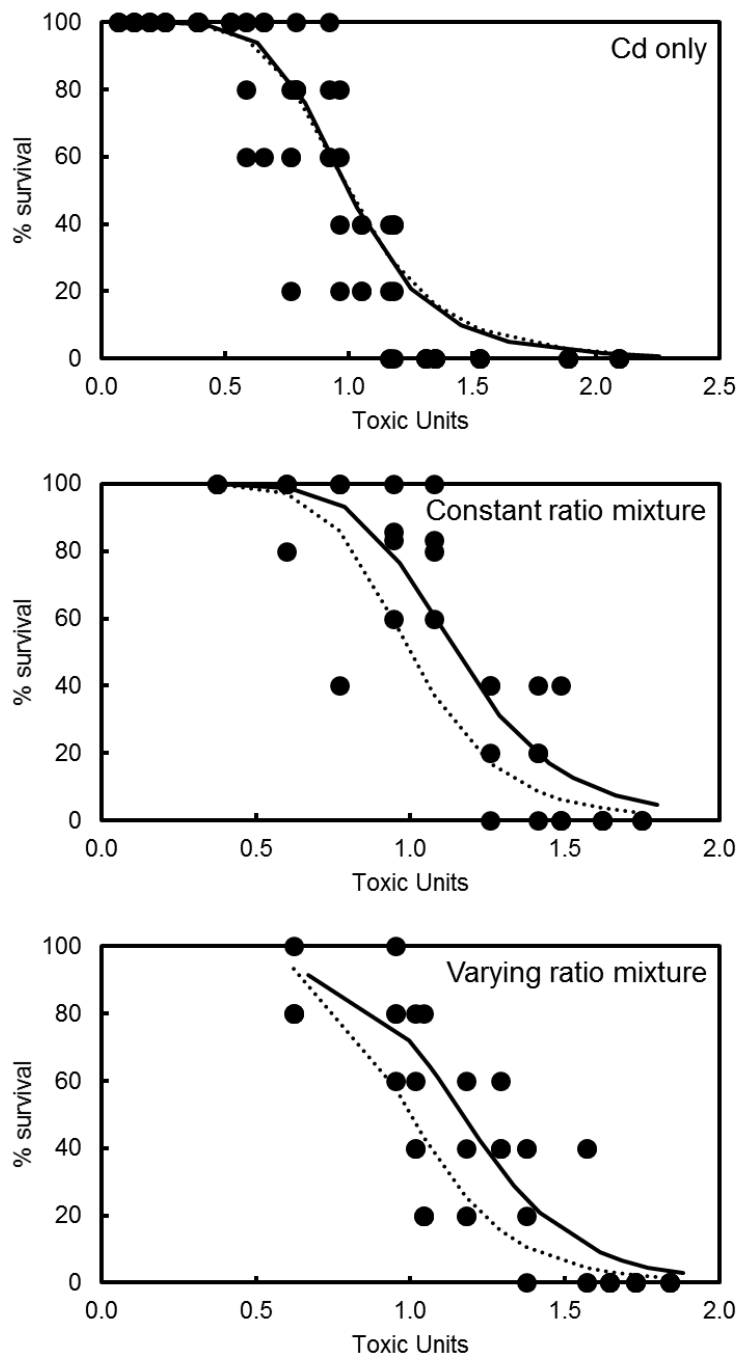


Figure 36. Modelling of Cd toxicity to *D. magna* in Cd-only exposures (top), the constant ratio U-Cd exposure series (middle) and the varying ratio U(VI)-Cd exposure series (bottom). Dotted lines: fit using CA reference model; solid lines: fit using CA model with synergistic/antagonistic deviation function.

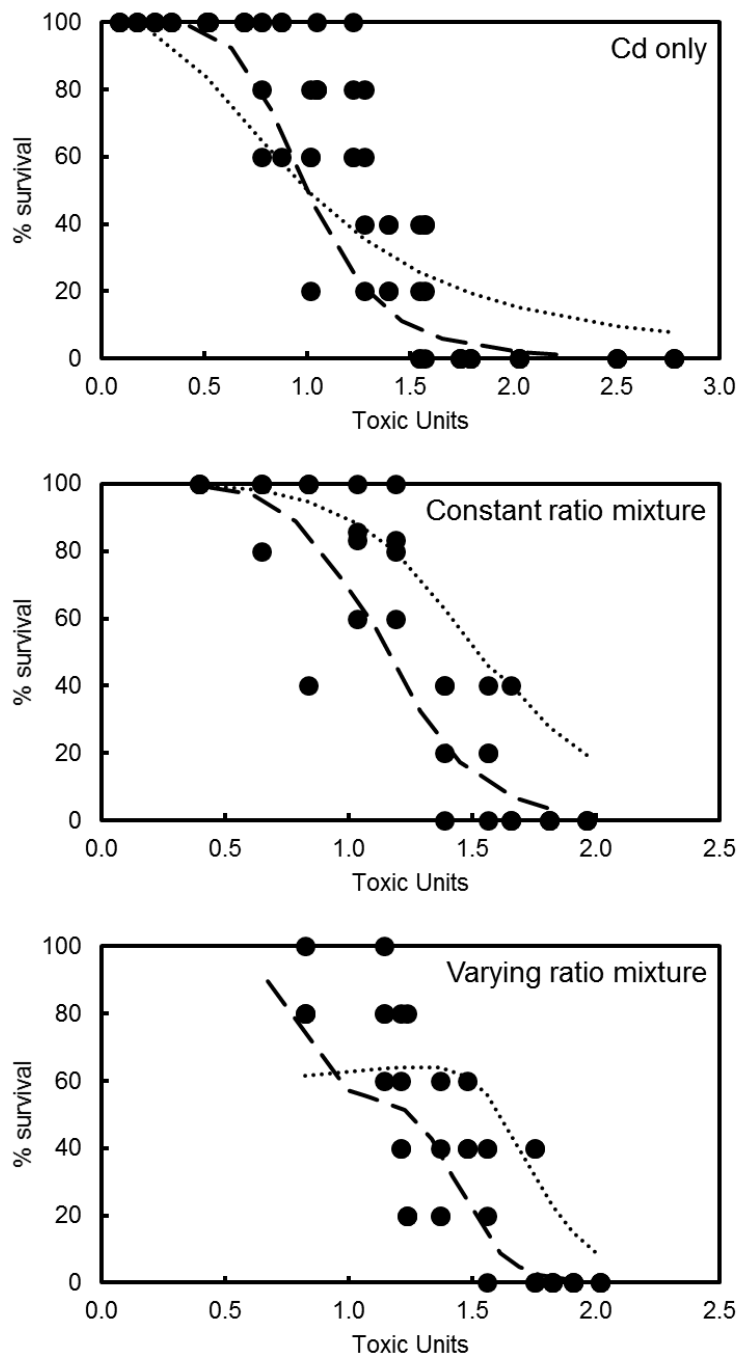


Figure 37. Modelling of Cd toxicity to *D. magna* in Cd-only exposures (top), the constant ratio U-Cd exposure series (middle) and the varying ratio U(VI)-Cd exposure series (bottom). Dotted lines: fit using IA reference model; dashed lines: fit using IA model with synergistic/antagonistic deviation function.

6 Discussion, Highlights and Conclusions

In these studies, we have measured and modelled the influence of major ion and trace metal competition on the exposure of U to test organisms and the toxic effects, under laboratory conditions. A necessary underpinning to this work was the production of an updated database of solution binding constants for the WHAM7 model, based on the outcomes of Deliverable N°.4.1 (Vandenhove et al., 2012b). The experimental BLM studies clearly showed that changing the exposure medium composition influenced U(VI) toxicity to all three organisms studied. Development of Biotic Ligand Models for all three organisms confirmed the first two hypotheses developed to guide the work (Section 2.2): The bioavailability of U(VI) to organisms will exhibit statistically significant variations in response to the exposure medium used and the variations in U(VI) bioavailability can be described by organism-specific Biotic Ligand Models (BLMs) that take into account the chemical speciation of U(VI) and competition of binding uranyl species with major cations.

Common patterns of uptake and toxicity for the three species tested, in response to changing water compositions, were sought. For *S. salar* and *L. minor*, the search for patterns was facilitated by the quantification of U(VI) uptake addition to toxicity. Particularly in toxicity tests on *S. salar*, where the onset of mortality occurred rather abruptly in relation to increasing dissolved U concentrations, modelled patterns of sublethal uptake to the gills provided a more subtle, graduated response to increasing exposure and the modifying influence of water chemistry than did mortality itself.

The clearest common pattern in the effect response for the three organisms was in relation to pH. There was a large effect of pH on endpoints when expressed as measured dissolved U (Figure 38). The EC50 for *S. salar* varied over 1.5 orders of magnitude over the pH range 5.5–7.9 and the EC50 for *D. magna* varied over two orders of magnitude over the pH range 6.0–8.0 (Figure 38). These are not large variations when compared to the variability in dissolved metal endpoints for other metallic toxicants; for example, De Schamphelaere and Janssen (2002) found a variation in EC50 for copper toxicity to *D. magna* of nearly an order of magnitude over the same pH range as that used for *D. magna* here. However, when toxicity is expressed in terms of the free ion, a distinct pattern is seen for U(VI). Comparing $\log(1/LC50_{M^{2+}})$ for U(VI) and Cu effects on *D. magna* (Figure 39) shows that as pH increases, the free uranyl ion in solution at the LC50 decreases much more rapidly than does the free copper ion. In other words, the apparent competitive effect of the proton on uptake is much larger for the free uranyl ion than it is for the copper ion. If the apparent competitive effect of the proton on U(VI) were of similar magnitude to that for copper, then we would expect to see a large decrease in the LC50 for dissolved U as pH increased, with concomitant decreases in uptake. This is due to the extent of U(VI) complexation by inorganic ligands (particularly carbonate) as the pH increases, higher than for copper and other trace metals, which reduces the free ion relative to the dissolved uranyl by several orders of magnitude. Uptake (i.e. accumulated U) for *S. salar* and *L. minor* did decrease with increasing pH, but not by as much as would be predicted by a conventional BLM. Similar trends in effect endpoints for all three organisms can be seen above pH6 (Figure 40).

This strong apparent proton competition means that the conventional BLM, where the free metal ion and competing ions bind to the biotic ligand on a 1:1 basis, does not work for U(VI). Strong effects of pH on U(VI) uptake and toxicity have previously been observed. Alves et al. (2008) studied U(VI) uptake and toxicity for the benthic amphipod *Hyaletta azteca* and successfully modelled the pH effect by assuming free uranyl–proton competition to occur at a site binding four protons. Their results are shown in Figure 40 for comparison with the organisms studied here. The slope of $\log(1/LC50_{UO_2,2+})$ against pH for *H. azteca* is 3.7, which is substantially higher than the slopes of approximately two found for our organisms above pH6. A note of caution, however, is required, since Alves et al. (2008) calculated U(VI) speciation using a different model/database combination to that used here. For complete consistency, a common approach to speciation modelling, including database composition, is ideally required.

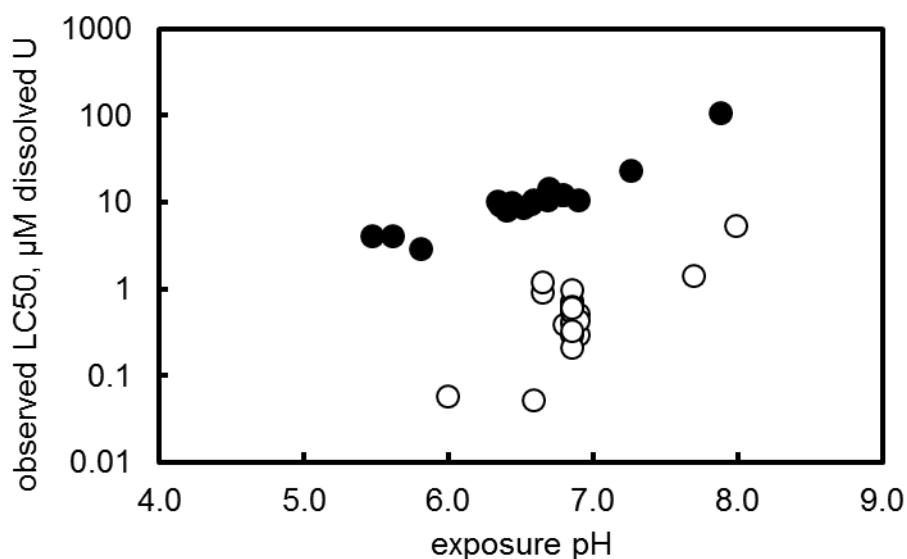


Figure 38. Observed endpoints (LC50s) for *S. salar* (closed points) and *D. magna* (open points) as a function of exposure medium pH.

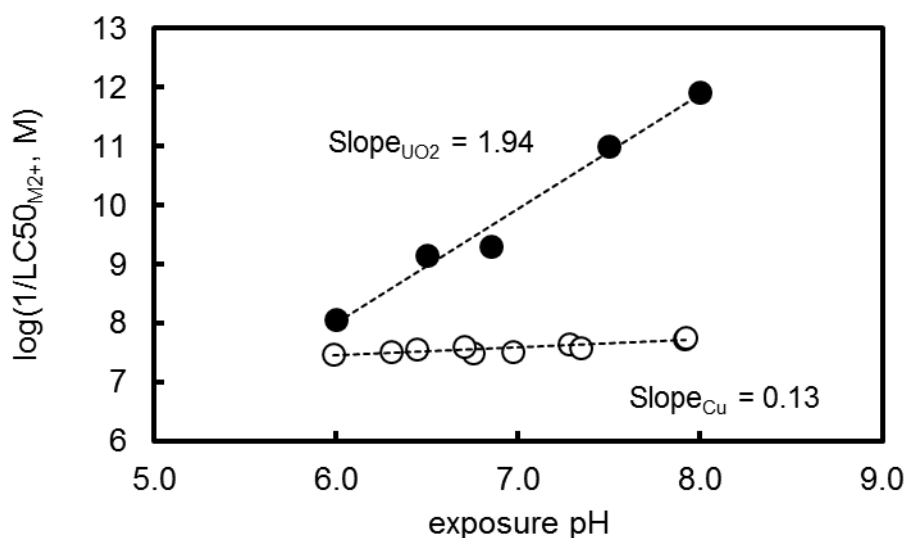


Figure 39. Comparison of pH effects on the LC50s of Cu (open points; De Schamphelaere and Janssen, 2002) and U(VI) (closed points; this study) for *D. magna*.

Fortin et al. (2007) studied the uptake of U(VI) by the green alga *Chlamydomonas reinhardtii* at pH5 and pH7 and found that the maximum uptake rate at pH7 was much larger than that at pH5. They concluded that “the simple proton–metal competition described by the biotic ligand model cannot successfully depict uranium–algae interactions”, which is in accordance with our findings. By conducting studies using three different organisms, we have provided strong evidence that this distinctive pattern of pH effect on uptake is a general phenomenon for U(VI) accumulation and toxicity to aquatic organisms.

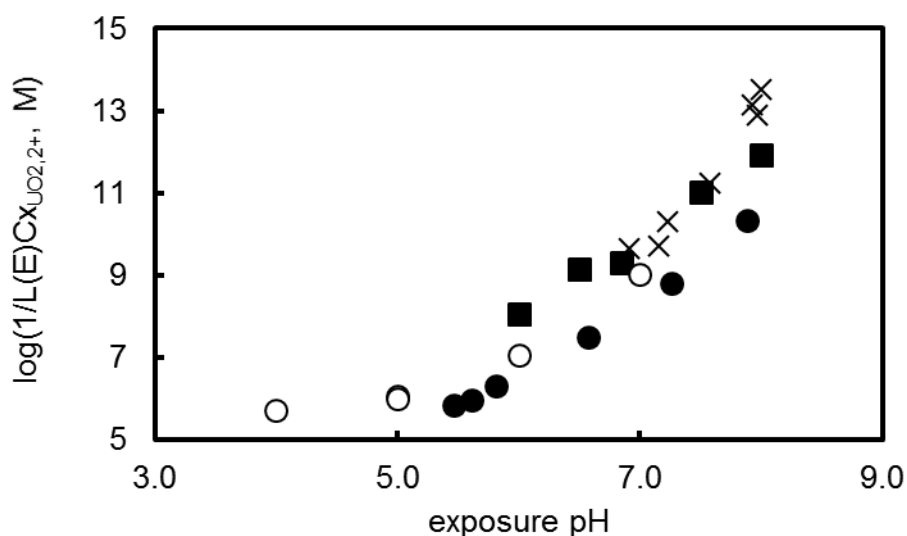


Figure 40. Comparison of pH effects on the 50% effect endpoints for *S. salar* (closed circles, LC50), *L. minor* (open circles, EC10) and *D. magna* (closed squares, LC50). Endpoints expressed as the free UO_2^{2+} ion. Crosses are the LC50 data of Alves et al. (2008) for *H. azteca*.

We used two alternative formulations for the BLM, to see whether either would prove demonstrably superior in modelling accumulation and toxicity:

- a single biotic ligand site (one-site model), allowing multiple U(VI) species to bind;
- two biotic ligand sites (two-site model), allowing only UO_2^{2+} to bind and forcing competition with H^+ at the second site.

In practice both models produced similar fits to the data and it was not possible to select one as superior, except in the case of *D. magna* where the two-site model could not reproduce the pH effect on toxicity. The similarity of the fits largely reflects the fact that the observed pH effects on toxicity can be reproduced either by allowing additional U(VI) species to bind (one-site model) or by formulating a site binding UO_2^{2+} and H^+ competitively with a fixed stoichiometry (two-site model). In the one-site model, where the stoichiometry of binding since relationship between the activities of UO_2^{2+} and the hydrolysis products UO_2OH^+ and $UO_2(OH)_2$ is a function of pH, allowing the hydrolysis products to bind allows for more flexibility in the relationship between bound U(VI) and pH than if only UO_2^{2+} . Similar considerations apply to the binding of the UO_2CO_3 species, given that important influence of pH on the activity of the CO_3^{2-} ion.

For *S. salar*, and particularly for *L. minor*, the extent of the pH effect was seen to change as pH was reduced, with a smaller pH effect on the apparent toxicity due to the free ion at low pH. For these organisms the two-site BLM could explain these effects, with a 'conventional' BL site dominating U(VI) uptake at low pH and a second site dominating at higher pH to describe the strong pH effects. For *S. salar*, the low pH site, while important to provide the optimal fit to the observed accumulation and toxicity, is important in a relatively small

proportion of the exposures and hence has limited data, hence we elected to constrain the *S. salar* model by fixing binding constants to the values obtained for *L. minor* as far as was possible. This provided a reasonable degree of consistency, although further work is required to better understand the influences on U(VI) uptake and toxicity at low pH, ideally including studies of the mechanism(s) by which U(VI) is taken up and exerts toxicity. For example, since the *L. minor* low pH site included competition from Mg^{2+} and Ca^{2+} , this was also included in the *S. salar* low pH site, despite the lack of empirical evidence for a competitive role for these ions on *S. salar*. Ideally, future studies should include major ion competition at multiple pHs to better understand how the competition operates.

For *D. magna*, extension of toxicity studies below pH6 was not possible due to the physiological limitations of the organism, and toxicity could be best explained using a one-site model with multiple U(VI) species binding in competition with the proton and the major ions Na^+ , Mg^{2+} and Ca^{2+} . Binding of multiple species of uranyl to the biotic ligand was required to explain the observed toxicity patterns. Precedent exists for allowing species other than free ion to bind; De Schampelaere et al. (2002) showed that binding of $CuCO_3^0$ (and $CuOH^+$) was required to extend an acute BLM for copper toxicity to *D. magna* above pH8, where $CuCO_3^0$ is an important copper species. Since complexation, particularly with carbonate, is important for U(VI) over a wider range of pH than for many trace metals such as Cu, it is perhaps not surprising that the binding of such species to the biotic ligand needed to be invoked to explain the observed toxicity patterns.

6.1 Biotic ligand modelling of uranium–cadmium mixture accumulation and toxicity

Modelling of mixture accumulation and toxicity produced generally contrasting results for the different organisms. In the case of *L. minor*, both CA and IA reference models gave good predictions of effect in the mixture experiments, with some small improvements afforded by allowing for non-additivity. The models however did not completely describe the accumulation data. Cadmium had a negligible effect on U(VI) accumulation, and this was reproduced by the model. However, U(VI) uptake lowered Cd accumulation, which was not reproduced by the model. For *S. salar*, similar patterns of accumulation were seen i.e. competitive inhibition of Cd uptake by U but negligible apparent effect of Cd on U(VI) uptake. Mixture modelling of effects on *S. salar* did not explain the observed trends; in particular the lack of observed mortality in the presence of either 4.2 or 8.4 μM nominal dissolved U was not reproduced by any of the BLMs. Clearly in this case there is scope for further research to better understand and simulate the competitive effects of U(VI) and Cd for this organism. Modelling of mixture effects on *D. magna* produced contrasting predictions of effect patterns depending on the reference mixture model employed, although the CA model gave superior fits to the IA model. Neither reference model was able to describe mixture effects without some optimisation for residual nonadditive behaviour, following optimisation for competition between uranyl and Cd at the biotic ligand. This tentatively suggests that interactions between the two metals that determine their effect in the mixtures cannot be completely described by competition for general uptake, at least as formulated in this work.

The hypothesis tested in applying the biotic ligand model approach to describing the mixture toxicity was Cationic trace metal co-contaminants will influence the bioavailability of U(VI).

The magnitude of this influence will be consistent with a BLM-based description of uptake competition. For *S. salar* and *L. minor* the first part of the hypothesis can be assessed from the observed accumulation data. In both cases uranyl accumulation does not appear to be influenced by the presence of Cd in solution, in the mixture designs employed. For both organisms the range of Cd solution concentrations required to produce the full range of effect for the target endpoint was insufficient to appreciably influence the uptake of U(VI). Conversely, U(VI) suppressed the uptake of Cd, similar to the suppressing effect of major ions, e.g. Ca and Mg in the case of U(VI) accumulation and effects on *L. minor*. Thus, U(VI) influenced the bioavailability of Cd, rather than the opposite, as was hypothesised. It must be emphasised that the effects of competition between two toxic metal species for uptake cannot be generalised solely on the basis of either their chemical activities or their affinities for the biotic ligand(s). Meyer et al. (2015) showed that for simple competition between cations for binding at a single biotic ligand, the extent of the binding of ions M1, M2 etc. is given by a set of terms $K_{M1} \cdot a_{M1}$, $K_{M2} \cdot a_{M2}$ etc., where K_M is the biotic ligand binding constant and a_M is the activity of the solution species. If the activity of M1 in solution increases it will displace M2 from the biotic ligand if $K_{M1} \cdot a_{M1} > K_{M2} \cdot a_{M2}$. Thus, the extent of competition is a function not only of the relative binding strengths but also of the chemical activities of the binding species in solution. The latter is a function both of the toxic potency (i.e. the range of dissolved concentrations required to be used in a toxicity test) and the aqueous chemistry of the element (i.e. the proportion that is free ionic form under the prevailing chemical conditions).

Fitting the mixture BLM for *D. magna* to the Cd only and U(VI)-Cd mixture data together allowed the optimisation of Cd binding and U(VI)-Cd competition at the biotic ligand, coupled with assessment of any residual nonadditivity. The results provide reasonable, albeit indirect evidence for nonadditivity in the combined toxicity beyond that which could be accounted for by competition between U(VI) species and Cd at the biotic ligand. Further research on mixture effects, particularly different water compositions, would allow more complete assessment of this finding.

A key issue to be addressed in mixture BLM development is whether the concentration addition or independent action approach is most appropriate for modelling. Competition among toxicants for uptake may contribute to deviations from reference mixture models when the medium concentrations are used to express the doses. Thus, from a practical point of view, mixture BLM modelling may seek to explain observations solely on the basis of this competition. However this does not necessarily preclude the possibility that toxicants may act with similar or dissimilar modes of action following BLM binding. The exception to this is where the BLM and the site of toxic action are the same; in this case, modelling competitive uptake at a single biotic ligand implies a common mode of toxic action and the concentration addition approach is appropriate. We have chosen in this work to apply both reference approaches in order to look for outcomes that may support one approach over the other. In the case of *D. magna*, we suggest that the results provide tentative support for the concentration addition approach. However, a better understanding of U(VI) uptake and toxicity mechanisms is needed to better rationalise and understand the discrepancies between observations and model outcomes in the mixture experiments. Recent research (Van Engelen et al, 2011; Burbank et al., 2015) is making a start at elucidating such mechanisms by investigating U(VI)

binding to specific receptor molecules in biological systems. If such initial results are confirmed then they could be used to derive a BLM with a more robust biochemical basis, rather than drawing on macroscopic data such as accumulation and toxicity outcomes.

6.2 *Extension of the BLM to other radionuclides*

There are clear possibilities for extension of the BLM approach to simulate the uptake and/or toxicity of other radionuclides, with some important caveats and potential issues to be considered, of which the most important are likely to be:

- the radionuclide must have an uptake mechanism consistent with the framework of the BLM, i.e. it must be taken up at a 'biotic ligand' e.g. an ion channel, in competition with solution ions;
- the equilibrium speciation of the radionuclide must be computable;
- the concentration range of the radionuclide for uptake and/or effects must be relevant to BLM application.

The current state of the art in the BLM is focused on explaining the bioavailability of elements that form cations in solution. There has been relatively little focus on BLM development for elements forming anions, such as As and Mo, and thus understanding of the effects of competition from other elements for their uptake is less well developed than for elements forming cations. This has implications for BLM development for important anion-forming radionuclides such as ⁹⁹Tc and ¹³¹I, since there is a weaker theoretical basis upon which to design experiments and select the likely major competing ions.

For cationic radionuclide elements e.g. Cs, Sr, Th and the transuranic elements, the possibilities for developing BLMs are clear. Of the examples listed Cs and Sr are the most amenable to BLM development since their solution chemistries are well known, as are their main competing ions (K and Ca respectively). Indeed, their competitive influence on uptake is already included in empirical models (e.g. Smith et al., 2009; Pinder et al., 2014), and Ca competition has been incorporated into a mechanistic model of Sr uptake by fish (Chowdhury & Blust, 2001). For Th and the transuranic elements, knowledge of their equilibrium speciation in waters is reasonable, with constants for binding to a range of inorganic ligands quantified, and constants for binding to natural organic matter available (e.g. Th, Am and Cm in Visual MINTEQ, Th, Np(VI), Am, Pu(IV), Pu(VI) and Cm in WHAM7). A crucial consideration is whether the assumptions underlying the BLM, i.e. that solution complexation of the metal, transport of the binding species to the cell membrane and establishment of binding equilibrium with the biotic ligand are all rapid (Section 1.2.1) are applicable to these elements at concentrations relevant for uptake and/or effects. It has been shown (Hudson and Morel, 1993) that biotic uptake of some trace metals in the open ocean, where dissolved concentrations can range as low as 1 pM, is controlled by the kinetic lability of the metal rather than by equilibrium assumptions, as the BLM assumes.

6.3 *Highlights and Conclusions*

- Extensive datasets on the accumulation of U(VI) by *S. salar* and *L. minor*, and the toxicity of U(VI) to *S. salar*, *L. minor* and *D. magna* under varying chemical exposure

conditions and in mixtures with a toxic non-radioactive metal, Cd, have been derived. These are the most significant datasets yet generated on the bioavailability of U(VI) to aquatic organisms and provide a firm basis for modelling.

- Biotic Ligand Models for U(VI) have been developed and parameterized for U(VI) accumulation by and toxicity to *S. salar* and *L. minor*, and for toxicity to *D. magna*. Distinct, common patterns of accumulation and toxicity in response to changing pH were found. This is the first time that BLMs for U(VI) have been developed in common for multiple species, and is a significant step forward in our ability to understand and predict the toxicity of U(VI) to aquatic organisms across varying water chemistries.
- Modelling of the interactions between U(VI) and Cd in combined exposures broadly suggested that competitive uptake is not the only mechanism required to explain the mixture toxicity patterns. This was best seen in the modelling of combined toxicity to *D. magna*.
- A better understanding of the mechanism of U(VI) toxicity to aquatic organisms is needed to further develop the modelling to provide robust predictions of uptake and toxicity of U(VI) in the presence of co-contaminants.

7 References

- Allen, H.E., Hall, R.H., Brisbin, T.D., 1980. Metal speciation. Effects on aquatic toxicity. *Environ. Sci. Technol.* 14(4), 441–443.
- Altenburger, R., Backhaus, T., Boedeker, W., Faust, M., Scolze, M., 2013. Simplifying complexity : Mixture toxicity assessment in the last 20 years. *Environ. Toxicol. Chem.* 32, 1685–1687.
- Alves, L.C., Borgmann, U., Dixon, D.G., 2008. Water-sediment interactions for *Hyalella azteca* exposed to uranium-spiked sediment. *Aquat. Toxicol.* 87, 187–199.
- Borgmann, U., Nowierski, M., Dixon, D.G. 2005. Effect of major ions on the toxicity of copper to *Hyalella azteca* and implications for the biotic ligand model. *Aquatic Toxicology* 73, 268–287.
- Brain, R.A., Solomon, K.R., 2007. A protocol for conducting 7-day daily renewal tests with *Lemna gibba*. *Nature Protocols* 2, 979-987.
- Burbank, K.A., Walker, R.A., Peyton, B.M., 2015. A molecular level mechanism for uranium (VI) toxicity through Ca²⁺ displacement in pyrroloquinoline quinone-dependent bacterial dehydrogenase. *J. Inorg. Biochem.* 149, 59–67.
- Calamari, D., Marchetti, R., Vailati, G., 1980. Influence of water hardness on cadmium toxicity to *Salmo gairdneri* rich. *Wat. Res.* 14, 1421–1426.
- Cedergreen, N., Kudsk, P., Mathiassen, S.K., Sorensen, H., Streibig, J.C., 2007. Reproducibility of binary-mixture toxicity studies. *Environ. Toxicol. Chem.* 26, 149-156.

- Charles, A. L., Markich, S. J., Stauber, J. L., De Filippis, L. F., 2002. The effect of water hardness on the toxicity of uranium to a tropical freshwater alga (*Chlorella* sp.). *Aquat. Toxicol.* 60, 61-73.
- Chowdhury, M.J., Blust, R., 2001. A Mechanistic Model for the Uptake of Waterborne Strontium in the Common Carp (*Cyprinus carpio* L.). *Environ. Sci. Technol.* 35, 669–675.
- Clifford, M, McGeer, J.C., 2010. Development of a biotic ligand model to predict the acute toxicity of cadmium to *Daphnia pulex*. *Aquat. Toxicol.* 98, 1–7.
- De Jonge, M., Tipping, E., Lofts, S., Bervoets, L., Blust, R., 2013. The use of invertebrate body burdens to predict ecological effects of metal mixtures in mining-impacted waters. *Aquat. Toxicol.*, 142–143, 294–302.
- De Schamphelaere, K. A. C., Janssen, C. R., 2002. A biotic ligand model predicting acute copper toxicity for *Daphnia magna*: The effects of calcium, magnesium, sodium, potassium, and pH. *Environ. Sci. Technol.* 36, 48–54.
- De Schamphelaere, K.A.C., Heijerick, D.G., Janssen, C.R., 2002. Refinement and field validation of a biotic ligand model predicting acute copper toxicity to *Daphnia magna*. *Comp. Biochem. Physiol. C* 133, 243–258.
- De Schamphelaere, K. A. C., Janssen, C. R., 2004. Development and field validation of a biotic ligand model predicting chronic copper toxicity to *Daphnia magna*. *Environ. Toxicol. Chem.* 23, 1365–1375.
- De Schamphelaere, K. A. C., Janssen, C. R., 2006. Bioavailability Models for Predicting Copper Toxicity to Freshwater Green Microalgae as a Function of Water Chemistry. *Environ. Sci. Technol.* 40, 4514–4522.
- Di Toro, D.M., Allen, H.E., Bergman, H.L., Meyer, J.S., Paquin, P.R., Santore, R.C., 2001. Biotic Ligand Model of the acute toxicity of metals. I. Technical basis. *Environ. Toxicol. Chem.* 20, 2383–2396.
- Dong, W., Brooks, S.C., 2006. Determination of the formation constants of ternary complexes of uranyl and carbonate with alkaline earth metals (Mg^{2+} , Ca^{2+} , Sr^{2+} , and Ba^{2+}) using anion exchange method. *Environ. Sci. Technol.* 40, 4689–4695.
- Fortin, C., Denison, F.H., Garnier-Laplace, J., 2007. Metal-phytoplankton interactions: modeling the effect of competing ions (H^+ , Ca^{2+} , and Mg^{2+}) on uranium uptake. *Environ. Toxicol. Chem.* 26, 242–248.
- Geipel, G., Amayri, S., Bernhard, G., 2008. Mixed complexes of alkaline earth uranyl carbonates: A laser-induced time-resolved fluorescence spectroscopic study. *Spectrochim. Acta A-Mol. Biomol. Spec.* 71, 53–58.
- Guillaumont, R., Fanghänel, T., Neck, V., Fuger, J., Palmer, D.A., Grenthe, I., Rand, M.H., 2003. Update on the Chemical Thermodynamics of Uranium, Neptunium, Plutonium, Americium and Technetium. OECD Nuclear Energy Agency, Issy-les-Moulineaux, France.
- Hamelink J. L., Landrum, P. F., Bergman, H. L., Benson, W. H., 1994. Bioavailability: Physical, Chemical and Biological Interactions. CRC Press, Boca Raton, FL, U.S.A..

- Hatano, A., Shoji, R., 2008. Toxicity of Copper and Cadmium in Combinations to Duckweed Analyzed by the Biotic Ligand Model. *Environ. Toxicol.* 23, 372–378.
- Horemans, N., Van Hees, M., Van Hoeck, A., Saenen, E., De Meutter, T., Nauts, R., Blust, R., Vandenhove, H., 2015. Uranium and cadmium provoke different oxidative stress responses in *Lemna minor* L. *Plant Biol.* 17, 91-100.
- Howarth, R.S., Sprague, J.B., 1977. Copper lethality to rainbow trout in waters of various hardness and pH. *Wat. Res.* 12, 455–462.
- Hudson, R.J.M., Morel, F.M.M., 1993. Trace metal transport by marine microorganisms: implications of metal coordination kinetics. *Deep Sea Research Part I: Oceanographic Research Papers* 40, 129–150.
- Iwasaki, Y., Kamo, M., Naito, W., 2015. Testing an application of a biotic ligand model to predict acute toxicity of metal mixtures to rainbow trout. *Environ. Toxicol. Chem.* 34, 754–760.
- Jonker, M.J., Svendsen, C., Bedaux, J.J.M., Bongers, M., Kammenga, J.E., 2005. Significance testing of synergistic/antagonistic, dose level-dependent, or dose ratio-dependent effects in mixture dose-response analysis. *Environ. Toxicol. Chem.* 24, 2701–2713.
- Kamo M, Nagai T. ,2008. An application of the biotic ligand model to predict the toxic effects of metal mixtures. *Environ. Toxicol. Chem.* 27,1479–1487.
- Kinniburgh, D. G., Milne, C. J., Benedetti, M. F., Pinheiro, J. P., Filius, J., Koopal, L. K., Van Riemsdijk, W. H., 1996. Metal ion binding by humic acid: Application of the NICA-Donnan model. *Environ. Sci. Technol.* 30, 1687–1698.
- Keizer, M.G., van Riemsdijk, W.H., 2009. ECOSAT User manual. Department of Soil Quality, Wageningen University, The Netherlands (<http://webdocs.alterra.wur.nl/internet/soq/research/ecosat/manual.pdf>).
- Lauren, D.J., McDonald, D.G., 1986. Influence of water hardness, pH, and alkalinity on the mechanisms of copper toxicity in juvenile rainbow trout, *Salmo gairdneri*. *Can. J. Fish. Aquat. Sci.* 43, 1488–1496.
- Meyer, J.S., Ranville, J.F., Pontasch, M., Gorsuch, J.W., Adams, W.J., 2015. Acute toxicity of binary and ternary mixtures of Cd, Cu, and Zn to *Daphnia magna*. *Environ. Toxicol. Chem.* 34, 799–808.
- Morel, F.M.M., 1983. *Principles of Aquatic Chemistry*. Wiley–Interscience, New York.
- Morgan, J.E., Morgan, A.J., 1998. The distribution and intracellular compartmentation of metals in the endogeic earthworm *Aporrectodea caliginosa* sampled from an unpolluted and a metal-contaminated site. *Environ. Pollut.* 99, 167–175.
- Norwood, W.P., Borgmann, U., Dixon, D.G., 2013. An effects addition model based on bioaccumulation of metals from exposure to mixtures of metals can predict chronic mortality in the aquatic invertebrate *Hyaella azteca*. *Environ. Toxicol. Chem.* 32, 1672–1681.

OECD, 1992. Test No. 203: Fish, Acute Toxicity Test. OECD Guidelines for the Testing of Chemicals, Section 2, OECD Publishing, Paris.

OECD, 2006. Test No. 221: Lemna sp. growth inhibition test. In. Guidelines for the Testing of Chemicals, Section 2. Effects on Biotic Systems. ISSN: 2074-5761 (online) DOI: 10.1787/20745761

Pagenkopf, G.K., 1983. Gill Surface Interaction Model for Trace–Metal Toxicity to Fishes: Role of Complexation, pH and Hardness. Environ. Sci. Technol. 17, 342–347.

Paquin, P.R., Gorsuch, J.W., Apte, S., Batley, G.E., Bowles, K.C., Campbell, P.G.C., Delos, C.G., Di Toro, D.M., Dwyer, R.L., Galvez, F., Gensemer, R.W., Goss, G.G., Hogstrand, C., Janssen, C.R., McGeer, J.C., Naddy, R.B., Playle, R.C., Santore, R.C., Schneider, U., Stubblefield, W.A., Wood, C.M., Wu, K.B. 2002. The biotic ligand model: a historical overview. Comparative Biochemistry and Physiology C–Toxicology & Pharmacology 133, 3–35.

Peters, A.; Lofts, S.; Merrington, G.; Brown, B.; Stubblefield, W.; Harlow, K., 2011. Development of biotic ligand models for chronic manganese toxicity to fish, invertebrates, and algae. Environ. Toxicol. Chem. 30, 2407–2415.

Pinder III, J. E., Rowan, D.J., Rasmussen, J.B., Smith, J.T., Hinton, T.G., Whicker, F.W., 2014. Development and evaluation of a regression-based model to predict cesium concentration ratios for freshwater fish. J. Environ. Radioact. 134, 89–98.

Popic, J.M., Salbu, B., Strand, T., Skipperud, L., 2011. Assessment of radionuclide and metal contamination in a thorium rich area in Norway. J. Environ. Monit. 13, 1730-1738.

Rosseland, B.O., Rognerud, S., Massabuau, J.-C., Grimalt, J.O., 2002. Protocol for Fish Sampling. EU-MOLAR project manual, <http://www.mountain-lakes.org/molar/manual/doc/FISH%20PROTOCOLS.doc> (accessed 1 July 2015).

Santore, R.C., Ryan, A.C., 2015. Development and application of a multimetal multibiotic ligand model for assessing aquatic toxicity of metal mixtures. Environ. Toxicol. Chem. 34, 777–787.

Sinley, J.R., Goettl, J.P., Jr., Davies, P.H., 1974. The Effects of Zinc on Rainbow Trout (*Salmo gairdneri*) in Hard and Soft Water. Bull. Environ. Contam. Toxicol. 12(2), 193–201.

Smith, J.T., Sasina, N.V., Kryshev, A.I., Belova, N.V., Kudelsky, A.V., 2009. A review and test of predictive models for the bioaccumulation of radiostrontium in fish. J. Environ. Radioact. 100, 950–954.

Thakali, S., Allen, H.E., Di Toro, D.M., Ponizovsky, A.A., Rooney, C.P., Zhao, F.J., McGrath, S.P., 2006. A Terrestrial Biotic Ligand Model. 1. Development and application to Cu and Ni toxicities to barley root elongation in soils. Environ. Sci. Technol. 40, 7085–7093.

Tipping, E., 2005. Cation Binding by Humic Substances. Cambridge University Press, Cambridge.

Tipping, E., Lofts, S., 2015. Testing WHAM– F_{TOX} with laboratory toxicity data for mixtures of metals (Cu, Zn, Cd, Ag, Pb). Environ. Toxicol. Chem. 34, 788–798.

- Tipping, E., Lofts, S., Sonke, J.E., 2011. Humic Ion-Binding Model VII: a revised parameterisation of cation-binding by humic substances. *Environ. Chem.* 8, 225–235.
- Tipping, E., Rey-Castro, C., Bryan, S., Hamilton-Taylor, J., 2002. Al(III) and Fe(III) binding by humic substances in freshwaters, and implications for trace metal speciation. *Geochim. Cosmochim. Acta*, 66, 3211.
- Unsworth, E.R., Jones, P., Cook, J.M., Hill, S.J., 2005. Uranium speciation in moorland river water samples: A comparison of experimental results and computer model predictions. *J. Environ. Monit.* 7, 559–567.
- Unsworth, E.R., Warnken, K.W., Zhang, H., Davison, W., Black, F., Buffle, J., Cao, J., Cleven, R., Galceran, J., Gunkel, P., Kalis, E., Kistler, D., Van Leeuwen, H.P., Martin, M., Noel, S., Nur, Y., Odzak, N., Puy, J., Van Riemsdijk, W., Sigg, L., Temminghoff, E., Tercier-Waeber, M. L., Toepperwien, S., Town, R. M., Weng, L.P., Xue, H. B., 2006. Model predictions of metal speciation in freshwaters compared to measurements by in situ techniques. *Environ. Sci. Technol.* 40, 1942–1949.
- Vandenhove, H., Horemans, N., Gilbin, R., Lofts, S., Bradshaw, C., Février, L., Spurgeon, D., Oughton, D., Thørring, H., Salbu, B., Steiner, M., Vaaramaa, K., Jensen, L.K., 2012a. Integrated Research and Experimental Plan under STAR-WP4. STAR WP4 Milestone MS43. EU project No: Fission-2010-3.5.1-269672.
- Vandenhove, H., Horemans, N., Gilbin, R., Lofts, S., Real, A., Bradshaw, C., Février, L., Thørring, H., Brown, J., Oughton, D., Mora, J.-C., Adam, C., Alonzo, F., Saenen, E., Spurgeon, D., Salbu, B., 2012b. Critical review of existing approaches, methods and tools for mixed contaminant exposure, effect and risk assessment in ecotoxicology and evaluation of their usefulness for radioecology. STAR Deliverable D-N^o4.1., 244p. EU project No: Fission-2010-3.5.1-269672.
- van der Lee, J., 1998. Thermodynamic and mathematical concepts of CHESSE. Ecole des Mines de Paris, Paris.
- Van Engelen, M.R., Szilagyi, R.K., Gerlach, R., Lee, B.D., Apel, W.A., Peyton, B.M., 2011. Uranium Exerts Acute Toxicity by Binding to Pyrroloquinoline Quinone Cofactor. *Environ. Sci. Technol.* 45, 937–942.
- van Gestel, C.A.M., M. Jonker, J.E. Kammenga, R. Laskowski, C. Svendsen. (Eds.). 2011. Mixture Toxicity: Linking Approaches from Ecological and Human Toxicology, CRC Press/Taylor and Francis Group, ISBN: 978-1-4398-3008-6, Boca Raton, London, New York. pp 320.
- Verboost, P.M., Van Rooij, J., Flik, G., Lock, R.A.C., Wendelaar Bonga, S.E., 1989. The movement of cadmium through freshwater trout brachial epithelium and its interference with calcium transport. *J. Exp. Biol.* 145, 185–197.
- Wildish, D.J., Carson, W.G., Carson, W.V., 1971. The effect of humic substances on copper and zinc toxicity to salmon, Fisheries Research Board of Canada Manuscript Report N^o. 1160. Fisheries Research Board of Canada, St. Andrews, New Brunswick, Canada.

Winter, A.R., Playle, R.C., Dixon, D.G., Borgmann, U., Wilkie, M.P., 2012. Interactions of Pb and Cd mixtures in the presence or absence of natural organic matter with the fish gill. *Ecotox. Environ. Saf.* 83, 16–24.

Zeman, F.A., Gilbin, R., Alonzo, F., Lecomte-Pradines, C., Garnier-Laplace, J., Aliaume, C., 2008. Effects of waterborne uranium on survival, growth, reproduction and physiological processes of the freshwater cladoceran *Daphnia magna*. *Aquat. Toxicol.* 86, 370–378.

Zitko, P., Carson, W.V., Carson, W.G., 1973. Prediction of Incipient Lethal Levels of Copper to Juvenile Atlantic Salmon in the Presence of Humic Acid by Cupric Electrode. *Bull. Environ. Contam. Toxicol.* 10, 265–271.

Zitko, V., Carson, W.G., 1976. A mechanism of the effect of water hardness on the lethality of heavy metals to fish. *Chemosphere* 5, 299–303.

8 Annex 1: List of papers and presentations issued from this work

List of submitted and published papers in national and international journals

Lofts, S., Février, L., Horemans, N., Gilbin, R., Bruggeman, C., Vandenhove, H. Assessment of co-contaminant effects on uranium and thorium speciation in freshwater using geochemical modelling. *Journal of Environmental Radioactivity*, accepted for publication.

Presentations at National and International scientific congress

Février L., Lofts S., Minko mi Ondo S.L., Lecomte T., Camilleri V., Carasco L., Gilbin R.. Toward a better understanding of uranium bioavailability to daphnids by accounting for cationic competition at the membrane interface. Presented at the 13th International Conference on the Biogeochemistry of Trace Elements (ICOBTE), Fukuoka, Japan, 12-16 July 2015.

Lofts, S., Février, L., Gilbin, R., Horemans, N., Lecomte, T., Minko Mi Ondo, S. L., Teien, H., Willrodt, C., Turtiainen, T., Vandenhove, H. Developing Biotic Ligand Models for uranium: research within the STAR EU Network of Excellence. Presented at the Society of Environmental Toxicology and Chemistry (SETAC) North America 35th Annual Meeting, Vancouver, Canada, 2014.

Horemans Nele, Van Hees May, Willrodt Christine Turtiainen Tuukka, Vandenhove Hildegard. Influence of pH and cations on the speciation, bioavailability and toxicity of uranium in *Lemna minor*. Presented at the Society of Environmental Toxicology and Chemistry (SETAC) Europe 34th Annual meeting, 12-14 May 2014, Basel, Switzerland.

9 Annex 2: One-site toxicity model results, *L. minor*

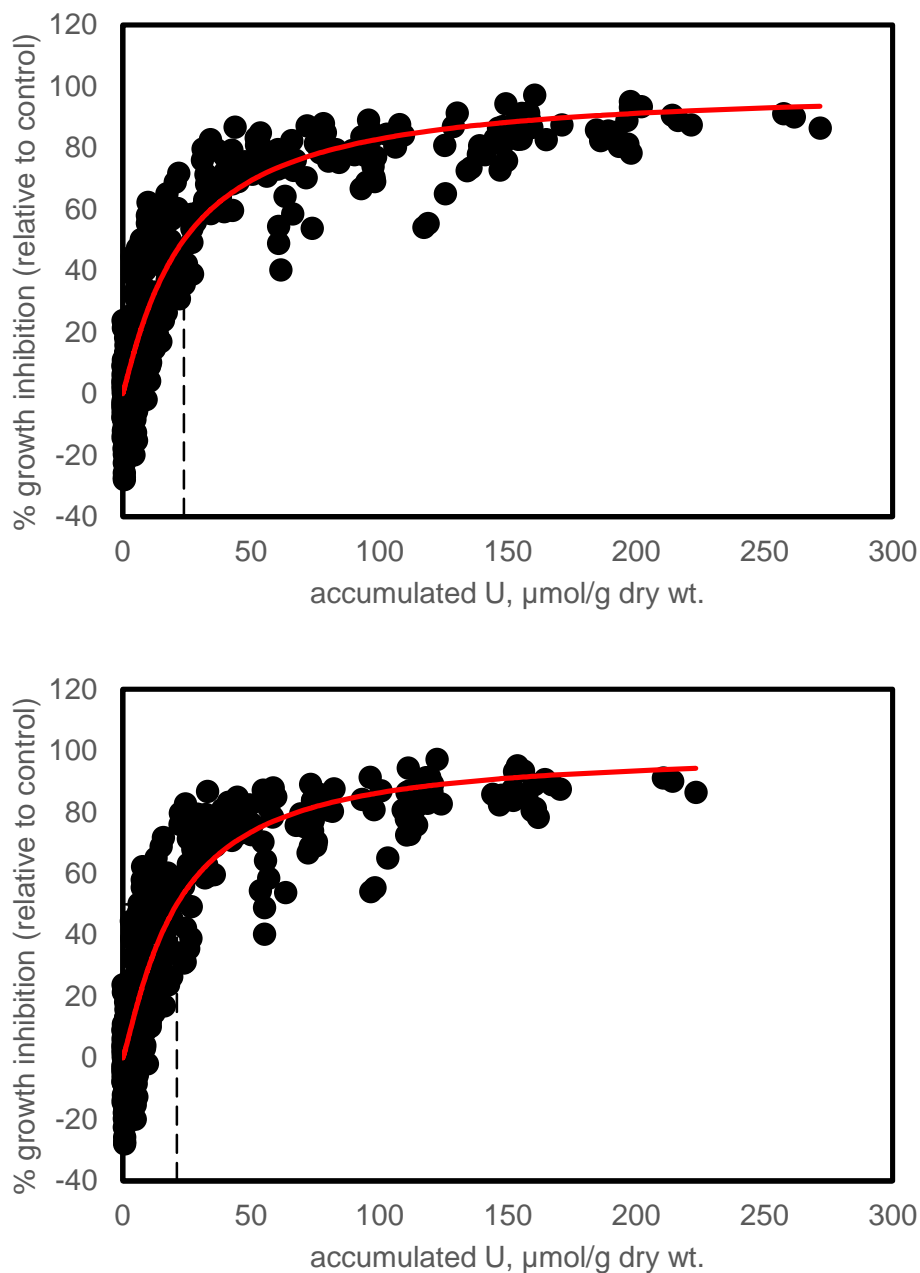


Figure A2-1. Observed and modelled growth inhibition of *L. minor* in response to U accumulation, plotted against modelled U accumulation, for the one-site unconstrained model (top) and the one-site constrained model (bottom). The dashed line marks the $\{UO_2-S\}_{L(E)C50}$.

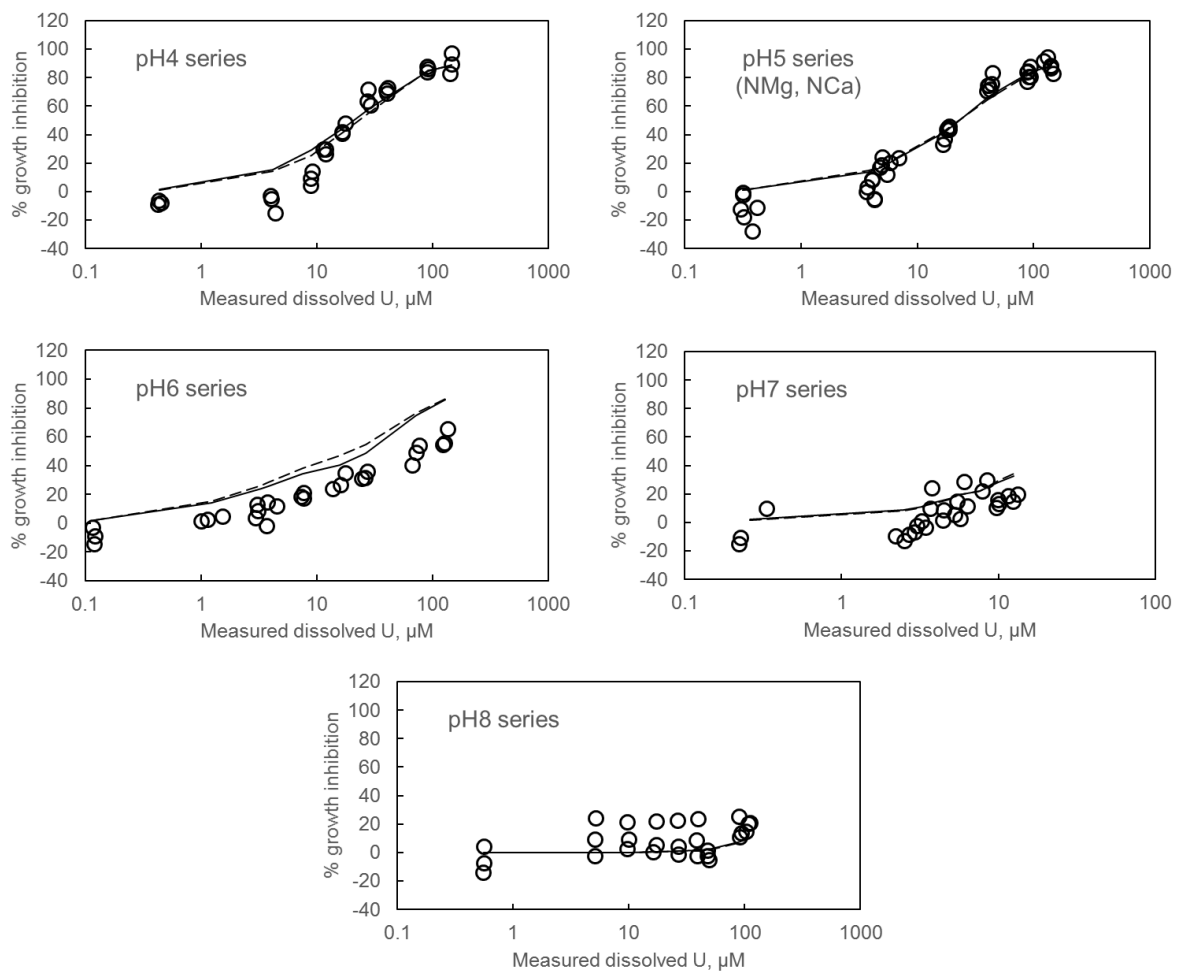


Figure A2-2. Observed and modelled growth inhibition of *L. minor* in the pH series of U exposures, plotted against the measured dissolved U (0.22µm filtered) in the exposures. Solid lines are the fits of the unconstrained one-site BLM, dashed lines are the fits of the constrained one-site BLM.

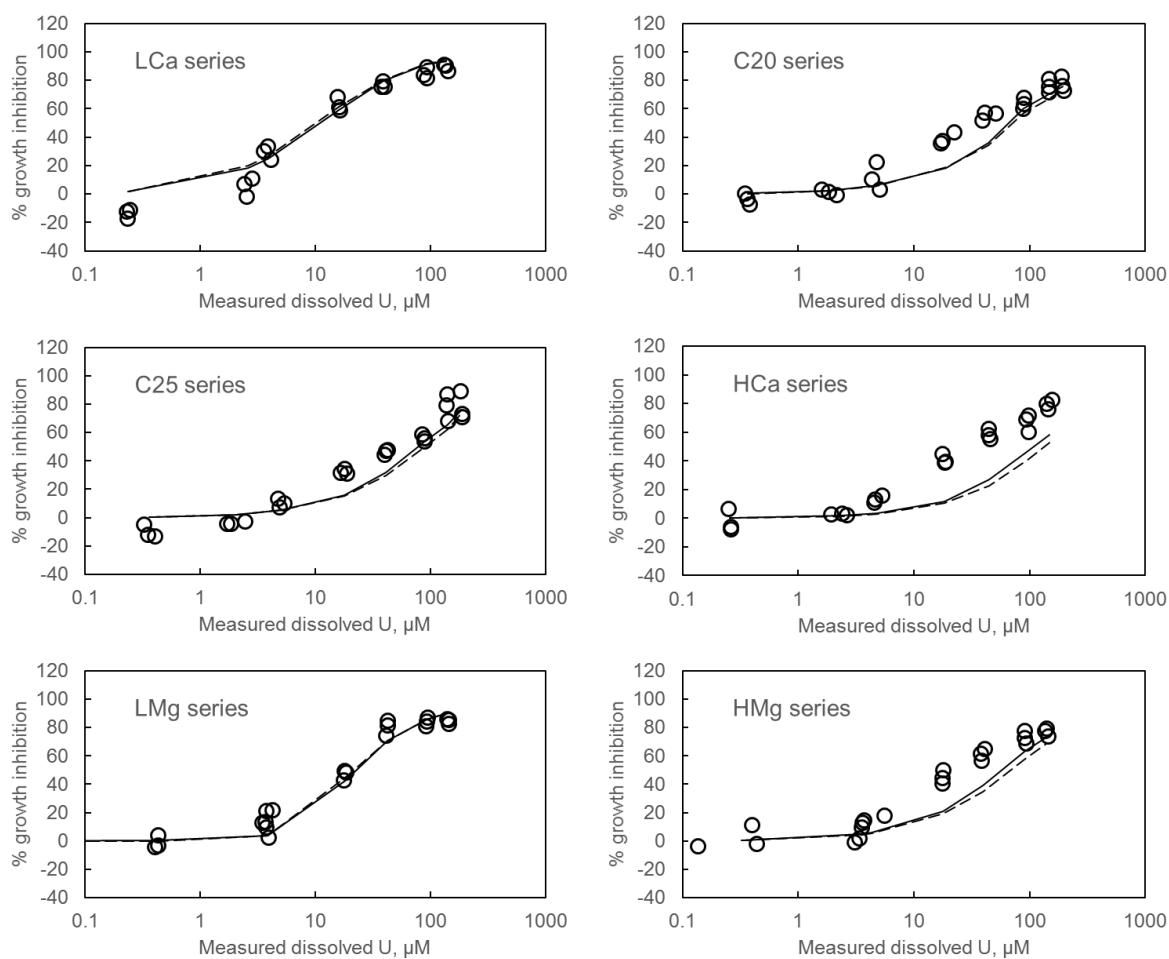


Figure A2-3. Observed and modelled growth inhibition of *L. minor* in the Ca and Mg series of U exposures, plotted against the measured dissolved U (0.22µm filtered) in the exposures. Solid lines are the fits of the unconstrained one-site BLM, dashed lines are the fits of the constrained one-site BLM.

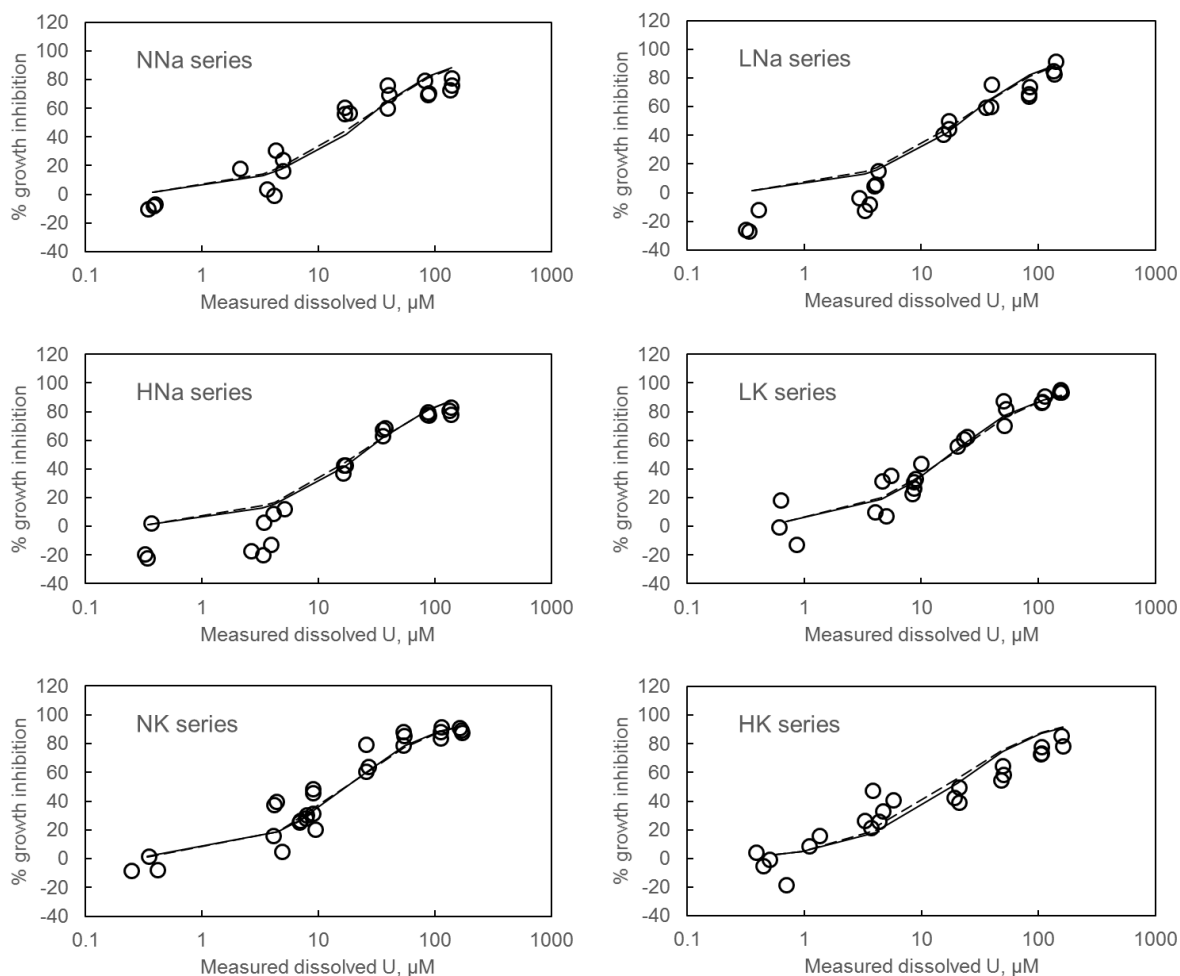


Figure A2-4. Observed and modelled growth inhibition of *L. minor* in the Ca and Mg series of U exposures, plotted against the measured dissolved U (0.22µm filtered) in the exposures. Solid lines are the fits of the unconstrained one-site BLM, dashed lines are the fits of the constrained one-site BLM.

10 Annex 3: One-site toxicity model results, *S. salar*

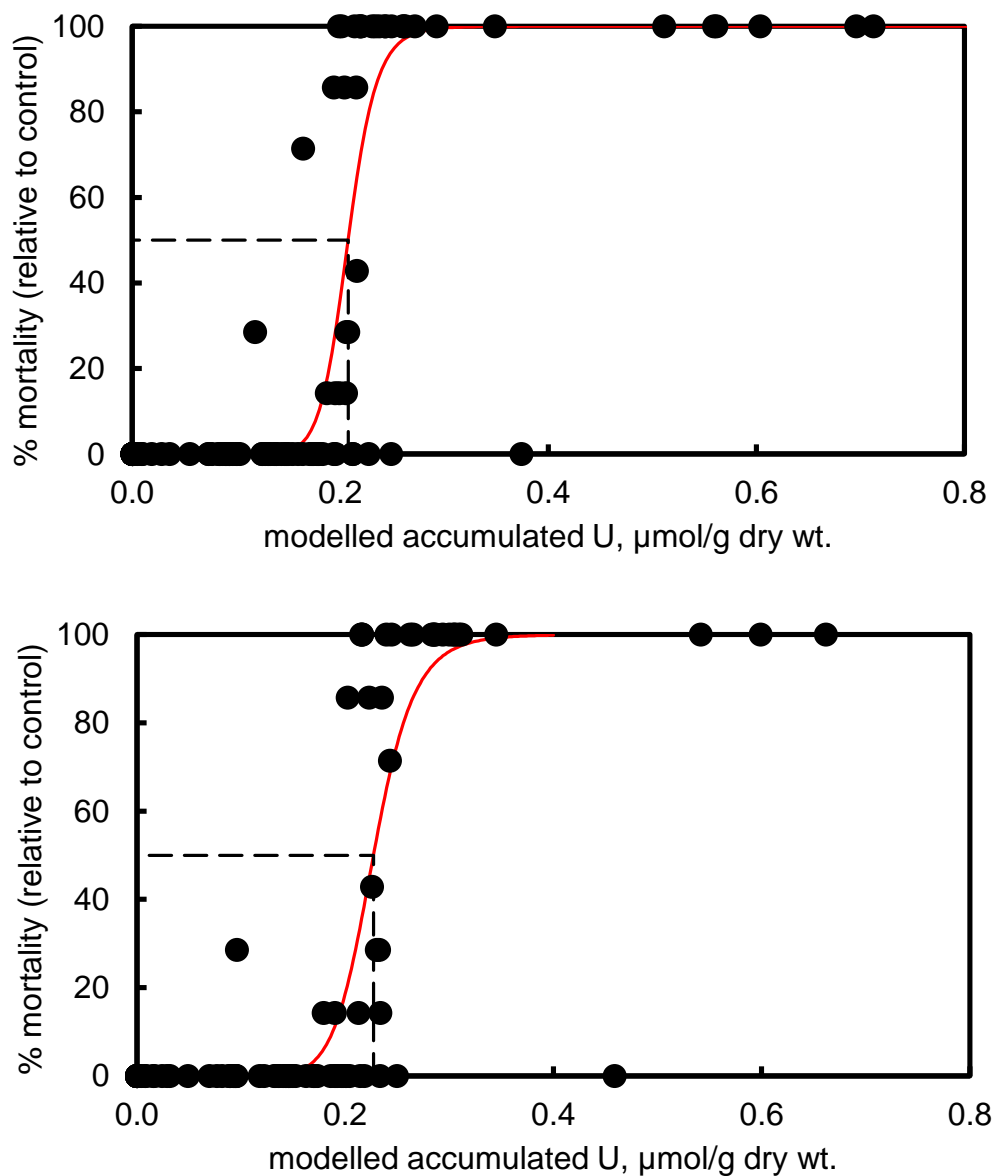


Figure A3-1. Observed and modelled mortality of *S. salar* in response to U accumulation, plotted against modelled U accumulation according to the unconstrained one-site model (top) and the constrained one-site model (bottom). The dashed line marks the $\{UO_2-S\}_{L(E)C50}$.

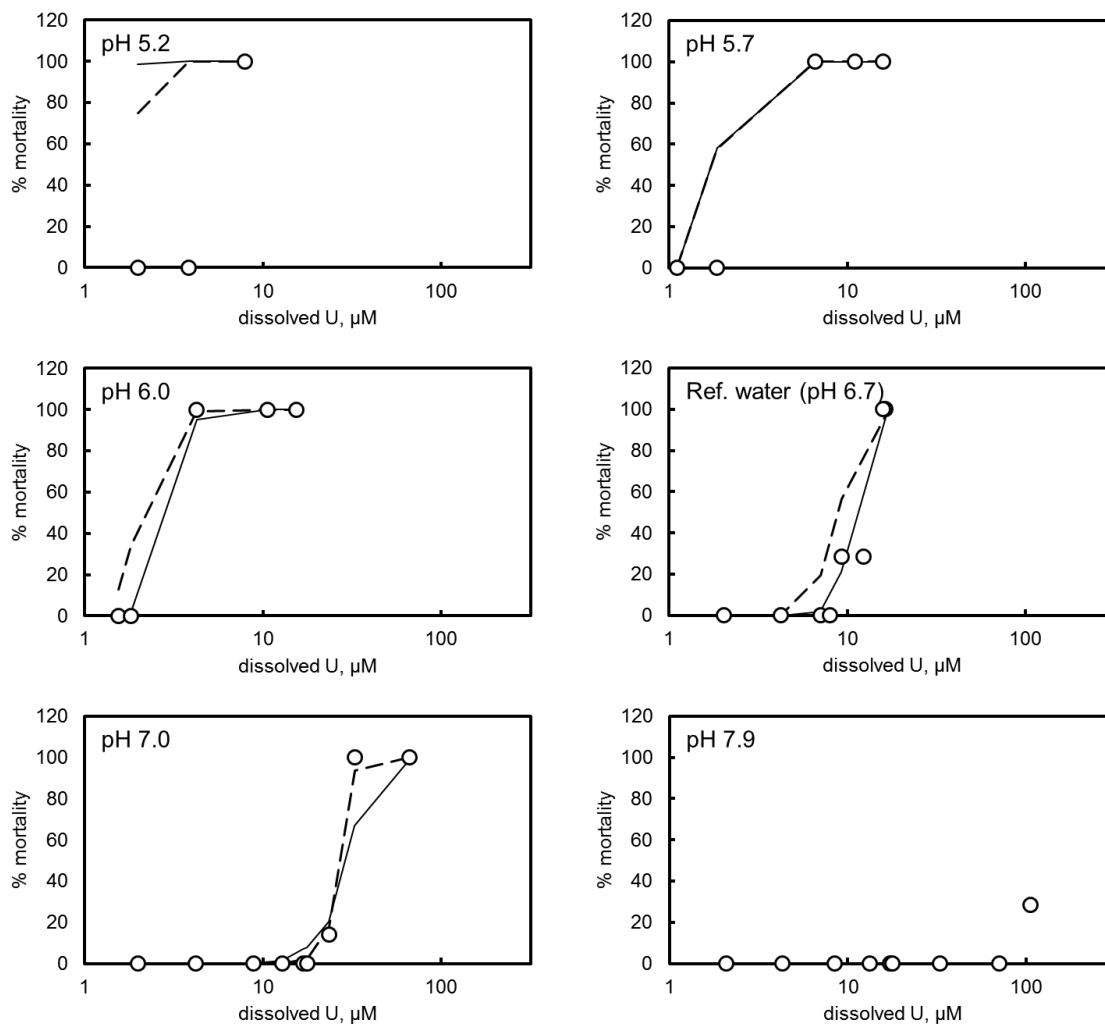


Figure A3-2. Observed and modelled mortality of *S. salar* in the pH series of U exposures, plotted against the measured dissolved U (0.45µm filtered). Solid lines: fits to the unconstrained one-site BLM; Dashed lines: fits to the constrained one-site BLM.

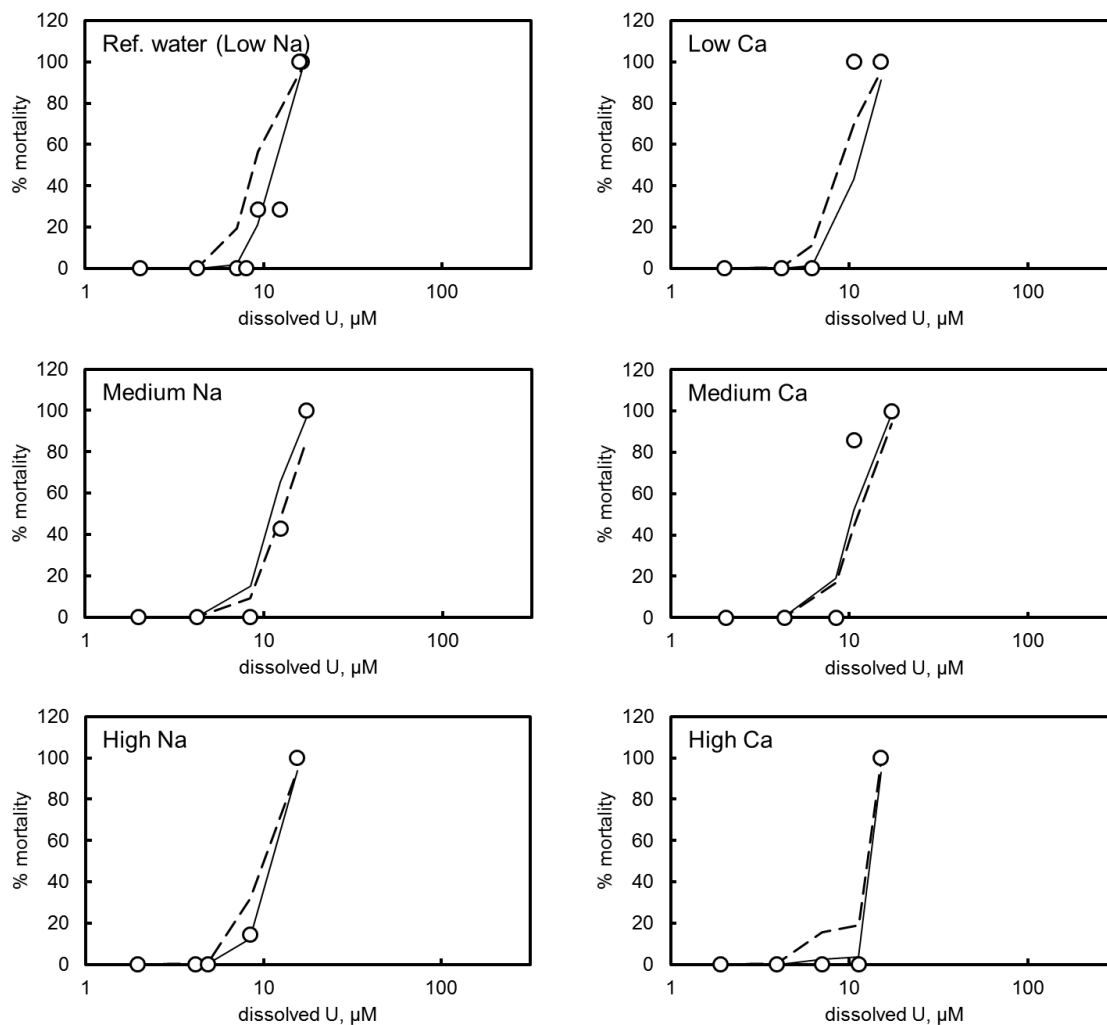


Figure A3-3. Observed and modelled mortality of *S. salar* in the Na and Ca series of U exposures, plotted against the measured dissolved U (0.45µm filtered). Solid lines: fits to the unconstrained one-site BLM; Dashed lines: fits to the constrained one-site BLM.

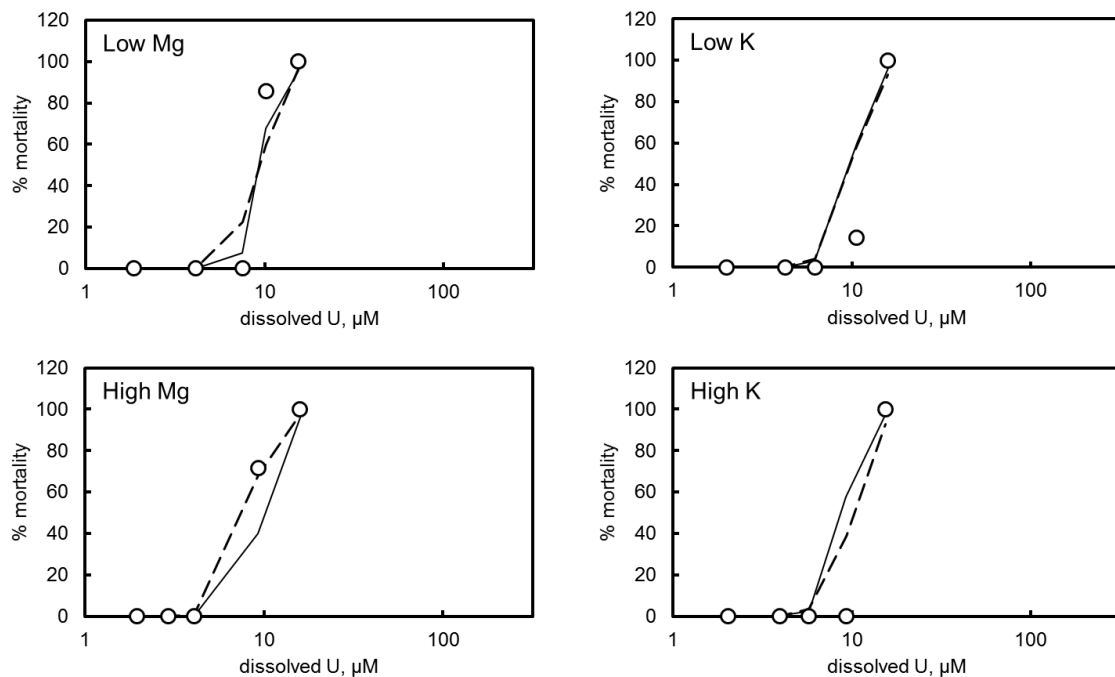


Figure A3-4. Observed and modelled mortality of *S. salar* in the Mg and K series of U exposures, plotted against the measured dissolved U (0.45µm filtered). Solid lines: fits to the unconstrained one-site BLM; Dashed lines: fits to the constrained one-site BLM.

11 Annex 4: Mixture BLM effect predictions, *S. salar*

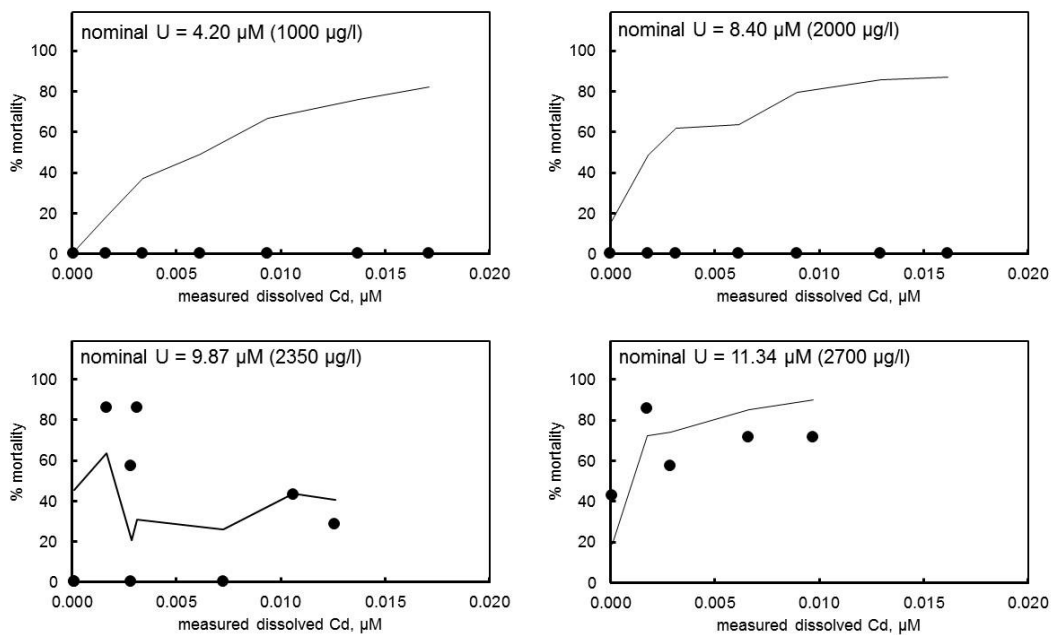


Figure A4-1. Modelled toxicity of U–Cd mixtures to *S. salar* using the constrained one-site BLM and concentration addition reference model . Data are presented in series where nominal dissolved U is constant and dissolved Cd is varied. Solid lines are the reference model predictions.

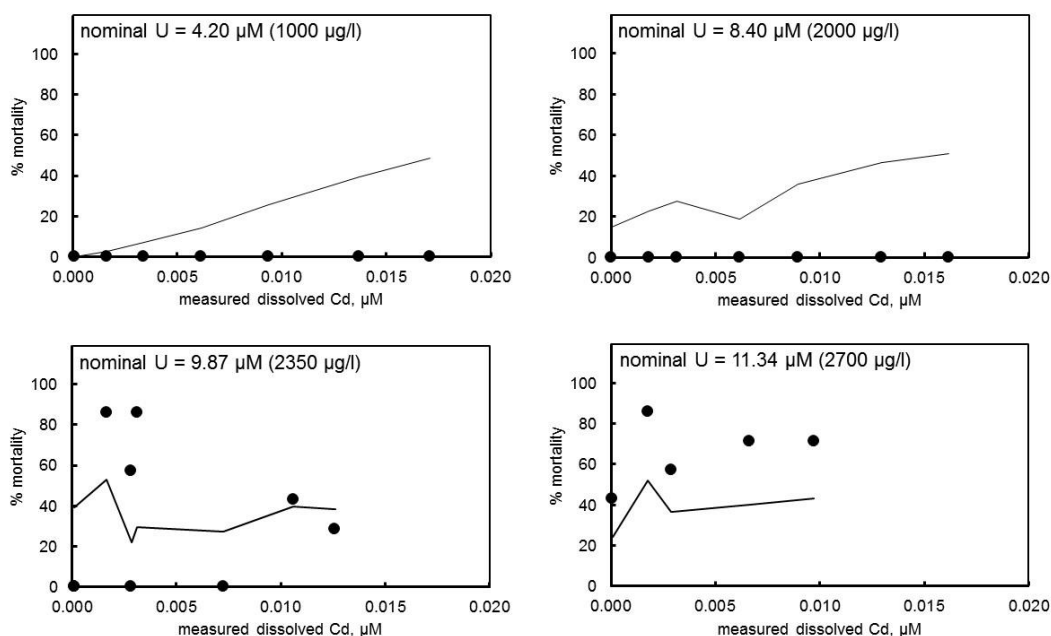


Figure A4-2. Modelled toxicity of U–Cd mixtures to *S. salar* using the constrained one-site BLM and independent action reference model . Data are presented in series where nominal dissolved U is constant and dissolved Cd is varied. Solid lines are the reference model predictions.

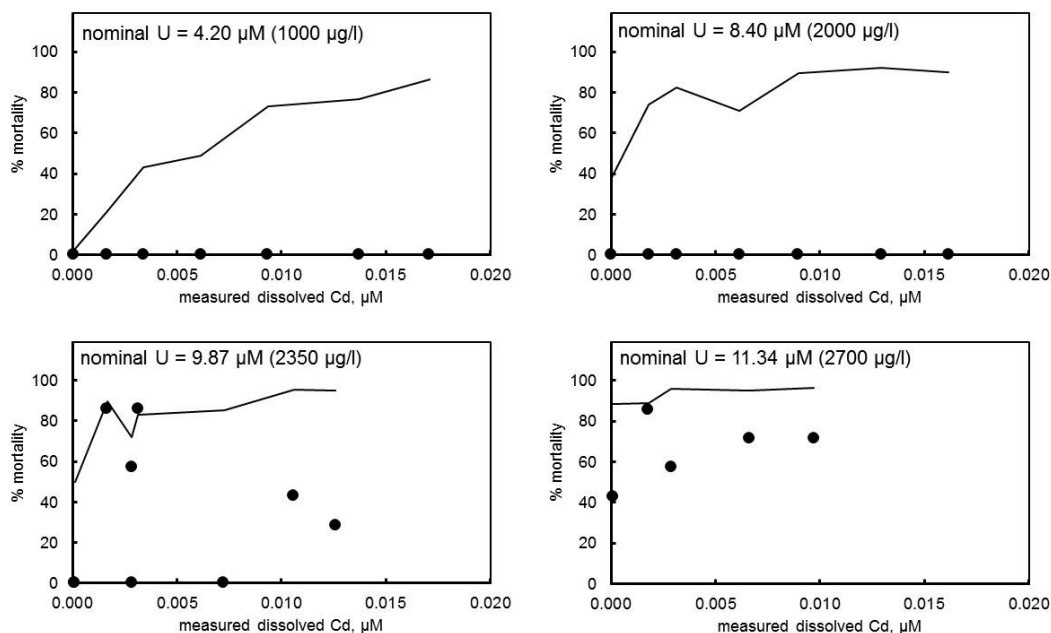


Figure A4-3. Modelled toxicity of U–Cd mixtures to *S. salar* using the two-site BLM and concentration addition reference model. Data are presented in series where nominal dissolved U is constant and dissolved Cd is varied. Solid lines are the reference model predictions.

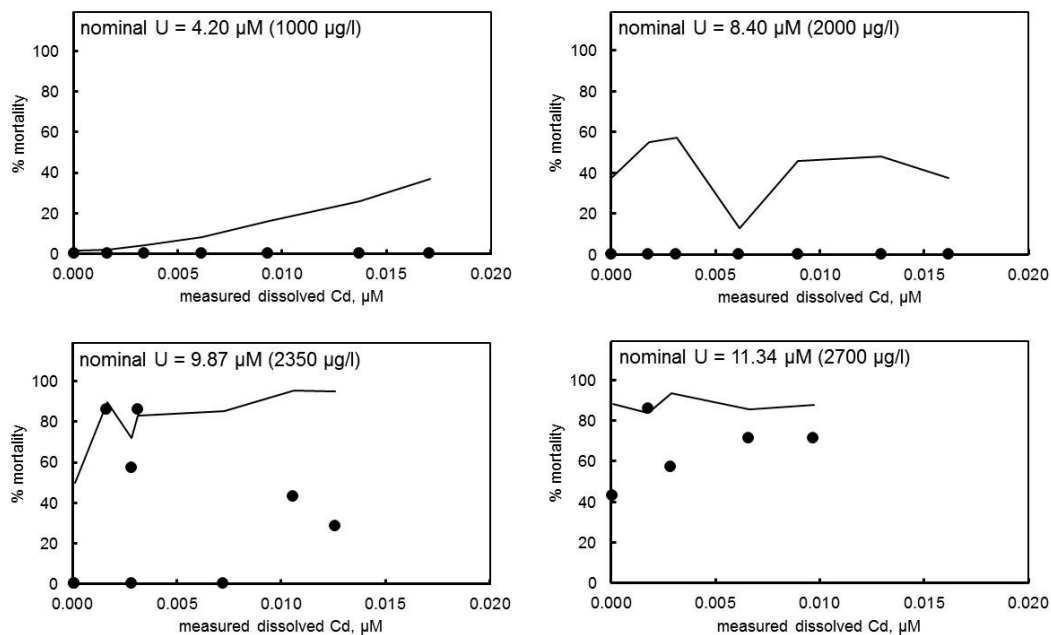


Figure A4-4. Modelled toxicity of U–Cd mixtures to *S. salar* using the two-site BLM and independent action reference model. Data are presented in series where nominal dissolved U is constant and dissolved Cd is varied. Solid lines are the reference model predictions.

12 Annex 5: Two-site model results, *D. magna*

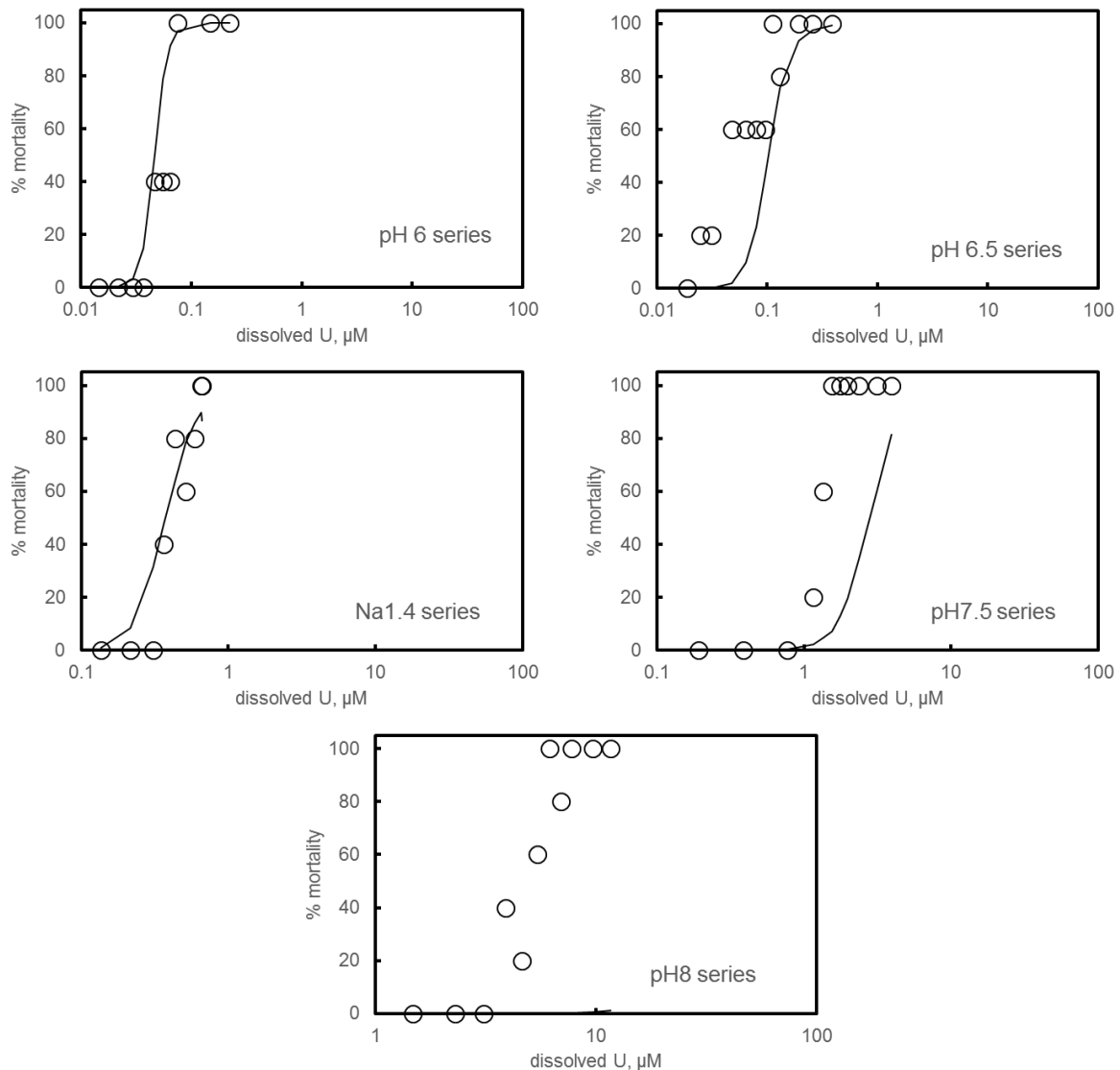


Figure A5-1. Best fit to the *D. magna* pH exposure series obtained using the two-site BLM.